



universität
wien

DISSERTATION

Titel der Dissertation

Recombination and packaging of flaviviruses

angestrebter akademischer Grad

Doktor/in der Naturwissenschaften (Dr. rer.nat.)

Verfasserin / Verfasser:	Taucher Christian
Matrikel-Nummer:	9956839
Dissertationsgebiet (lt. Studienblatt):	Genetik und Mikrobiologie
Betreuerin / Betreuer:	Univ.-Prof. DDr. Christian W. Mandl
Wien, am Juni 2009	

Danksagung

Mein Dank gilt insbesondere Prof. Christian Mandl und Prof. Franz X. Heinz, die großen Anteil am Inhalt der vorliegenden Arbeit haben.

Weiters möchte ich allen Mitarbeitern des Instituts für Virologie für ihre wertvolle Unterstützung danken.

Zum Schluss möchte ich noch den wichtigsten Personen in meinem Leben danken. Meiner unschätzbaren Frau Cornelia und meinem Sohn Vinzent. Beide sorgen stets dafür dass ich nicht den Kopf für die wesentlichen Dinge im Leben verliere.

Content

SUMMARY	5
ZUSAMMENFASSUNG.....	7
INTRODUCTION.....	9
1. Genus <i>Flavivirus</i> , Family <i>Flaviviridae</i>	9
1.1. Epidemiology and disease	10
1.1.1. Japanese encephalitis virus (JEV)	10
1.1.2. West Nile virus (WNV).....	10
1.1.3. Tick-borne encephalitis virus (TBEV)	11
1.2. Molecular Organization of Flaviviruses.....	11
1.2.1. Genome organization and virus particle.....	12
1.2.2. Flavivirus life cycle.....	13
1.2.3. Entry and Genome replication.....	13
1.2.4. Assembly and Egress	14
1.2.5. Flavivirus packaging and the capsid protein	15
2. RNA Recombination	16
2.1. Mechanism of RNA recombination: Replicase driven template switch	17
2.2. Types of RNA recombination	19
2.2.1. Type I Homologous recombination or similarity essential recombination	19
2.2.2. Type II Aberrant homologous or similarity-assisted recombination	20
2.2.3. Type III Non-Homologous or similarity non essential recombination	20
2.3. Factors favoring RNA recombination	21
2.3.1. Available data on animal viruses	21
2.3.2. Lessons from plant viruses.....	22

2.3.2.1. Brome mosaic bromovirus (BMV)	22
2.3.2.2. Turnip crinkle virus (TCV)	23
2.3.3. Involvement of host genes.....	24
2.4. Generation of defective interfering RNA (DI RNA)	25
2.5. The extent of recombination in the family Flaviviridae.....	26
2.5.1. Genus Flavivirus	26
2.5.2. Genus Pestivirus	28
2.5.3. Genus Hepacivirus	29
2.6. Recombination in other positive stranded RNA virus families.....	29
2.6.1. Picornaviruses	29
2.6.2. Coronaviruses.....	30
2.6.3. Alphaviruses.....	30
2.7. Recombination in negative stranded RNA virus families.....	31
2.8. Recombination of Retroviruses	32
AIMS.....	33
Manuscript 1.....	35
Manuscript 2.....	81
Manuscript 3.....	109
References	110

SUMMARY

The flaviviruses include several important human pathogens of global medical importance. Diseases caused by the dengue viruses, West Nile virus (WNV) and Japanese encephalitis virus (JEV) have been classified as emerging diseases and are continuing to spread into new territory. The overall objective of this thesis was to address two fundamental issues that underlie the biology of flaviviruses: recombination among flavivirus genomes and packaging of the viral genome. To this end, an innovative trans-complementation system was established in this thesis. This system consists of two genomes each lacking a different part of the viral structural protein genes. Thus, neither of these so-called replicons is able to produce infectious virions by itself. When introduced together into the same host cell, however, they are able to complement each other and both replicons can be packaged into virion particles. Thus, these two replicons can be repeatedly passaged together providing ample opportunity for recombination events potentially generating full-length, infectious genomes. This system was applied to three different flaviviruses, i.e. tick-borne encephalitis virus (TBEV), WNV, and JEV

Surprisingly, in no case the recombination trap produced wild-type genomes by exact, homologous cross-over events different from the general assumption that this would be the most likely event to occur. Intermolecular recombination yielding infectious full-length viruses was observed for one of the three viral systems, namely JEV. However, rather than generating wild-type genomes, aberrant homologous recombination resulted in recombinant JE viruses with unnatural gene arrangements and reduced growth properties compared to wild-type virus. In spite of the absence of any inter-molecular recombination events, the TBEV recombination trap evolved defective genomes with larger deletions presumably by a intra-molecular recombination process. The resulting mutants lacked part of a nonstructural protein gene and were thus by themselves incompetent for RNA replication. However, in the

presence of the other replicon (or an infectious virus) these defects could be complemented in trans leading to successful replication of these mutants which thus represent proper sense 'defective interfering particles'.

The fact that all of these deletion mutants could be packaged into virions demonstrated that these sequences were not essential for the packaging process. To analyze the requirements for packaging within the capsid protein in more detail, the WNV capsid protein was subjected to a specific deletion analysis. Artificially introduced deletions into a conserved hydrophobic region were mostly well tolerated. Spontaneously emerging pseudorevertants surprisingly included two mutants with significantly extended deletions removing more than a third of the entire capsid protein. Further analysis confirmed that those minimal capsids allowed packaging of the viral genome.

In summary, this thesis demonstrates that flavivirus genomes have a very low propensity, if any, for homologous recombination and provides the first laboratory recombination system yielding an aberrant homologous recombination event between flavivirus genomes. Furthermore, the data indicate that flavivirus genomes can readily undergo intramolecular recombination events leading to extended deletion mutations. The spontaneously formed defective interfering particles as well as viable capsid deletion mutants provided information on requirements for packaging of the viral genome.

ZUSAMMENFASSUNG

Das Genus Flavivirus umfasst eine Reihe wichtiger menschlicher Krankheitserreger. So sind zum Beispiel das Dengue, West Nile oder Japanische Enzephalitis Virus als wiederaufkommende Erreger klassifiziert worden und dringen in neue Gebiete vor. Das Ziel dieser Doktorarbeit war, zwei wichtigen Aspekten der Biologie von Flaviviren auf den Grund zu gehen: einerseits die Rekombination von Flaviviren und andererseits die Verpackung des viralen RNA Genoms. Hierfür wurde ein neuer, innovativer Ansatz entwickelt. Das Grundprinzip beinhaltet zwei defekte Viren, so genannte Replikons, denen jeweils unterschiedliche Viruspartikelbausteine fehlen wodurch sie keine infektiösen Viruspartikel mehr bilden können. Beide Replikons besitzen jedoch die Fähigkeit in einer Wirtszelle das virale Genom zu vervielfältigen und in Proteine zu übersetzen. Wenn beide Viren in der gleichen Zelle vorhanden sind, kodieren sie für alle Proteine, die für ein Viruspartikel nötig sind. Tatsächlich konnten wir zeigen, dass beide Replikons in infektiöse Partikel verpackt werden. Allerdings ist das System nicht so effizient wie ein einzelnes Genom auf dem alle Virusbausteine kodiert sind. Aus diesem Grund können „Ganzlängengenome“, die durch Rekombination der beiden defekten Genome entstehen können, in Zellpassagen gesucht werden. Dieses System wurde auf die drei Flaviviren Frühsommermeningoenzephalitis Virus (FSME), WNV und JEV angewandt.

Interessanterweise, wurde in keinem Fall exakte homologe Rekombination zu Wildtype Virus beobachtet, obwohl dies als sehr wahrscheinlich galt. Allerdings konnte Rekombination zu infektiösen Ganzlängen Viren in einem der drei Virussystemen gezeigt werden. Beim JE Virus führte ungenaue homologe Rekombination zu Viren mit ungewöhnlicher Genomstruktur und im Vergleich zum Wildtype Virus reduzierten Wachstum.

Obwohl keine intermolekulare Rekombination zu infektiösen Viren beim FSME Virus gefunden werden konnte, entwickelten sich die defekten FSME Viren durch den Verlust von

Sequenzen, herbeigeführt wahrscheinlich durch einen intramolekularen Rekombinationsprozess. Den entstandenen Mutanten fehlte ein Teil eines Nichtstrukturproteins wodurch sie nicht mehr in der Lage waren ihr RNA Genom zu vervielfältigen. Allerdings konnte dieser Defekt in Anwesenheit eines Replikons (oder eines infektiösen Virus) kompensiert werden. Die Mutanten erlangten dann wieder die Fähigkeit ihr Genom zu vervielfältigen und stellten damit im eigentlichen Sinn defekte hemmende RNA Moleküle dar.

Die Tatsache, dass diese Mutanten in Viruspartikel verpackt werden konnten, zeigte, dass die ihnen fehlenden Sequenzen nicht für die Verpackung wichtig waren. Um die Anforderungen an das Kapsidprotein für die Verpackung genauer zu analysieren, wurde das Kapsidprotein des WNV genauer untersucht. Die Wegnahme von kurzen Sequenzen in einer konservierten, hydrophoben Region wurde vom Virus zwar toleriert. In zwei Fällen traten jedoch Revertanten auf, denen mehr als ein Drittel der Sequenz für das WNV Kapsidprotein fehlten. Eine genauere Analyse zeigte, dass diese reduzierten Kapside ausreichten um das virale Genom zu verpacken.

Zusammenfassend zeigt diese Dissertation, dass Flaviviren eine sehr geringe Tendenz zu homologer Rekombination aufweisen. Zugleich beschreibt sie das erste Rekombinationssystem im Labor, das ein ungenaues Rekombinationsereignis zwischen Flavivirus Genomen zeigen konnte. Darüber hinaus deuten die Ergebnisse darauf hin, dass Flaviviren eher zu intramolekularer Rekombination neigen, was zum Verlust von Sequenzen führt. Die spontan entstandene defekten hemmenden RNA Moleküle sowie die funktionstüchtigen WNV Kapsid Mutanten lieferten Informationen über die Verpackung des viralen Genoms.

INTRODUCTION

1. Genus *Flavivirus*, Family *Flaviviridae*

The family *Flaviviridae* consists of three genera: *Pestivirus*, *Hepacivirus* and *Flavivirus*. The Genus *Flavivirus* is the largest genus comprising over 70 viruses, many of which are important human pathogens. Although, some flaviviruses have no known vector, most members are either transmitted by mosquitoes or ticks which also constitutes two different genetic lineages. Further, the members of the genus *Flavivirus* can be grouped serologically into different groups (figure 1).

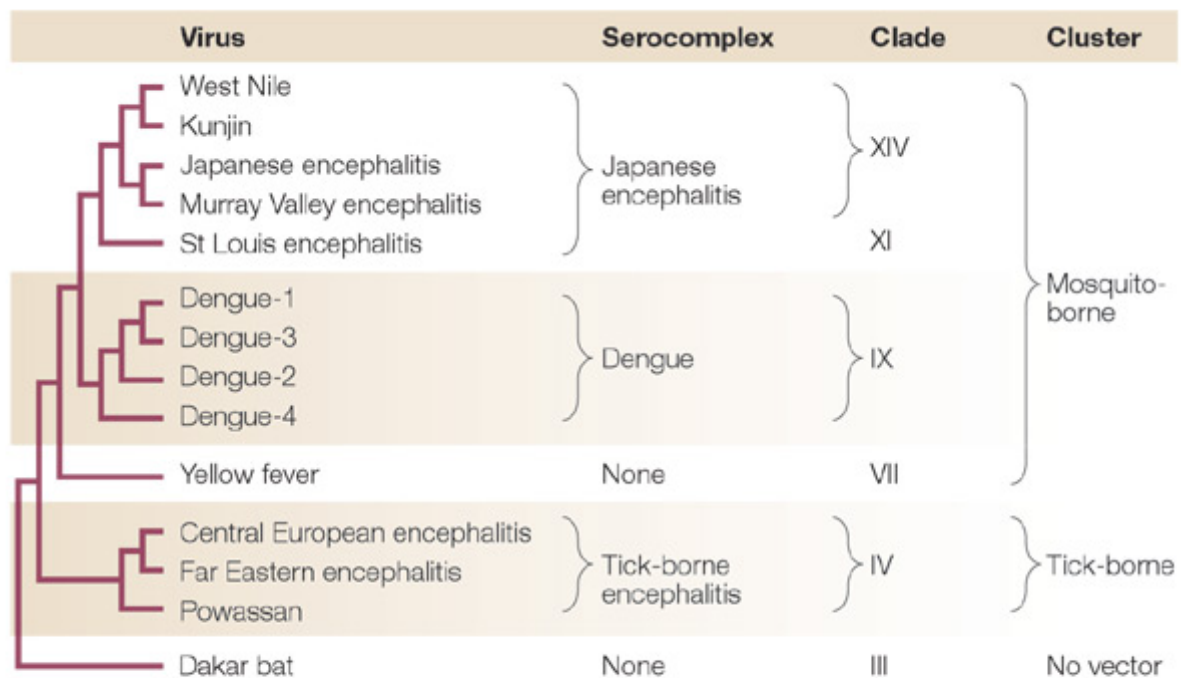


Figure 1. *Flavivirus* classification. *Flaviviruses* can be grouped into different groups according to serological (serocomplex), phylogenetical (clades) or transmitting vector (cluster) (106).

1.1. Epidemiology and disease

1.1.1. Japanese encephalitis virus (JEV)

JEV is the most important cause of viral encephalitis in eastern and southern Asia, with 30,000-50,000 cases reported annually. Most infections are asymptomatic but 25-30% of the reported cases result in fatal disease and 50% in neurological sequelae (93). Clinical disease varies from non-specific febrile illness to meningoencephalitis, aseptic meningitis or polio-like acute flaccid paralysis (137). JEV is transmitted in a zoonotic cycle between mosquitoes and pigs and/or water birds. Humans become infected only coincidentally and are dead end host. There exist two licensed vaccines, the Chinese SA14-14-2 strain, which due to international safety requirements cannot be used outside of China and a Vero cell produced formalin inactivated SA-14-14-2 strain by Intercell (IXIARO®) which has just been licensed for use in Europe and the US.

1.1.2. West Nile virus (WNV)

Two distinct lineages have been defined for WNV: Lineage 1 includes the NY-99 strain that was responsible for the introduction of WNV to the US and Kunjin which represents an attenuated subtype circulating in Australia. Lineage 2 includes several African strains but all reported cases of severe illness were caused by strains of lineage 1 (117). The transmission cycle of WNV is maintained in a bird-mosquito-bird cycle and humans are only incidental hosts (93). When humans become infected, in most cases WNV causes a mild febrile illness or the infection remains asymptomatic. However, in 1 out of 150 infections a severe and sometimes fatal encephalitis, meningoencephalitis or hepatitis have been reported, especially

in elder patients (118). Although, a number of different WNV vaccines are at the stage of clinical trials (18)(47) at the moment exists only a veterinary vaccine that has been successfully used in horses (18).

1.1.3. Tick-borne encephalitis virus (TBEV)

Three subtypes of TBEV have been phylogenetically defined: European, Far Eastern and Siberian (31). In Western Europe the principal vector for TBEV is *Ixodes ricinus* while in Eurasia it is *Ixodes persulcatus*. Typically, TBEV is transmitted in a zoonotic cycle between ticks and small vertebrate hosts, mainly rodents, although larger animals like birds or deer can get infected as well. Occasionally, the direct transmission to humans drinking unpasteurized milk from infected goat, sheep or cow has been reported (122). Approximately 70% of TBEV infections are asymptomatic, the remaining percentage can develop an febrile illness after an incubation period of 3 to 7 days after the tick bit. Symptoms include fever, headache, malaise and nausea. After an asymptomatic phase that may last from 1 to 33 days, in about one third of the patients, fever returns accompanied with symptoms affecting the central nervous system, such as meningitis or meningoencephalitis. A small percentage of patients sustain long-lasting or permanent neurological sequelae. The case fatality rate is below 1% with infections of the Western subtype but can be as high as 40% with the Far Eastern subtype. In Austria about 90% of the population is vaccinated with a formalin inactivated whole virus vaccine which originally has been developed with major input from scientists of the Institute of Virology in Vienna.

1.2. Molecular Organization of Flaviviruses

1.2.1. Genome organization and virus particle

Flaviviruses are positive-stranded RNA viruses. The 11kb-long genome contains a cap structure at its 5' end but no poly-A tail at its 3' end. It encodes only a single open reading frame which is translated into a polyprotein. Posttranslational cleavages by viral and host proteases yield three structural proteins: the membrane (M), envelope (E) and capsid (C) proteins, as well as seven non-structural proteins that are essential for viral replication (figure 2)(90) (89).



Figure 2. Schematic drawing of a Flavivirus full-length genome. C, capsid; M, membrane; E, envelope; NCR, non-coding region.

For example, NS5 is the viral RNA-dependent RNA polymerase (RdRp) and NS-3 is a multifunctional protein containing a serine protease domain at its N-terminus necessary for the processing of the viral polyprotein and helicase domain at its C-terminus which is part of the viral replication complex. Non-coding regions that are rich in RNA secondary structure are located at both ends of the genome. These structures have been associated with diverse functions controlling replication and translation of the RNA genome (97). Flavivirus virions are composed of a single copy of the positive-stranded RNA genome that is packaged by the capsid protein C into a nucleocapsid. The nucleocapsid is engulfed by a lipid envelope containing the surface glycoproteins prM and E (figure 3).

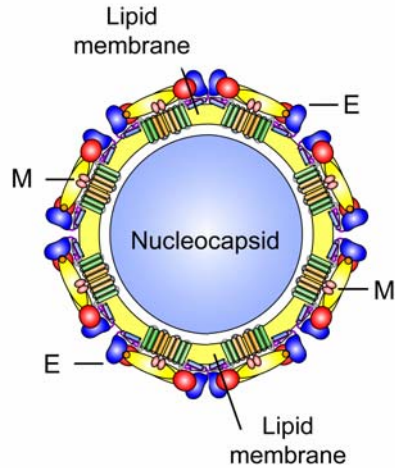


Figure 3. Schematic drawing of a mature Flavivirus virion. The nucleocapsid which lacks a defined form is surrounded by a host derived lipid bilayer in which the surface glycoproteins M and E are inserted (140).

1.2.2. Flavivirus life cycle

1.2.3. Entry and Genome replication

Flaviviruses attach to the surface of a host cell by a yet unidentified receptor. An involvement of heparin sulfate (HS) during attachment and entry has been suggested but its availability on the host is not essential for virus uptake (95). Although, no specific cellular receptor has been identified, it was established that Flaviviruses enter the cell by receptor mediated endocytosis via clathrin coated pits (24). After endocytosis, viral particles are found in uncoated prelysosomal vesicles, where fusion of viral and host membrane occurs (89). The RNA genome is released into the cytoplasm where replication takes place at the perinuclear membrane in virus induced vesicular packets. First, the plus-strand of the viral genome directs the synthesis of the viral polyprotein in association with the host membrane (figure 4). Once the viral polymerase and other essential proteins are synthesized, the viral RNA is copied. RNA replication of the viral genome starts with the synthesis of a negative-strand RNA from

which new viral genomic RNA is produced. The process of replication is asymmetric, leading to a 10- to 100-fold excess of positive-strands over negative strands (25).

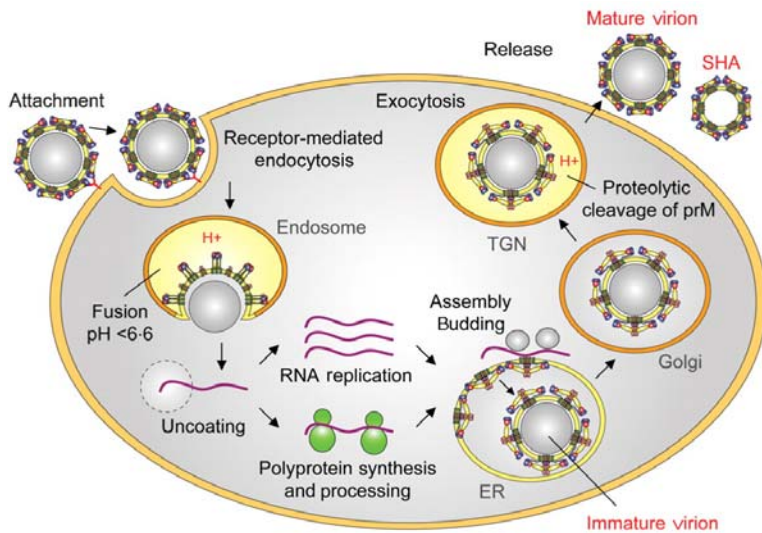


Figure 4. *Flavivirus* life cycle (140).

1.2.4. Assembly and Egress

The glycoproteins prM and E drive budding at the membrane of the endoplasmic reticulum (ER)(106). Subviral particles devoid of a nucleocapsid are routinely observed as a by-product of flavivirus infections (3) and can be produced by recombinant expression of the two viral surface proteins prM and E alone (2). However, preformed nucleocapsids are usually not observed in flavivirus-infected cells, indicating that virion formation is a coordinated process between the membrane-associated capsid protein and prM-E heterodimers in the ER. After intracellular budding at the endoplasmic reticulum immature particles are transported through the trans-Golgi network, followed by the cleavage of prM by the host protease furin. Mature virions and subviral particles are subsequently released from the host cell by exocytosis (139).

1.2.5. Flavivirus packaging and the capsid protein

For many viruses, specific elements on the packaged genome (such as the psi signal on retrovirus genomes) or specific protein determinants have been identified which ensure the specificity and efficiency of this crucial process. Although it is clear that flaviviruses also package their genome with high specificity and efficiency, the determinants that underlie this process are essentially unknown. On the RNA level, it has been speculated that specific RNA elements present in the terminal non-coding regions may function as packaging signals (97), but there is no experimental evidence for this hypothesis. Some studies suggest that packaging is tightly coupled to and dependent on RNA replication (70). Other studies indicate that non-structural proteins may also be involved in this process (83).

On the protein level, positively charged regions of protein C appear to be involved in RNA binding, but no specificity has been demonstrated for this binding (72). Further it is believed that a hydrophobic sequence element which is present at a conserved position in all flavivirus capsid protein sequences (figure 5) plays an important role in packaging. The functional importance of this conserved internal hydrophobic domain has been demonstrated by studies with a variety of flaviviruses. For example, characterization of TBEV capsid deletion mutants showed that the proportion of infectious virions to non-infectious capsidless subviral particles shifted towards subviral particles with increasing deletion length (77). In addition large deletions were tolerated only upon the acquisition of additional mutations increasing the hydrophobicity of the protein (80). Further, studies on YFV protein C (115) and WNV(131), showed that removal of the entire helix α_2 , which includes the conserved domain produced a noninfectious phenotype. In DENV, removing large parts of this hydrophobic domain abolished the ability to dimerize in vitro(149) which is a prerequisite for the formation of the nucleocapsid and the ability to associate with the ER membrane (98). Taken together, these

studies underlined the important role of the conserved internal hydrophobic sequences in virion assembly.

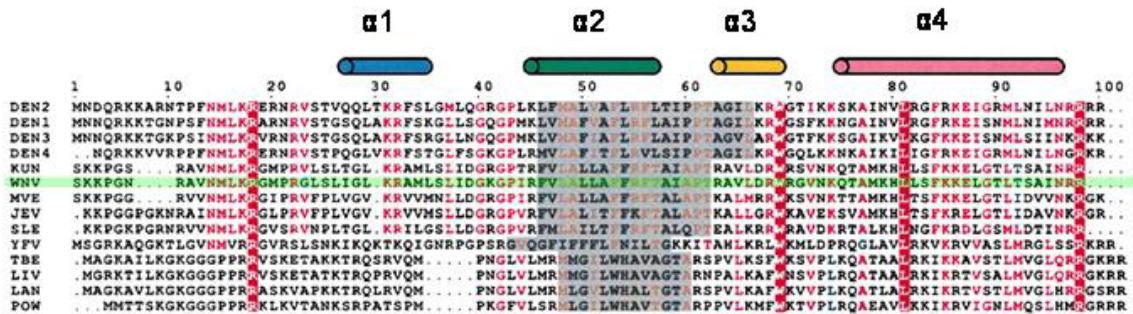


Figure 5: Multiple sequence alignment of flavivirus capsid proteins. Residues with high similarity (>50%) are red, and the conserved residues highlighted. The secondary structure is indicated at the top. The conserved hydrophobic region of flaviviruses is shaded gray. KUN, Kunjin; MVE, Murray Valley encephalitis; SLE, St. Louis encephalitis; YFV, yellow fever; LIV, loupin ill; LAN, Langat; POW, Powassan virus.(92)

2. RNA Recombination

The versatility of RNA viruses depends on divers and rapid genetic changes. Error-prone viral polymerases can cause single nucleotide substitutions at high rates and allow them to quickly adapt to new environmental challenges (62). In addition, it has become increasingly clear that many RNA viruses add the capacity to exchange genetic material with one another to their evolutionary repertoire. RNA recombination has been observed in all types of viruses using RNA as a carrier of genetic information: in positive-sense, single-stranded RNA viruses ((84)), in negative-sense, single-stranded RNA viruses ((142)), in double-stranded RNA viruses ((113)) and in retroviruses ((156)). Moreover, it has been shown that RNA recombination enables the exchange of genetic material not only between the same or similar

viruses but also between distinctly different viruses ((153)). There are also examples in which host derived sequences have been identified in viral RNAs: For example a sequence from 28S rRNA inserted in the hemagglutinin gene of an influenza virus (67) and a tRNA sequence in Sindbis virus RNA (105) or an ubiquitin-coding sequence in bovine viral diarrhea virus (99).

2.1. Mechanism of RNA recombination: Replicase driven template switch

DNA recombination progresses according to a breakage and joining mechanism, involving hetero-duplex formation of the two recombining molecules (Holliday junction). In contrast, the most accepted model for RNA recombination is a replicase-driven template switch mechanism. Here, recombinants are formed during the replication when the viral polymerases jumps or switches from one RNA template (donor RNA) to another (acceptor RNA). The strongest evidence in favor for this mechanism is provided by the work of Kirkegaard and Baltimore on homologous recombination in poliovirus (74). In this study, after super-infection of wild-type virus (guanidine sensitive and temperature resistant) with a double mutant (guanidine resistant and temperature sensitive) the production of progeny resistant to guanidine and temperature was monitored. Interestingly, co-infection in two consecutive steps resulted in the inhibition of the replication of the first virus and yielded more than 100 fold difference in the yield of recombinants depending on which restrictive factor was applied at super-infection. Specifically, the number of recombinants was high when the cells were super-infected with the wild-type virus at an elevated temperature and low when the cells were super-infected with the mutant virus in the presence of guanidine. Accordingly, such an asymmetric result could not be produced by a breaking and joining mechanism inasmuch as the parental genomes were equally abundant in each case but because of the asymmetric influence of restriction factors on RNA synthesis. Moreover, a later study showed that the frequency of recombination events increased throughout the replication cycle of the virus

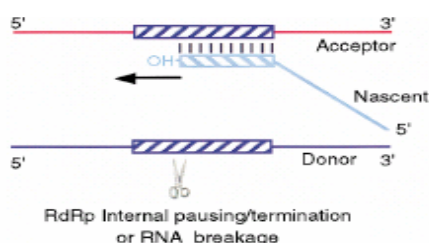
(61). The dependency of recombination on RNA replication for homologous recombination has further been confirmed in a RNA recombination system for brome mosaic bromovirus where mutations within the two virus-encoded components of the replicase influenced the frequency of recombinants (107) (110). Another piece of evidence came from the study of aberrant homologous recombination of Turnip crinkle virus, which detected non-templated nucleotides at the site of cross-over. This finding further supports the hypothesis that recombination simultaneously takes place with replication (17). Even though, this model represents the most accepted mechanism, it is still unclear if it is operative in all RNA viruses. For example, studies on Brome mosaic virus showed that mutations in the viral polymerase selectively decreased only non-homologous recombination but did not affect the frequency of homologous recombination (35). Therefore, an additional mechanism has been proposed for RNA recombination. The generation of a recombinant sequence can also be conceived via breaking the parental sequences and joining the resulting fragments. The first evidence of a nonreplicative transesterification mechanism was obtained in the in vitro Q β phage system which employed Q β phage replicase to detect replicable RNA species generated from nonreplicable RNA fragments (23). Interestingly, these studies revealed that non-homologous recombination occurred in the absence of replication while homologous recombination was observed in a control experiment, in which the same RNA fragments were incubated in the presence of dNTPs and a reverse transcriptase (112). However, the presence of Q β replicase required for amplification of the recombinant molecules did not fully exclude a replicative mechanism. Further reports of non-replicative recombination exist for picornavirus between overlapping 5' and 3' RNA fragments of the poliovirus genome (45) but in this study the 3' fragment contained the complete RdRp and therefore it could not be excluded that minimal levels of translation led to expression of the viral polymerase promoting recombination via a replicative template switch mechanism. In the genus *Pestivirus* of the family *Flaviviridae*, transfection of overlapping 5' and 3' fragments of the bovine viral diarrhea virus, each

lacking different essential parts of the viral RdRp gene yielded recombinant full-length genomes demonstrating at last the existence of a viral polymerase independent mechanism for RNA recombination (38). However, the exact mechanism remains to be elucidated.

2.2. Types of RNA recombination

Initially, RNA recombination has been typed as homologous and non-homologous. However, this definition was adapted from DNA recombination and can not easily be applied to RNA recombination. Due to the mechanism of template switching sequence pairing seems less important for facilitating recombination between RNA than between DNA molecules. Other factors such as RNA secondary structures (see below) have been described to redirect the re-initiation point of the viral replicase. This means that even though homologous sequences are present on donor and acceptor strand the point of cross-over may not be determined by sequence matches. Therefore, examination of recombination end products can be misleading, however according to current theories including the structure of intermediates and the recombination machinery the following three types of recombination have been proposed (84)(110).

2.2.1. Type I Homologous recombination or similarity essential recombination.

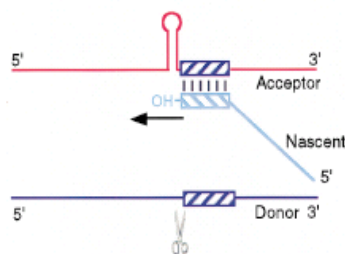


Homologous recombination occurs if substantial sequence similarity on donor and acceptor strand is provided and part of this sequence is the major determinant of the recombination event which directs the cross-over to a region of identical

sequence. The created RNA molecules retain the exact sequence and structural organization of the parental RNAs. Most of RNA recombination involving full-length viral genomes, such as recombination of picornaviruses, is of this type.

2.2.2. Type II Aberrant homologous or similarity-assisted recombination

Similar to type I recombination, there is homology between the parental RNAs of type II recombination. The difference is that cross-over does not occur at homologous or compatible sites. This imprecise template switch often leads to sequence alterations (insertion, duplication or deletions) at the site of cross-over. In addition, to sequence similarity, other factors such as RNA secondary structures can influence both the frequency and position of recombination. This type of recombination is unique to RNA recombination. It is particularly common, when defective RNAs are involved in recombination.

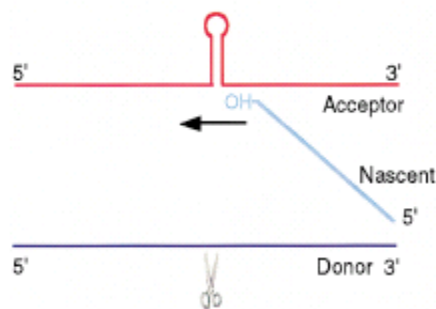


(110)

2.2.3. Type III Non-Homologous or similarity non essential recombination

Type III recombination includes events between two RNA molecules that either share no sequence homology or there is no apparent requirement for sequence similarity or identity. Type III recombination would therefore be independent of base-pairing and other factors such as polymerase binding sequences or hetero-duplex formation between parental RNAs may be involved in re-initiation of the replicase. The frequency of non-homologous recombination is

rarely reported. One explanation for this is that many recombination systems involve selection of viable or replication competent recombinant genomes. Non-homologous recombination often changes the genome structure which increases the probability of non-viable recombinants. Therefore, possible non-homologous recombinants exhibit growth deficiencies and need to further evolve to gain fitness to become detectable. Such additional adaptation often involves deletion of redundant sequences which can lead to recombinant viruses with a wild-type like genome organization which would indicate a homologous recombination event.



(110)

2.3. Factors favoring RNA recombination

2.3.1. Available data on animal viruses

In general, examination of cross-over points suggests that RNA recombination is a chance event and thus each nucleotide in an RNA molecule may serve as target for recombination (133). It has been suggested that a combination of structure and/or sequence on the donor strand that serves momentarily to slow the elongation rate of the viral polymerase can provide the kinetic window allowing the switch between templates(61). In accordance with this hypothesis, studies of recombinant inter-typic RNA virus genomes of poliovirus revealed that all identified cross-over sites were flanked by or located within RNA secondary structures and a continuous identical sequence in the cross-over region of minimal 5 nucleotides was

observed in the described homologous recombinant genomes (144)(123). Similarly, a study on mouse hepatitis virus reported the possible involvement of RNA secondary structure in recombination of coronaviruses (5). Interestingly, the frequency of homologous recombination decreased when the degree of sequence homology between co-infecting polioviruses molecules was reduced (74) (144). To gain more knowledge of the mechanism of RNA recombination, in-vitro recombination systems have been created and even though no consensus sequence has been identified to be essential for RNA recombination, a wide spectrum of RNA motifs supporting recombination or increasing its frequency have been characterized. For example, bovine viral diarrhea virus polymerase NS5B (family *Flaviviridae*, genus *Pestivirus*) was shown to be able to produce RNAs longer than template length in vitro, because of the enzyme switching template either at the 5' end or within the template RNA (73). Analysis of template sequence and RNA secondary structure revealed that the sequence within 7 nucleotides from the 5'terminus of the template (or donor) RNA could affect the frequency of recombination. While a high propensity for recombination with G-C rich base pairing near the site of cross-over was observed, no simple correlation between the recombination frequency and the number of hydrogen bonds between the template and the nascent transcript was observed, indicating the existence of other contributing factors. In addition, comparative analysis with other viral polymerases indicated that the structure/function of the replicase also greatly affects the frequency of template switch (73).

2.3.2. Lessons from plant viruses

2.3.2.1. Brome mosaic bromovirus (BMV)

Brome mosaic bromovirus genomes consists of three separate RNA molecules designated RNA1, RNA2 and RNA3. RNA1 and RNA2 encode BMV replicase proteins 1a and 2a,

respectively. RNA3 encodes movement and coat proteins. Recombinantly active mutants of RNA3 can be constructed by insertion of artificial sequences. Non-homologous recombination or recombinants with imprecise cross-over were observed after insertion of 66 nts in RNA 3 which were complementary to a respective region on RNA 1. Insertion of the corresponding region in direct orientation did not give detectable RNA1/3 recombinants (109). Further studies with this system revealed that longer heteroduplexed regions supported recombination at higher frequency than shorter ones. Also, shorter than 30 nt heteroduplexed regions did not induce RNA1/3 recombinants at detectable level (107). Analysis of homologous recombinants generated between RNA2/3 defined that 15 or longer sequence identity between RNA2 and RNA3 can support efficient, while 5 and 9nt long common regions supported only reduced levels of homologous recombination. No recombinants were detected when the common region was 4 or none. Introduction of mismatch mutations reduced the number of recombinants and at the same time caused a shift in the location of cross-overs towards the non-mutagenized portion (107). Further, AU-rich sequences were frequently detected at crossover regions and were shown to support high frequency recombination (108). In addition, the presence of GC rich sequences was shown to function as recombination enhancers (110). These observations indicated that homologous recombination is different from non-homologous recombination with respect to sequence/structure requirements. While hetero-duplex formation and strong RNA secondary structures favored non-homologous recombination, local sequence homology and AU-rich sequences played a major role in homologous recombination of brome mosaic bromovirus.

2.3.2.2. Turnip crinkle virus (TCV)

In contrast to the bromovirus family, the genome of Turnip crinkle carmovirus (TCV) is composed of a single positive-sense RNA of 4kb. The virus genome is frequently associated

with a number of subviral RNAs, including satellite, defective-interfering and chimeric RNAs (111). RNA species of the latter two groups were shown to be the products of natural recombination (17). In vivo examination of recombination between common sat RNA D and sat RNA C suggested the involvement of a hairpin structure (motif1-hairpin) on the acceptor RNA (=sat RNA C) for high frequency of recombination between these two RNAs. In-vitro studies of this process helped to develop a model which suggested that the motif1-hairpin is involved in recruitment of the RdRp during re-initiation of synthesis following template switch. In addition, a short base-paired region formed between the acceptor RNA and the nascent RNA was shown to influence the frequency of recombination (111). This suggested that according to a template switch mechanism, the viral RdRp can dissociate with the nascent transcript and then re-initiation at the motif1-hairpin is assisted by the base-paired region and 3' terminal extension is facilitated. These studies confirm the assumption that both RNA secondary structures and local sequence pairing play a role in mediating RNA recombination.

2.3.3. Involvement of host genes

Beside the obvious involvement of the viral proteins of the replication complex (107) (61) (35) in RNA recombination, several host genes were shown to influence both the occurrence and frequency of RNA recombination (132) (21). Analysis of the effect of a single-gene deletion library of *Saccharomyces cerevisiae* on recombination of a positive strand RNA virus (Family *Tombusviridae*) led to the identification of four host genes inducing recombination and five other genes inhibiting it. The genes able to suppress RNA recombination were shown to be involved in the RNA metabolism/degradation (table 1). Based on the known function of genes able to increase the frequency of recombination, the authors suggested that either a change in intracellular transport of viral and/or host proteins (or possibly protein-viral RNA complexes) to the site of recombination (PEP7 and DC11), and/or differences in the lipid

content/structure of the membranous compartment (IPK1, CH02, and DCI1), which contains the virus replicase, influences RNA recombination efficiency.

Table.1. Names and functions of host genes affecting RNA recombination

Gene	Molecular function/biological process
	<i>Supressors</i>
CTL1	Polynucleotide 5'-phosphatase
MET22/HAL2	3'(2'),5'Bisphosphate nucleotidase
HUR1	unknown
XRN1	5'-3' exoribonuclease
UBP3	Ubiquitin-specific protease
	<i>Accelerators</i>
PEP7/VPS19	Unknown/Golgi to vacuole transport
IPK1	Inositol/phosphatidylinositol kinase
CHO2/PEM1	Phosphatidylethanolamine N-methyltransferase
DCI1	Dodecenoyl-CoA Δ -isomerase

2.4. Generation of defective interfering RNA (DI RNA)

Not all RNA viruses have been shown to be able to undergo intermolecular RNA recombination (i.e. Vesicular stomatitis virus, West Nile virus, Tick-borne encephalitis virus, Newcastle disease virus and RNA phages). However, nearly all RNA viruses generate recombinant subgenomic deletion particles designated defective interfering particles (DI particles). These RNA genomes retain all cis-acting regulatory sequences required for replication and packaging of the RNA, but their replication depends on enzymes and structural proteins provided by infectious helper virus. Notably, their replication interferes with closely related viruses able to act as helpers (121). DI RNAs are most efficiently generated under conditions in which many infectious virus genomes simultaneously infect the same cell (55). It has been suggested that DI RNAs arose by intermolecular recombination according to the copy choice model (17)(116)(87) (King, A.M.Q. 1988. Genetic recombination in positive strand RNA viruses, p150-185. In E. Domingo, J.J. Holland, and P.

Ahlquist (ed.), RNA genetics II. CRC Press, Inc., Boca Raton Fla.). One obvious example is the generation of DI RNA of Sindbis virus, in which tRNA sequences are incorporated at the 5' terminus of the virion RNA (146). Some satellite RNAs of TCV (discussed above) also contain nonviral sequences of unknown origin (17). Further, structural analysis of a DI RNA of influenza virus supports the hypothesis of intermolecular recombination for its generation (34). The analyzed RNA has been shown to consist of several discontinuous regions, some of which were derived from RNA-1 and others from RNA-3. Thus, it may represent a true recombinant RNA between two different RNA molecules, although both RNAs belong to the same virus. Moreover, it was shown that coronavirus recombination occurred more frequently within a hypervariable region (5), in which deletions commonly occur after virus passage in tissue culture or animals. Thus, the same RNA secondary structure, i.e. strong stem-loop structures, may be responsible for both deletions (intramolecular) and recombination (intermolecular) by causing a pause in RNA transcription. In conclusion, the generation of DI RNA, the occurrence of deletions, insertions or duplication as well as true recombination of viral genomes may all be linked to the model of template switch, in which the viral polymerase jumps either within or between the same (intramolecular) or between different (intermolecular) templates of replication.

2.5. The extent of recombination in the family Flaviviridae

2.5.1. Genus Flavivirus

Most phylogenetic evidence indicates that evolution of Flaviviruses is clonal, with diversity generated largely by the accumulation of point mutations rather than recombination events (46). However, some sequence-based phylogenetic studies have suggested the occurrence of homologous recombination among strains of the same viral species. Several recent

publications have identified recombinant Flaviviruses by computational sequence analysis of viral isolates from infected patients. These studies suggested that homologous recombination had occurred between closely related virus strains of all four dengue virus serotypes (57)(143)(1), JEV (147) and St. Louis encephalitis virus (147). However, there is a complete lack of direct experimental evidence for Flavivirus recombination occurring in, for example, double-infected cells or animals.

The controversy over whether or not Flavivirus genomes can recombine carries significant practical importance. A commentary by Seligman and Gould published in the *Lancet* (130) warned against the use of live Flavivirus vaccines because of the danger of creating new chimeric viruses with unpredictable biological properties if recombination occurs with other Flaviviruses that circulate in the environment and accidentally infect vaccinees. This report caused a stir among scientists and health officials because live Flavivirus vaccines (e.g. against YFV) are an invaluable and much-needed tool to combat life-threatening diseases (103). Several studies have provided at least indirect evidence that the propensity of Flavivirus RNA to undergo homologous recombination is low or nonexistent. Recombination events were not observed in any trans-complementation packaging studies in which replication competent defective virus genomes can be packaged by in-trans expressed structural proteins. These systems include expression plasmids, cell lines that have been modified to constitutively express Flavivirus structural proteins and alphavirus-based expression systems. However, since recombination may depend on Flavivirus RNA replication, the fact that the structural proteins in these systems were expressed either from cellular mRNAs or alphavirus-derived mRNAs, could mean that the necessary conditions for recombination were not provided in these experiments. In another study, replication-deficient Flavivirus genomes carrying disabling mutations in one of the non-structural proteins were successfully complemented by replicating helper RNA, leading to the production of single-round-infectious particles (68). Although recombination was not observed under these

conditions either, the experimental design of this study probably would not have allowed low-frequency events to be detected. No experimental studies with the purpose of achieving inter-species recombination have been described so far.

On the other hand, several studies have shown that Flavivirus genomes can spontaneously acquire deletion or sequence-duplication mutations (33)(80). Such mutations are thought to occur by a mechanism in which the RNA polymerase falls off from the template and re-initiates synthesis at a site further upstream or downstream. A similar event is assumed to occur during recombination of RNA, when the polymerase dissociates from the first template and then continues synthesis from a different template (see above Generation of DI RNA). The observation that spontaneous deletions and duplications readily occur provides indirect evidence that the Flavivirus replication complex is capable of undergoing processes of the kind that can lead to recombination.

2.5.2. Genus Pestivirus

In the case of pestiviruses, such as bovine viral diarrhea virus, heterologous RNA recombination is frequently observed in nature and is responsible for changes in viral pathogenicity (99, 100). RNA recombination was first observed in connection with the molecular characterization of cytopathogenic (cp) BVDV strains that are involved in the induction of lethal mucosal disease in cattle (14). Further studies of cp pestiviruses revealed that most cp strains evolved from persisting non-cp viruses by recombination (100). As a result, cp pestiviral genomes harbor genomic alterations that frequently include insertions of cellular mRNA or viral sequences as well as deletions or duplications of viral sequences (10, 12)(99, 100). In cell culture passages such cp strains were shown to lose the phenotype altering sequences by reverting to non-cp viruses (11)(7). Both homologous and non-homologous recombination mechanisms - the latter being more frequent - have been

described in this context. Surprisingly, under laboratory conditions, recombination has been demonstrated with BVDV even with non-replicating defective virus genomes suggesting a polymerase independent recombination mechanism (for comparison, see the above chapter on “Mechanism of RNA recombination”) (38).

2.5.3. Genus Hepacivirus

The genus *Hepacivirus* consists of only one established species Hepatitis C virus (43) , which is classified into six genotypes and several additional subtypes. Similarly to the genus *Flavivirus*, recombination in the genus *Hepacivirus* has been demonstrated only indirectly by phylogenetic analysis of different isolates. By such means, intra-genotypic (27)(26) as well as inter-genotypic (63) homologous recombinant viruses were identified. Despite these findings and the frequent co-detection of multiple genotypes in patients (64)(59)(29) the available data suggests that RNA recombination plays only a minor role in the evolution of HCV. In one study, only one out of 89 analyzed sequences turned out to be a recombinant virus (27). In another study, monitoring of HCV co-infected patients failed to detect recombinant viruses, even though some patients were infected with the same subtype (13).

2.6. Recombination in other positive stranded RNA virus families

2.6.1. Picornaviruses

The family *Picornaviridae* comprises several important pathogens, such as poliovirus or foot-and-mouth-disease virus. Poliovirus is the best studied virus regarding RNA recombination. It has been shown to exhibit the highest rate of homologous recombination ($10^{-5}/nt$ or 1% for every 1700nts) (22), but non-homologous recombination was suggested to be almost equally

efficient (82). Frequent detection of recombinant viruses after vaccination with polio vaccine strain raised the issue of the stability and safety of the vaccine (16)(101). Generally, recombination occurred more readily between more closely related picornaviruses and was shown to decrease as the genetic relationship diverged. However, this may only reflect the greater probability of viable recombinant genomes between closely related viruses rather than the influence of homologous sequences on the actual recombination frequency.

2.6.2. Coronaviruses

Coronaviruses contain a positive-sense RNA genome that is unusually large (31kb), which is almost twice the size of the next largest viral RNA (paramyxovirus). The discovery of RNA recombination of murine hepatitis coronavirus (MHV) was the first proof that also other RNA viruses than picornaviruses are capable of this mechanism (85). Studies indicated that similar to picornaviruses, coronaviruses can recombine at high frequency because the isolated recombinant viruses showed evidence of multiple cross-overs, sometimes even outside of the selection markers (66)(65)(94). The estimated rate of recombination was as high as for picornaviruses (10^{-5} /nt or 1% for every 1700nts) (88). Recombination mapping of cross-over sites of MHV revealed that the recombination frequency was higher near the 3' end, indicating a possible involvement of subgenomic mRNAs in recombination (36, 37). So far, only homologous recombination has been detected between coronaviruses. The absence of non-homologous recombination in coronaviruses may reflect their rigid viral RNA or protein structure requirements for optimal viral growth.

2.6.3. Alphaviruses

In contrast to picorna- and coronaviruses, homologous recombination in alphaviruses seems to be uncommon concerning data obtained from recombination studies under laboratory conditions (150)(51). Only one study also identified homologous recombinants in the lab (120). Intriguingly, a homologous recombinant virus was discovered in nature. Recombination between Eastern equine encephalitis virus and a virus related to Sindbis virus resulted in the lineage of Western equine encephalitis virus (50). Interestingly, one of the putative crossover sites in WEEV RNA was located in the middle of the structural protein-coding region, such that the structural proteins of WEEV have two different origins, with the capsid protein gene being derived from EEV and the rest of the structural proteins being derived from Sindbis virus.

2.7. Recombination in negative stranded RNA virus families

Little is known about the recombination mechanism of negative stranded RNA viruses because the available data was almost exclusively obtained by phylogenetic analysis of isolated genome sequences. Recombinant viruses have been reported in arenavirus (4) and (20), hantavirus (75), (136), influenza A virus (44), measles virus (126), and Newcastle disease virus (HN gene) (19). Generally, negative-sense RNA viruses have lower rates of recombination than positive-sense RNA viruses (119). This assumption is supported by a single report of RNA recombination under experimental conditions for a nonsegmented negative strand RNA virus (respiratory syncytial virus) (138). In a classical co-infection experiment with different marker mutations and consecutive plaque purification only one recombinant virus was detected. The genome of the recombinant virus was generated by double cross-over between the parental viruses involving non-homologous as well as homologous recombination events (138).

2.8. Recombination of Retroviruses

The fact that retrovirus particles contain two copies of the RNA genome and that transcription makes use of both RNAs results in an extraordinary high propensity for recombination (141)(58). Estimates for the recombination rate of HIV in vivo are as high as 1.4×10^{-4} recombination events / site / generation, which is about fivefold greater than the average point mutation rate (134). Recombination is believed to occur during the reverse transcription process according to the template switch mechanism of the copy-choice model. Intriguingly, recombination predominantly occurs between co-packaged RNA genomes and co-infection with two different viruses does not yield a high number of recombinants. This suggests that each particle provides its own reverse transcriptase and the copied RNA genomes are not freely exchanged with other RT-reactions in the cytoplasm of the same cell. This compartmentalization of the replication location is also observed for many other RNA viruses replicating in the cytoplasm. In this context it is important to note that host genes involved in the induction or maintenance of membranous structures were shown to influence the frequency of recombination. In conclusion, the physical separation of RNA genomes from different virus particles within a cell may pose a critical constraint on the occurrence of recombination of other “haploid” RNA viruses replicating in the cytoplasm.

AIMS

This thesis addresses two fundamental issues that underlie the biology of flaviviruses: Recombination among flavivirus genomes and determinants of flavivirus genome packaging. These two main objectives can be subdivided into four individual goals.

Goal 1: Establishment of a reciprocal trans-complementation system

The reciprocal trans-complementation system will involve two different replicons, each lacking part of the structural protein coding region, which is, however, present in the other one, will be simultaneously introduced into the same host cell. Together, the two replicons will express all of the structural components necessary for particle formation. Replication of both replicons in the same cell will lead to the expression of all of the components necessary for particle production. This will allow to study whether the replicons can be packaged and released in the form of single-round-infectious virus like particles (VLPs). Transfer onto fresh cells of supernatants containing sufficient concentrations of VLPs to allow double infections of cells with VLPs containing both replicons may again lead to VLP production, and these passages will be repeated as many times as desired.

Goal 2: Assessment of the propensity for intermolecular recombination

Replication of two complementary replicons may lead to recombination between the two complementing genomes, yielding a full-length infectious virus genome. In contrast to the replicon-containing VLPs, the recombined infectious virion will not depend on double infections of cells for its propagation and can thus be enriched by subsequent cell culture passages. After several limiting dilution passages, it is anticipated that a recombined virus will have completely outgrown the two parental replicons and can be characterized by standard techniques (Northern blot, PCR, sequence analysis). Complementing replicons of three

different flaviviruses, TBEV, JEV and WNV will be tested in this “recombination trap”. If recombination to infectious viruses is observed, the recombined genomes will be tested for infectivity and growth properties will be assessed in vector and host cells.

Goal 3: Study of other mechanisms involved in adaptation of flaviviruses

If no recombination to infectious viruses is observed, the defective viruses involved in the reciprocal trans-packaging system will be analyzed and tested for adaptive mutations. Such mutations may include point mutations, deletions or generation of defective interfering RNAs. Analysis of these mutations on the efficiency of the reciprocal packaging will allow new insights into flavivirus packaging. Further, it will be interesting to observe whether the defective viruses show a greater propensity for intermolecular recombination to infectious viruses than for intramolecular changes.

Goal 4: Analysis of capsid in flavivirus packaging. An internal hydrophobic sequence within the flaviviral capsid protein was shown to play an important role in the assembly of infectious TBEV and YFV virions. To systematically test the functional role of hydrophobic residues and to define common features of the flavivirus capsid various deletions ranging from 4 to 14 amino acids will be introduced into the capsid protein of WNV. Resuscitating mutations will be selected in cell culture passages and will allow insights into the basic requirements of the nucleocapsid for flavivirus packaging.

Manuscript 1

A *trans*-Complementing Recombination Trap Demonstrates a Low Propensity of Flaviviruses for Intermolecular Recombination

Christian Taucher¹, Angelika Berger¹ and Christian W. Mandl^{12*}

1 Institute of Virology, Medical University of Vienna, Vienna, Austria

2 Present address: Novartis Vaccines and Diagnostics, Inc., Cambridge, MA, USA

*Corresponding Author

Christian W. Mandl

Institute of Virology

Medical University Vienna

Kinderspitalgasse 15

A-1095 Vienna, Austria

Tel:+43 1 40490 79500, Fax: +43 1 404909795

E-mail: christian.mandl@meduniwien.ac.at

Author Contributions

CT and CWM conceived and designed the experiments. CT and AB performed the experiments. CT and CWM analyzed the data. CT and CWM wrote the paper.

Abstract

Intermolecular recombination between the genomes of closely related RNA viruses can result in the emergence of novel strains with altered pathogenic potential and antigenicity. Although recombination between flavivirus genomes has never been demonstrated experimentally, the potential risk of generating undesirable recombinants has nevertheless been a matter of concern and controversy with respect to the development of live flavivirus vaccines. As an experimental system for investigating the ability of flavivirus genomes to recombine, we developed a "recombination trap", which was designed to allow the products of rare recombination events to be selected and amplified. To do this, we established reciprocal packaging systems consisting of pairs of self-replicating subgenomic RNAs (replicons) derived from tick-borne encephalitis virus (TBEV), West Nile virus (WNV), and Japanese encephalitis virus (JEV) that, due to different deletions in the region encoding their structural proteins, individually lacked the ability to produce infectious virions but could complement each other *in trans* and thus be propagated together in cell culture over multiple passages. Any infectious viruses with intact, full-length genomes that were generated by recombination of the two replicons would be selected and enriched by endpoint-dilution passage, as was demonstrated in a spiking experiment. Using the recombination trap, we detected two aberrant recombination events using the JEV system, both of which yielded unnatural genomes containing duplications. Infectious clones of both of these genomes yielded viruses with impaired growth properties. Despite the fact that the replicon pairs shared approximately 600 nucleotides of identical sequence where a precise homologous crossover event would have yielded a wild-type genome, this was not observed in any of these systems, and the TBEV and WNV systems did not yield any viable recombinant genomes at all. Our results show that intergenomic recombination can occur with flaviviruses but that its

frequency appears to be very low and therefore probably does not represent a major risk in the use of live attenuated flavivirus vaccines.

Author Summary

Effective live vaccines against the flaviviruses yellow fever virus and Japanese encephalitis virus have been in use for decades, and tetravalent live vaccines against dengue viruses are currently undergoing clinical testing. Recently, concerns that flavivirus strains might have the potential to exchange genetic information by recombination – and generate new strains with undesirable properties – have led some researchers to question the safety of using live flavivirus vaccines. In the present study, we have developed a "recombination trap", a sensitive experimental system for studying flavivirus recombination. This system consists of a pair of defective viral genomes, so-called replicons, that are mutually dependent because each provides the other with an essential protein required for making virus particles. The replicons are propagated together in cell culture for multiple generations under conditions that favor the positive selection of any viable virus particles that might arise due to recombination. Surprisingly, we observed not a single homologous recombination event using recombination traps designed for three different flaviviruses, tick-borne encephalitis virus, West Nile virus, and Japanese encephalitis virus (JEV). With JEV, however, we twice observed the generation of a recombinant virus with an unnatural genome organization that had arisen through a more random process known as aberrant homologous recombination. These viruses were impaired in their growth properties. This is the first time that recombination of flavivirus genomes has been observed in the laboratory. Our data suggest that homologous recombination occurs infrequently, if at all, with flaviviruses and therefore probably does not represent a major risk when using live flavivirus vaccines.

Introduction

RNA viruses are able to undergo rapid genetic changes in order to adapt to new hosts or environments. Although much of this flexibility is due to the error-prone nature of the RNA-dependent RNA polymerase, which generates an array of different point mutations within the viral population (62), recombination is also a common and important mechanism for generating viral diversity (55, 84, 110, 153). Recombination occurs when the RNA-dependent RNA polymerase switches templates during replication -- an event that is favored when both templates share identical or very similar sequences. Three types of RNA recombination have been identified: homologous recombination occurs at sites with exact sequence matches; aberrant homologous recombination requires sequence homology, but crossover occurs either upstream or downstream of the site of homology, resulting in a duplication or deletion; and non-homologous (or illegitimate) recombination is independent of sequence homology (84, 110).

When the same cell is infected by viruses of two different strains, or even different species, recombination between their genomic RNAs can potentially lead to the emergence of new pathogens. A case in point is the emergence of western equine encephalitis virus (WEE), a member of the genus *Alphavirus*, family *Togaviridae*, which arose by homologous recombination between eastern equine encephalitis virus and Sindbis virus (50).

Some mammalian RNA viruses can recombine at a frequency that is detectable in experimental settings (6, 8, 150), and phylogenetic analysis of partial or complete genome sequences suggests that RNA recombination is a widespread phenomenon. Naturally occurring recombinant viruses have been identified in almost every family of positive-stranded RNA viruses (84, 153).

RNA recombination is increasingly being recognized as an important parameter to consider in the development of vaccines containing live attenuated viruses (153). Experience

with live poliovirus vaccines has already shown that new strains can indeed arise in vaccinees due to recombination between vaccine strains, and possibly between vaccine strains and other viruses (16, 28). The potential hazards of homologous recombination events involving live vaccine strains has become a concern and an obstacle to the development of flavivirus vaccines. Flaviviruses are members of the genus *Flavivirus*, family *Flaviviridae*, a family which also includes the genera *Pestivirus* and *Hepacivirus*. Several of the flaviviruses are important human pathogens, such as Japanese encephalitis virus (JEV), West Nile virus (WNV), the dengue viruses, yellow fever virus, and tick-borne encephalitis virus (TBEV).

Live vaccines for the prevention of some flaviviral diseases are already in widespread use. Vaccines containing the live yellow fever virus strain 17D, one of the first viral vaccine strains ever developed, have been in continuous use since the 1950s, with over 500,000 administered doses per year (124). A live vaccine against JEV containing the attenuated strain SA-14-14-2 has been widely used in China since 1988 and also shows an excellent safety record so far (91).

Although there has never been a report of a pathogenic flavivirus strain arising due to recombination involving attenuated vaccine strains (103), the urgent necessity to develop tetravalent vaccines containing all four serotypes of dengue virus – two such vaccines are currently undergoing clinical testing (125) -- has recently brought the recombination issue to the forefront of discussion among researchers, regulators, and vaccine producers (103). It has been suggested that recombination, either between the strains present in a multivalent vaccine or between an attenuated vaccine strain and a wild-type strain, could lead to the emergence of new viruses with unpredictable properties (130).

So far, recombination between flavivirus genomes has not been demonstrated directly in the laboratory. However, phylogenetic analysis of partial genome sequences available in the GenBank database has suggested that homologous recombination may have occurred between closely related strains of dengue virus (57, 143, 148, 154), JEV (147), and St. Louis

encephalitis virus (147). An experimental approach for assessing the ability of flavivirus genomes to recombine is therefore urgently needed.

Flavivirus virions are composed of a single-stranded, positive-sense RNA genome that is packaged by the capsid protein C into a nucleocapsid. The nucleocapsid is covered by a lipid envelope containing the surface glycoproteins prM and E. These glycoproteins drive budding at the membrane of the endoplasmic reticulum (ER) during the assembly stage and mediate entry of the virus into host cells (106). Replicons, defined as self-replicating, non-infectious RNA molecules, can be generated by deleting parts or all of the region coding for the structural proteins C, prM, and E from the viral genome but maintaining all seven of the nonstructural proteins and the flanking noncoding sequences, which are required *in cis* for RNA replication (76). By providing the missing structural protein components *in trans*, replicons can be packaged into virus-like particles that are capable of a single round of infection (41, 52, 71, 128).

Typically, researchers developing novel replicating vaccines, especially ones that involve multiple components, make an effort to come up with strategies to prevent recombination, for example by "wobbling" codons, i.e., replacing codons in homologous regions with synonymous ones encoding the same amino acid but consisting of a different nucleotide triplet (135, 152). In this study, in order to assess the propensity of flavivirus genomes to recombine, we took an opposite approach, establishing a "recombination trap" that favors the selection and sensitive detection of recombination products. This system takes advantage of the ability of replicon pairs containing deletions in their structural protein genes to complement each other *in trans* and thus be propagated together in cell culture, and by passage at limiting dilution, it allows infectious RNA genomes arising by recombination between the two replicons to be preferentially selected.

Using the recombination trap, we have now obtained the first direct evidence of recombination between flavivirus genomes in the laboratory. Aberrant homologous

recombination was observed twice with JEV replicons, resulting in viruses with unnatural gene arrangements and reduced growth properties compared to wild-type JEV. No infectious recombinants of any kind were obtained when TBEV or WNV replicons were used. Interestingly, we never detected a fully infectious wild-type genome arising by homologous recombination in any of these systems. The results of this study show that the propensity of flavivirus genomes to recombine appears to be quite low and suggest that recombination does not represent a major risk in the use of live attenuated flavivirus vaccines.

Results

Establishment of a reciprocal packaging system

As a tool for testing the propensity of flaviviruses for recombination, we established a reciprocal packaging system to allow the co-cultivation of two different defective viruses for prolonged passages. This system consisted of two replicons, each of which contained a deletion in a region of the RNA genome that encodes structural proteins that are essential for virus assembly. Individually, each of these replicons was incapable of forming infectious virus particles due to the lack of an essential component for virion assembly, but when present together in the cytoplasm of the same cell, they were capable of complementing each other *in trans*, thus allowing each of the defective genomes to be packaged and propagated as single-round infectious (or pseudoinfectious) particles and allowing co-passage of these replicons in cell culture. By conducting passages at limiting dilution, functional revertant wild-type virus genomes resulting from recombination between the two replicons could potentially be selected and enriched.

To set up the two-component trans-complementation system, we took advantage of two previously described and characterized TBEV replicons called ΔC (78) and ΔME -eGFP (42). As shown in Fig. 1, replicon ΔC consisted of a full-length TBEV genome containing a 186-bp deletion in the region encoding the capsid (C) protein, and ΔME -eGFP lacked the entire region encoding the envelope proteins prM and E. In addition, ΔME -eGFP contained an additional artificial cistron inserted in the 3' noncoding region (3' NCR) that allowed the expression of the enhanced green fluorescent protein (eGFP) under the control of an IRES element.

To test the ability of these replicons to complement each other and to be packaged into infectious particles, BHK-21 cells were first transfected with each of the *in vitro*-synthesized, capped replicon RNAs, either individually or in combination. Transfected cells containing

replicon ΔC were identified using an immunofluorescence assay with a monoclonal antibody recognizing the envelope protein E, which was expressed in ΔC but not in ΔME -eGFP. Using a rhodamine-conjugated secondary antibody for detection, the cells containing ΔC RNA appeared red under the fluorescence microscope (Fig. 2, left), as did control cells infected with the full-length wild-type (WT) genomic RNA, which also expressed the E protein. Transfected cells containing replicon ΔME -eGFP appeared green under the fluorescence microscope.

When BHK-21 cells were transfected by electroporation with an equal mixture of the two replicons (Fig. 2, bottom left), it was observed one day after transfection that some cells were positive for eGFP (green cells), some for E (red cells), and some for both (yellow cells in the merged image), indicating that they contained both ΔC and ΔME -eGFP.

Supernatants from each of the transfected cell cultures were then applied to fresh BHK-21 cells, and the cells were tested 24 h later for the presence of E and eGFP (Fig. 2, right). After one passage, the cells treated with the supernatant from the cotransfected culture (ΔC + ΔME -eGFP) again showed a mixed pattern of green, red, and yellow cells, indicating that each of the replicons had been packaged into infectious particles and that a subset of the cells had been coinfecting with both replicons. As expected, the supernatants from cells transfected with defective ΔC or ΔME -eGFP RNA alone apparently did not produce infectious particles, and these replicons could not be propagated further. Also as expected, the supernatants from the positive control cells that had been transfected with full-length infectious genomic RNA (WT) were able to infect fresh cells, as indicated by positive red staining for the viral E protein (Fig. 2, top right).

In this passage experiment, the presence of cells containing both ΔC and ΔME -eGFP suggested that the frequency of coinfection was high enough to enable a further round of trans-complementation and packaging of replicon RNAs. To test this, the supernatants from passage 1 were again transferred to fresh cells, and, as shown in Fig. 2 (bottom right, "Passage

2"), a similar pattern was observed, with cells containing ΔC , ΔME -eGFP, or both. These experiments demonstrate that replicons ΔC and ΔME -eGFP, when used together, constitute a reciprocal packaging system that can be propagated in cell culture by serial passage.

Analysis of individual foci

Next, we infected fresh BHK-21 cells with various dilutions of supernatants containing the mixture of packaged ΔC and ΔME -eGFP replicons, added a methylcellulose overlay, and fixed and stained the cells 50 hours later using an anti-TBEV polyclonal antibody and an alkaline-phosphatase-conjugated secondary antibody to detect the formation of infectious foci. As shown in Fig. 3A, the mixture of packaged replicons formed foci that were smaller than those formed by wild-type TBE virus, demonstrating that the ability of infectious material to spread from replicon-containing cells was impaired compared to that of the virus control. Furthermore, unlike wild-type virus, which showed a linearly proportional decrease in the number of plaques formed with increasing dilution, the number of foci formed with the packaged replicon mixture decreased very sharply with increasing dilution (data not shown). This sensitivity to dilution is consistent with what would be expected if two particles, one containing ΔC and the other containing ΔME -eGFP, were required to make one infectious unit (i.e., one focus-forming unit).

To examine the foci more closely, cells were again infected with different dilutions of the ΔC and ΔME -eGFP mixture and overlaid with nitrocellulose as above, but instead of staining with polyclonal serum and alkaline phosphatase, the cells were fixed and prepared for detection of E and eGFP by fluorescence microscopy as described in the previous section. An example of a typical focus formed by infection with a mixture of packaged ΔC and ΔME -eGFP replicons at high dilution is shown in Fig. 3B. In the merged images, each of these foci could be seen to consist of a mixed population of cells, some of which were green (ΔME -eGFP), some red (ΔC), and some yellow ($\Delta C + \Delta ME$ -eGFP), similar to what was observed

earlier in confluent monolayers shown in Fig. 2. This means that each of the foci was formed by infection of neighboring cells by particles containing ΔC or ΔME -eGFP RNA, or by both types of particles simultaneously. Importantly, examination of more than 100 individual foci in this manner did not reveal any that consisted of only red-stained E-protein-producing cells, which would have been expected if a wild-type revertant virus had arisen in the population due to recombination between the replicons.

Competition between replicons and full-length viral genomes

In contrast to the defective replicon-containing particles, a fully infectious virion carrying a full-length genome would not depend on multiple infection of the same cell for its propagation, and if it were present in the population, it could be enriched by subsequent cell culture passages at high dilution. To test this principle experimentally, we carried out an experiment similar to the ones described above, except this time we spiked the mixture of packaged replicons with 10 focus-forming units (ffu) of wild-type TBE virus to see whether the full-length genome would eventually become dominant after serial passage at limiting dilution. For this experiment, however, instead of ΔME -eGFP, we used a replicon called ΔME (41), which was identical to ΔME -eGFP except that it had a normal viral 3' end and lacked the artificial cistron encoding eGFP (Fig. 1). Lysates of infected BHK-21 cells were analyzed after the initial infection and after three endpoint-dilution passages by northern blotting using a probe recognizing the nonstructural region of the genome. As shown in Fig. 4A, the replicons were initially detected after infection, but after the three passages, only a single band was observed, corresponding in size to the full-length genome. The presence of the wild-type virus genome replacing the two replicons was confirmed by a set of RT-PCRs (Fig. 4B) and sequencing (not shown). RT-PCR 1 was specific for the wild-type sequence, whereas RT-PCRs 2 and 3 yielded specific bands for replicons ΔC and ΔME , respectively, as well as a larger band for the wild-type RNA. After three passages, only the products specific for the

wild-type sequence were obtained by all three RT-PCR assays (Fig. 4B). This experiment thus showed that the full-length viral genome had displaced the replicons during passage in cell culture and demonstrates that this system can be used as a "recombination trap" for selecting potential wild-type revertants within the population of replicating RNAs.

Application of the recombination trap

The replicon constructs used in the previous set of experiments for establishing the reciprocal packaging system, although identical in the region encoding the nonstructural genes, contained only a small stretch of 27 identical nucleotides between the C and prM genes where a single homologous recombination event could result in the creation of a full-length genome by restoring the missing capsid gene in ΔC (Fig. 1). Therefore, in order to increase the likelihood of such an event, we constructed a new replicon to use in place of ΔME that increased the region of identical sequence between the deleted regions. This construct, called ΔE , had all of the E gene deleted (nt 973-2460) but retained the entire prM gene as a 572-nt region of common sequence identity where homologous recombination with ΔC could potentially take place (Fig. 1). In addition to the TBEV constructs, we also made analogous ΔC and ΔE replicons using genomic clones of the mosquito-borne flaviviruses West Nile virus (WNV) and Japanese encephalitis virus (JEV) (Fig. 1).

The recombination trap was then put to use by cotransfecting BHK-21 cells with the TBEV, WNV, and JEV ΔC and ΔE replicon pairs and carrying out multiple endpoint-dilution passages to favor the selection and enrichment of any viruses with full-length genomes that might arise by recombination. Full-length infectious clones of each virus were used as controls. After 10 endpoint passages, intracellular RNA was analyzed by gel electrophoresis and northern blotting with virus-specific probes (Fig. 5A). As expected, each of the full-length, wild-type controls yielded a single major band. In the case of TBEV, transfection with ΔC together with ΔME or ΔE resulted in two major bands (Fig. 5A, left panel, lanes 3 and 4)

that corresponded in size to the original replicons (lanes 5, 6 and 7), suggesting that the two original replicons had been co-passaged and maintained throughout the entire 10 passages. Likewise, cotransfection of ΔC and ΔE from WNV also yielded both replicon bands (Fig. 5A, middle panel, lane 3).

In contrast to these results, however, in the case of JEV, northern blotting revealed only a single band after passage of the $\Delta C + \Delta E$ pair, suggesting that the replicons were not propagated as a pair and that a recombination event might have occurred. This phenomenon was observed in two completely separate experiments. Northern blot analysis of earlier passages indicated that replacement of the original pair of replicons with the new band had already occurred in the third and fifth passage, respectively (data not shown). The relative positions of the bands in the gel suggested that the final RNA recombination products were not identical in size in the two experiments (Fig. 5A, right panel, lanes 3 and 4).

As a more sensitive and precise means of assessing whether recombinant RNA molecules were present in the population, we devised RT-PCR assays for detecting the restoration of deleted regions of the TBEV, WNV, and JEV genomes (see Materials and Methods). In these assays, neither of the original replicons could be amplified due to the lack of one of the primer-binding sites, but recombinants containing both of these sites would yield a PCR product. As shown in Fig. 5B, in the case of TBEV and WNV (left and middle panels, respectively), the RT-PCR assay yielded a product in the case of the WT control, but not with the passaged replicon pairs, indicating that no detectable reversion to wild-type TBEV or WNV had occurred via inter-replicon recombination. With JEV, however, a clearly different situation was observed (Fig. 5B, right panel). Positive RT-PCR results were obtained not only with the WT control (lane 1) but also with the combination of ΔC and ΔE in the two separate experiments (lanes 3 and 4). The first of these PCR products (lane 3) appeared to be larger than the one obtained using the wild-type genome, whereas the second (lane 4) was approximately the same size. These results provided positive evidence that recombination

events had indeed occurred with the JEV system. Other RT-PCR assays that were designed to detect the original replicons (see Materials and Methods) failed to yield detectable amplification products from the passaged JEV samples, indicating that both replicons had been completely displaced by the new recombinant in both of these experiments (data not shown).

These newly selected recombinant genomes were then reverse-transcribed and sequenced. Both of them were found to contain all of the components of the JEV genome, but neither corresponded in its arrangement to a wild-type genome. Recombinant 1 (Fig. 6A, top), which was obtained in experiment 1, was composed of replicon ΔE sequence from its 5' end up to nt 2761 and still included the original deletion of nt 978 to 2477 in the E gene. The remainder of the genome was derived from replicon ΔC and included the entire region extending from the beginning of prM to the 3' terminus, thereby resulting in an aberrant genome containing a partial duplication of the NS1 region and a complete duplication of the prM region between prM and E. Recombinant 2 (from experiment 2) resembled the wild-type JEV except that it contained a tandem duplication of nucleotides 393-455, corresponding to the NS2B/3 protease cleavage site between C and prM (Fig. 6A, bottom).

Growth properties of JEV recombinants

To characterize their biological properties, infectious clones of the recombinant 1 and recombinant 2 genomes were made as described in Materials and Methods. Full-length RNA was synthesized from these templates and used to transfect BHK-21 cells, which in turn released infectious particles into the cell supernatant. These viruses were then characterized by testing them in a standard plaque assay using Vero cells and by carrying out a multistep growth curve experiment using both BHK-21 cells and the mosquito cell line C6/36.

The plaque morphology produced by these viruses in Vero cells is shown in Fig. 6B. It was observed that the recombinant 1 virus produced large plaques that looked similar to those

produced by wild-type JEV. The recombinant 2 virus, on the other hand, produced small plaques, suggesting that this virus was impaired in its ability to spread to other cells.

The growth curves shown in Fig. 6C, performed using an MOI of 0.01, show that both recombinants had impaired growth properties compared to wild-type JEV. Recombinant 2 grew extremely poorly in BHK-21 cells, whereas the growth rate of recombinant 1 was only moderately reduced compared to wild-type JEV. However, the titer of recombinant 1 fell sharply after two days due to a strong cytopathic effect (CPE). In C6/36 cells, both of the recombinants grew about an order of magnitude more slowly than the wild type, and recombinant 1 did not produce an unusually strong CPE in these cells.

These results suggest that although passage at limiting dilution apparently gave the two aberrant full-length recombinant forms of JEV a growth advantage over the original replicon pair, their growth properties would not have allowed them to prevail over a wild-type virus, had one been present in the population. We therefore conclude that although aberrant recombination events did occur in the JEV system, a normal wild-type revertant was not produced by a simple homologous crossover in any of the experiments with JEV, WNV, or TBEV.

Discussion

Using a “recombination trap”, an experimental system designed to detect even rare recombination events between two self-replicating RNA molecules, we analyzed the propensity for intermolecular recombination of three flaviviruses, TBEV, WNV, and JEV. The inclusion of long overlapping regions between the two trans-complementing replicons in our recombination trap provided ample opportunity for homologous crossover events to generate recombinants with wild-type genomes. Surprisingly, however, no such event was detected in any of the three flaviviral systems, even after prolonged co-passaging, indicating

that exact homologous recombination occurs rarely, if at all, with these viruses. However, we did detect two aberrant recombination events in the JEV system, each of which gave rise to infectious virus progeny with an unnatural genome organization and an impaired growth phenotype.

The potential for unwanted recombination has been a topic of considerable controversy in the context of live flavivirus vaccine and vector development. Until now, the only evidence for flavivirus recombination has been inferred from sequence data from certain natural isolates (56, 57, 143, 147, 148). However, there has been a lack of general agreement about the significance of these observations, and due to the lack of appropriate experimental systems, it has not yet been verified under laboratory conditions that flavivirus genomes actually recombine. The recombination trap described here provides for the first time a sensitive system to address this issue experimentally, and the results obtained using this system represent the first direct observation of recombination between replicating flavivirus-derived RNA molecules in the laboratory. From this study, we can draw three major conclusions that are relevant for flavivirus vaccine and vector development:

(i) Homologous recombination among flavivirus genomes, if it occurs at all, is a very rare event. The sensitivity of the recombination trap was demonstrated by the spiking experiment, which showed that as little as 10 infectious units of wild-type virus resulted in the complete displacement of the two replicons by the infectious wild-type virus within three passages. It is reasonable to assume that a single recombination event that gives rise to an infectious genome would produce at least 10 infectious particles and would thus outgrow the parental replicons within three passages or less. Flavivirus replicons typically multiply to 10^4 copies per cell (79, 129), and because the experimental conditions used allowed multiple rounds of infection at each passage, we estimate that at least 10^4 cells per passage would have been co-infected with complementary replicons, providing approximately 10^8 molecules that could potentially participate in a recombination event. Thus, a homologous crossover event

resulting in the generation of wild-type virus – which could have happened at any position within the extended stretch of overlapping sequence identity between the two replicons – would have been selected at a frequency as low as one in 10^8 per passage. However, the generation of wild-type virus was never observed for any of the three flaviviruses although they were tested over 10 passages.

(ii) Aberrant recombination apparently does occur, at least for certain flaviviruses. Despite the fact that extensive overlaps of identical sequence were present in our replicon pairs to favor crossover events at homologous positions to regenerate wild-type genomes, the only recombination events observed were aberrant ones that generated unnatural, rearranged forms of the JEV genome. As with homologous recombination, longer sequence overlaps between the recombination partners provide more potential non-identical crossover sites and would thus be expected not only to increase the likelihood of aberrant recombination within the overlap region but also the statistical chances of such an event producing a viable genome. Our results also raise the question whether ‘wobbling’ the codons of the overlap region, as has been used by some researchers to avoid homologous recombination, would actually reduce the recombination frequency if it is indeed confirmed that most crossovers are of the aberrant type. Furthermore, it remains unclear why no aberrant recombination was observed in the TBEV and WNV systems in spite of equivalent experimental conditions and sequence design.

It is possible that this kind of recombination is favored by yet undefined RNA structures that were present in our JEV sequence but not in those of the other two flaviviruses. These questions can be addressed in future experiments with the recombination trap.

(iii) If recombinants arise, they are likely to have an impaired growth phenotype. Aberrant recombination, which occurs by a crossover event at non-identical genome positions, generates an unnatural genome organization with sequence duplications. In the case of the JEV recombinants generated and analyzed in this study, this unnatural genome structure apparently caused growth defects, as demonstrated by a reduced-plaque-size

phenotype and/or growth kinetics in different host cells. This suggests that under natural conditions, progeny virus derived from such aberrant recombination events would, in most cases, have little, if any, chance to compete against the parental wild-type virus.

Overall, these conclusions suggest that recombination may turn out not to be a major concern with regard to live flavivirus vaccines and self-replicating flavivirus vectors. Our observations are in good agreement with the fact that, in spite of decades of use of live flavivirus vaccines and the co-circulation of several flaviviruses in several endemic areas in the world, there has not been a single report of a naturally occurring recombinant involving a vaccine strain or of recombination between members of different flavivirus species. Furthermore, although numerous experiments with chimeric flaviviruses have clearly demonstrated that artificially constructed interspecies recombinants can be viable (49, 54, 60, 102, 104), such recombinants have never been observed to arise under natural conditions.

The low rate of recombination, even under conditions strongly favoring the selection of recombinants, suggest that recombination probably plays, at most, a minor role in the biology and evolution of flaviviruses, and this highlights a striking difference between flaviviruses and many other RNA viruses (84). Coronaviruses, for example, frequently undergo precise homologous recombination (88), and vaccine strains of poliovirus (a picornavirus) have been observed to recombine with each other and with other enteroviruses (16, 101). Recombination is also a major driver of genetic diversity and viral evolution of retroviruses such as HIV (58, 141), and homologous recombination has also been reported among plant RNA viruses. For other viruses, such as alphaviruses and pestiviruses, aberrant homologous recombination, and even non-homologous recombination, appear to be more common than homologous recombination, but its frequency is still significant (9, 10, 50, 99, 100, 120). In fact, first-generation packaging systems for alphavirus vectors suffered from the risk of frequently observed recombination events between helper and vector replicons, regenerating infectious virus (150) – a problem that has been addressed by the development

of tripartite packaging systems and other genetic modifications to prevent successful recombination. In the case of the pestiviruses, which belong to the same viral family as the flaviviruses, sequences of cellular origin can be acquired by non-homologous recombination, driving alterations in viral pathogenicity(10, 12). Homologous recombination in these viruses was reduced in a pestivirus study when the sequence identity between recombination partners was reduced(39).

How may the low propensity for recombination between flaviviruses be explained at the molecular level? RNA recombination is thought to occur through a process in which the RNA replication complex falls off its template and continues RNA synthesis on a different template. A similar process is probably involved in the generation of deletion or duplication mutations during RNA replication (17, 87). Here, the replication complex also falls off and reinitiates, but it does so on the same template molecule upstream or downstream from its previous position, thus generating, respectively, duplications and deletions. Spontaneous deletion and duplication mutations, in contrast to intermolecular recombination events, are frequently observed in flaviviruses (80, 127). If, however, the flavivirus replication complex, similar to that of other RNA viruses, is capable of releasing its template and continuing RNA synthesis at another location, why would it not be able to freely switch templates in the course of this process and thus generate a recombined RNA product? One possible explanation would be that replication takes place in individual, secluded compartments within the infected cell that predominantly contain RNA derived from a single template molecule (81, 151). An alternative explanation would be that the RNA template somehow remains associated with the replication complex at a site other than the active site, which would favor re-initiation on the same RNA molecule after a temporary release of the template from the active site of the synthetase.

The use of trans-complementation systems such as the ones described here as recombination traps will allow more detailed investigation of the types of recombination

events that flavivirus genomes are capable of undergoing as well as their relative frequencies. In addition, the generally low propensity of flavivirus replicons for recombination makes it possible for them to be used as reliable tools to study complementation of individual genes derived from different viral strains or species.

Materials and Methods

Cells. BHK-21 cells were grown in Eagle's minimal essential medium (Sigma) supplemented with 5% fetal calf serum (FCS), 1% glutamine and 0.5% neomycin (growth medium) and maintained in Eagle's minimal essential medium supplemented with 1% FCS, 1% glutamine, 0.5% neomycin and 15 mM HEPES, pH 7.4 (maintenance medium). Vero cells (ATCC CCL-81) were grown in Eagle's minimal essential medium supplemented with 10 % FCS, 30 mM L-glutamine, 100 units of penicillin, and 1 µg/ml streptomycin. Plaque assay infections were done in medium containing 1% FCS. *Aedes albopictus* C6/36 cells were grown in Eagle's minimal essential medium (without NaHCO₃) supplemented with 10% FCS, 20 mM L-glutamine, 100 units of penicillin, 1 µg/ml streptomycin, 13 mM sodium hydroxide, 19 mM HEPES, pH 7.4, and 0.2 % 50x tryptose-phosphate. For growth curve analysis, the FCS concentration was reduced to 1%.

Plasmids and cloning procedures. Plasmid pTNd/c, used for generating infectious TBEV, contains a full-length genomic cDNA insert of TBEV strain Neudoerfl (GenBank accession number U27495) cloned in plasmid pBR322 (96). RNA transcribed from this plasmid was used as the TBEV wild-type virus control. Plasmid pTNd/5' contains a 5' cDNA fragment of the same viral genome (96). Full-length DNA templates for *in vitro* transcription of TBEV plasmids were generated as described previously (77).

pTBEV- Δ C, a derivative of pTNd/c containing a large deletion (62 amino acids) of the sequence coding for the capsid protein as well as individual mutations in the signal sequence of the capsid protein, was used as the DNA template for *in vitro* synthesis of replicon Δ C. It has been described in an earlier publication (76) in which it was called C (Δ 28-89)-S. The plasmids for production of replicons Δ ME (41) and Δ ME-eGFP (42) were also described previously.

Plasmid pTBEV- Δ E, the template for generating TBEV replicon Δ E, was constructed by first performing PCR using the primers 5'-tttaccggtttacgctgatgttggtgcgctgtgga-3' and 5'-ttccatcgatagtgtagctagcaggccatgagca-3' with pTNd/5' as a template and then cloning this PCR product into pTNd/5' using the restriction enzymes AgeI and ClaI.

For the construction of plasmid pWNV- Δ C, the template for generating the WNV Δ C replicon, two DNA fragments were made by amplifying portions of the plasmid clone pWNV-K1 (127), which contains nucleotides 1-3339 of WNV strain NY99 (isolate Crow V76/1). The first fragment was made using the primers 5'-aggtgtccacagggtagcca-3' and 5'-ttttgatccttttagcatattgacagccc-3' and then digesting the resulting product with PacI and BamHI. The second fragment was made using primers 5'-tctcggatcctcaaaacaaaagaaaagagg-3' and 5'-aataggggttccgcgaca-3' and digestion with BamHI and NotI. These fragments were then mixed with a third fragment generated by digestion of the plasmid pWNV-K4 (containing nucleotides 3282-11029 from the same WNV strain) with PacI and NotI. Ligation of these three fragments resulted in an intermediate construct containing nucleotides 1-3339 of the WNV genome but lacking nucleotides 151-393 in the C gene, which were replaced by a BamHI restriction site. An additional SalI restriction site was created by introducing silent nucleotide substitutions at positions 151 and 156 using a site-directed mutagenesis kit (Invitrogen) with the primers 5'-gtgtctggagcaacatgggt**CgaC**ttggttctcg-3' and 5'-acctatgttgctccagacactccttccaag-3' (bold capital letters indicate mutated nucleotides). The full-length DNA template for RNA synthesis was generated by digestion of pWNV-K1- Δ C and

pWNV-K4 with BstEII, followed by *in vitro* ligation using T4 DNA ligase (Invitrogen) and linearization by digestion with NotI.

For construction of plasmid pWNV-ΔE, pWNV-K1 was used as a template for mutagenic PCR using the primers 5'-ttttcaccagtgctgctgtaagctggggccacca-3' and 5'-ttttagatctcgatgtctaagaaaccaggagg-3'. Restriction digestion of the PCR product and WNV-K1 with BglII and AclI generated fragments that were ligated to form pWNV-K1-ΔE. This partial clone was further digested with PacI and BstEII, and the resulting fragment was cloned into pWNV-K4, yielding full-length DNA plasmid pWNV-ΔE. This full-length plasmid was linearized by NotI digestion before use as a template for *in vitro* RNA transcription.

All constructs containing JEV sequences were based on JEV strain SA-14 (China), which was kindly provided by Peter Mason, Yale University. A 5' clone, pJEV-K3, containing nucleotides 1-5616, a 3' clone, pJEV-K4, containing nucleotides 5595-10977, and a full-length clone, pJEV/c, containing the whole genome (nt 1-10977) of the wild-type virus in pBR322 were generated using standard cloning techniques (manuscript in preparation).

For construction of pJEV-ΔC, mutagenic PCR was first performed using the primers 5'-ggcatcgattagtggaatacgcgggtag-3' and 5'-aaattaattaatacactcactatagagaa-3' with plasmid pJEV-K3 as the template. This PCR product and plasmid pJEV-K3 were both digested with ClaI and PacI and ligated, forming the intermediate construct pJEV-K3-ΔC. pJEV-K3-ΔC and pJEV/c were then digested with PacI and AgeI, and the smaller fragment of pJEV/c was replaced by the corresponding fragment of pJEV-K3-ΔC, yielding the full-length cDNA clone pJEV-ΔC.

For construction of pJEV-ΔE, mutagenic PCR was performed using the primers 5'-aggcagcccctaggaccagaaccacgttttctgttcgt-3' and 5'-ttttacgcgtggtattaccatcctcctgctgttggtcgtccggcttacagtgacacttggatgtgccattg-3' and plasmid pJEV-K3 as the template. This PCR product and plasmid pJEV-K3 were both digested with AvrII and MluI and ligated together to make the intermediate construct pJEV-K3-ΔE. pJEV-

K3-ΔE and pJEV/c were then digested with PacI and BamHI, and the smaller fragment of pJEV/c was exchanged with the corresponding pJEV-K3-ΔE fragment, yielding the full-length cDNA clone pJEV-ΔE.

Infectious clones of JEV recombinants 1 and 2 were made as follows: Cytoplasmic RNA that indicated the presence of a full-length virus in the northern blot analysis was transcribed into cDNA as described below for RT-PCR. Then, PCR with primers 5'-tcgagagattagtgcagttt-3' and 5'-cagtagcacaagtcactatggac-3' was used to generate a fragment that was digested with ClaI and AgeI and exchanged with the corresponding ClaI/AgeI fragment of pJEV-K3. Each of these intermediate constructs was cut with AgeI and ligated to AgeI-digested pJEV-K4 to form the full-length DNA templates for *in vitro* transcription.

RNA transfection. *In vitro* transcription and transfection of BHK-21 cells by electroporation were performed as described previously (79, 96, 114). RNA was synthesized from full-length cDNA clones or *in vitro*-ligated full-length templates (see above) using reagents of the T7 Megascript kit (Ambion) according to manufacturer's protocol. The template DNA was digested by incubation with DNase I, and the quality of the RNA was checked by electrophoresis in a 1% agarose gel containing 6% formalin. RNA was purified using an RNeasy Mini kit (Qiagen) and quantified spectrophotometrically. Equimolar amounts of RNA were then introduced into BHK-21 cells by electroporation using a Bio-Rad Gene Pulser (1.8 kV, 25 μF, 200 Ω). For cotransfections, equal amounts of RNA (~1.1 10¹² copies) of each construct were mixed before electroporation.

Immunofluorescence assays. Twenty-four hours after transfection or infection, BHK-21 cells were fixed for 20 min with 4% paraformaldehyde in PBS (pH 7.4) and then washed two times for 5 min with PBS (pH 7.4) and permeabilized with ice-cold methanol for 6 min at -20°C. After three washes with PBS (pH 7.4) and blocking with 3% BSA in PBS (pH 7.4) for

30 min at room temperature, intracellular E protein was visualized by sequential incubation with a monoclonal mouse antibody against E (1E9) (48) and a Rhodamine-Red-X-conjugated anti-mouse IgG antibody (Jackson Immune Research Laboratory). Simultaneously, eGFP fluorescence was enhanced by incubation with a polyclonal rabbit-antibody against GFP (Abcam: ab6556), followed by incubation with a fluorescein-isothiocyanate (FITC)-conjugated anti-rabbit IgG antibody (Jackson Immune Research Laboratory).

For single-focus immunofluorescence, BHK-21 cells were seeded into 24-well tissue culture plates containing microscope coverslips. The confluent monolayer was infected in parallel with the dilutions used for the focus assay. Accordingly, cells were treated in the same way and covered with a 3% carboxymethyl cellulose overlay dissolved in maintenance medium. After 50 hours, cells were washed three times with ice-cold PBS (pH 7.4) and then processed for double immunofluorescence staining. Microscopic observation and documentation were accomplished by using a LSM 510 scanning confocal microscope (Zeiss) and the included software.

Focus assay. Supernatants from BHK-21 cells were collected at passage 1 on day 3 postinfection. Serial dilutions of supernatants were applied to confluent monolayers of BHK-21 cells. After a 3-h incubation, supernatants were removed and cells were covered with a 3% carboxymethyl cellulose overlay dissolved in maintenance medium. Fifty hours after infection, cells were fixed with acetone-methanol (1:1) for 10 min at -20°C and treated with polyclonal rabbit anti-TBEV serum. Antibody-labeled cells were detected using an immunoenzymatic reaction consisting of sequential incubation with goat anti-rabbit immunoglobulin G-alkaline phosphatase and the corresponding enzyme substrate (SigmaFast Red TR/Naphthol AS-MX tablets).

Endpoint passages. Supernatants of infected cells were sequentially diluted, and 200 μ l of each dilution was applied to fresh BHK-21 cells grown in 24-well plates (Nunc). After three days, half of the medium was replaced by fresh medium, and after six days, protein E released into the supernatant was detected using a four-layer enzyme-linked immunosorbent assay (ELISA) (53) in the case of TBEV and a haemagglutination assay (HA) (127) in the case of WNV and JEV. After six days, the highest dilution yielding a positive signal in ELISA or HA was cleared of cell debris, sequentially diluted and used for infection of fresh BHK-21 cells.

Northern blot analysis. Template DNA for synthesis of RNA probes for northern blotting was generated using the following primers and templates: TBEV: template pTNd/c and primers agagagcagaaggattga and tacttaatacgactcactataggtgtgcaagacacccttg generated a probe binding to nucleotides 4093-4773 in wild-type virus. WNV: template pWNV-K4 and primers agcggctgttggtatggtatg and taatacgactcactataagctgcactcctcttcct generated a probe binding to nucleotides 3448-4107 in wild-type virus. JEV: template pJEV-K4 and primers aatggctgctggtacggaatgga and taatacgactcactatacatggtcttttctctcgtg generated a probe binding to nucleotides 3456-4103 in wild-type virus. After phenol-chloroform purification of the template DNA, the T7 promoter sequence (underlined) fused to each reverse primer allowed RNA synthesis using a T7 MAXIscript In Vitro Transcription Kit (Ambion). The probe RNA was labeled by using 0.4 μ l of 10 mM Bio-11-UTP (Ambion) instead of UTP. Probe RNA was separated from free nucleotides using Micro Bio-Spin 30 columns (BioRad).

Cytoplasmic RNA was extracted from BHK-21 cells 24 hours after transfection or infection. Ten μ g of total RNA was applied to a 1% agarose gel, and northern blotting was carried out according to the instructions of the NorthernMax-Gly Kit (Ambion). Blotted RNA was detected using a BrightStar BioDetect Kit (Ambion).

RT-PCR. Reverse transcription-polymerase chain reaction (RT-PCR) was performed using the same cytoplasmic RNA used for the northern blot analysis, with the primers for cDNA synthesis and PCR listed in Table 1. cDNA fragments of the 5' terminal part of each virus genome including the entire sequence coding for the three structural proteins capsid, prM and E was synthesized using a reverse primer binding to the sequence coding for NS1 of each virus (Table 1). Subsequently, primers binding to sequences absent in both or only one of the replicons were used for specific amplification of full-length or replicon cDNA fragments of the structural region of TBEV, WNV, or JEV (Table 1). Each PCR was carried out using an Advantage® HF2 PCR Kit (Clontech), and amplicons were subjected to 1% agarose gel electrophoresis as well as automated sequence analysis as described before (79).

Plaque assays. Vero cells were grown to 80% confluence in 12-well plates and incubated for 1 h with virus suspensions serially diluted in maintenance medium. The cells were subsequently overlaid with EMEM containing 5% FBS (PAA), 1.5% glutamine (200 mM, Cambrex), 1% penicillin/streptomycin (10,000 U/ml penicillin, 10 mg/ml streptomycin, Sigma), 15 mM HEPES and 0.25% agarose (Sigma). Four days after infection, the cells were fixed and stained with a solution containing 4% formaldehyde and 0.1% crystal violet.

Multistep growth curves. Stock preparations of JEV recombinants were generated by collecting supernatants of BHK-21 cells transfected with these mutants at day 3 posttransfection. For analysis of growth properties of recombinant JEV viruses, C6/36 mosquito cells grown in 6-well plates were infected with wild-type JEV or JEV recombinant stock preparations at a low multiplicity of infection (MOI 0.01). Aliquots of supernatants (500 µl) were taken at different time points, and virus titers were determined by plaque assay.

Acknowledgments

We are grateful to Steven L. Allison for his invaluable assistance during data evaluation and preparation of the manuscript. We thank Regina Kofler for her participation in mutant construction and Franz X. Heinz for providing materials and reagents. Finally, we are grateful to the staff of the microbial ecology department of the University of Vienna for their help with the use of the LSM 510 scanning confocal microscope.

References

1. Jenkins GM, Rambaut A, Pybus OG, Holmes EC (2002) Rates of molecular evolution in RNA viruses: a quantitative phylogenetic analysis. *J Mol Evol* 54: 156-165.
2. Worobey M, Holmes EC (1999) Evolutionary aspects of recombination in RNA viruses. *J Gen Virol* 80 (Pt 10): 2535-2543.
3. Lai MM (1992) RNA recombination in animal and plant viruses. *Microbiol Rev* 56: 61-79.
4. Holland J, Spindler K, Horodyski F, Grabau E, Nichol S, et al. (1982) Rapid evolution of RNA genomes. *Science* 215: 1577-1585.
5. Nagy PD, Simon AE (1997) New insights into the mechanisms of RNA recombination. *Virology* 235: 1-9.
6. Hahn CS, Lustig S, Strauss EG, Strauss JH (1988) Western equine encephalitis virus is a recombinant virus. *Proc Natl Acad Sci U S A* 85: 5997-6001.
7. Baric RS, Fu K, Schaad MC, Stohlman SA (1990) Establishing a genetic recombination map for murine coronavirus strain A59 complementation groups. *Virology* 177: 646-656.
8. Becher P, Orlich M, Konig M, Thiel HJ (1999) Nonhomologous RNA recombination in bovine viral diarrhea virus: molecular characterization of a variety of

- subgenomic RNAs isolated during an outbreak of fatal mucosal disease. *J Virol* 73: 5646-5653.
9. Weiss BG, Schlesinger S (1991) Recombination between Sindbis virus RNAs. *J Virol* 65: 4017-4025.
 10. Cammack N, Phillips A, Dunn G, Patel V, Minor PD (1988) Intertypic genomic rearrangements of poliovirus strains in vaccinees. *Virology* 167: 507-514.
 11. Cuervo NS, Guillot S, Romanenkova N, Combiescu M, Aubert-Combiescu A, et al. (2001) Genomic features of intertypic recombinant sabin poliovirus strains excreted by primary vaccinees. *J Virol* 75: 5740-5751.
 12. Roukens AH, Visser LG (2008) Yellow fever vaccine: past, present and future. *Expert Opin Biol Ther* 8: 1787-1795.
 13. Liu ZL, Hennessy S, Strom BL, Tsai TF, Wan CM, et al. (1997) Short-term safety of live attenuated Japanese encephalitis vaccine (SA14-14-2): results of a randomized trial with 26,239 subjects. *J Infect Dis* 176: 1366-1369.
 14. Monath TP, Kanesa-Thanan N, Guirakhoo F, Pugachev K, Almond J, et al. (2005) Recombination and flavivirus vaccines: a commentary. *Vaccine* 23: 2956-2958.
 15. Sabchareon A, Lang J, Chanthavanich P, Yoksan S, Forrat R, et al. (2004) Safety and immunogenicity of a three dose regimen of two tetravalent live-attenuated dengue vaccines in five- to twelve-year-old Thai children. *Pediatr Infect Dis J* 23: 99-109.
 16. Seligman SJ, Gould EA (2004) Live flavivirus vaccines: reasons for caution. *Lancet* 363: 2073-2075.
 17. Holmes EC, Worobey M, Rambaut A (1999) Phylogenetic evidence for recombination in dengue virus. *Mol Biol Evol* 16: 405-409.

18. Tolou HJ, Couissinier-Paris P, Durand JP, Mercier V, de Pina JJ, et al. (2001) Evidence for recombination in natural populations of dengue virus type 1 based on the analysis of complete genome sequences. *J Gen Virol* 82: 1283-1290.
19. Uzcategui NY, Camacho D, Comach G, Cuello de Uzcategui R, Holmes EC, et al. (2001) Molecular epidemiology of dengue type 2 virus in Venezuela: evidence for in situ virus evolution and recombination. *J Gen Virol* 82: 2945-2953.
20. Worobey M, Rambaut A, Holmes EC (1999) Widespread intra-serotype recombination in natural populations of dengue virus. *Proc Natl Acad Sci U S A* 96: 7352-7357.
21. Twiddy SS, Holmes EC (2003) The extent of homologous recombination in members of the genus *Flavivirus*. *J Gen Virol* 84: 429-440.
22. Mukhopadhyay S, Kuhn RJ, Rossmann MG (2005) A structural perspective of the flavivirus life cycle. *Nat Rev Microbiol* 3: 13-22.
23. Kofler RM, Aberle JH, Aberle SW, Allison SL, Heinz FX, et al. (2004) Mimicking live flavivirus immunization with a noninfectious RNA vaccine. *Proc Natl Acad Sci U S A* 101: 1951-1956.
24. Gehrke R, Ecker M, Aberle SW, Allison SL, Heinz FX, et al. (2003) Incorporation of tick-borne encephalitis virus replicons into virus-like particles by a packaging cell line. *J Virol* 77: 8924-8933.
25. Harvey TJ, Liu WJ, Wang XJ, Linedale R, Jacobs M, et al. (2004) Tetracycline-inducible packaging cell line for production of flavivirus replicon particles. *J Virol* 78: 531-538.
26. Khromykh AA, Varnavski AN, Westaway EG (1998) Encapsidation of the flavivirus kunjin replicon RNA by using a complementation system providing Kunjin virus structural proteins in trans. *J Virol* 72: 5967-5977.

27. Scholle F, Girard YA, Zhao Q, Higgs S, Mason PW (2004) trans-Packaged West Nile virus-like particles: infectious properties in vitro and in infected mosquito vectors. *J Virol* 78: 11605-11614.
28. Shustov AV, Mason PW, Frolov I (2007) Production of pseudoinfectious yellow fever virus with a two-component genome. *J Virol* 81: 11737-11748.
29. Widman DG, Ishikawa T, Fayzulin R, Bourne N, Mason PW (2008) Construction and characterization of a second-generation pseudoinfectious West Nile virus vaccine propagated using a new cultivation system. *Vaccine* 26: 2762-2771.
30. Mandl CW, Ecker M, Holzmann H, Kunz C, Heinz FX (1997) Infectious cDNA clones of tick-borne encephalitis virus European subtype prototypic strain Neudoerfl and high virulence strain Hypr. *J Gen Virol* 78 (Pt 5): 1049-1057.
31. Kofler RM, Heinz FX, Mandl CW (2002) Capsid protein C of tick-borne encephalitis virus tolerates large internal deletions and is a favorable target for attenuation of virulence. *J Virol* 76: 3534-3543.
32. Gehrke R, Heinz FX, Davis NL, Mandl CW (2005) Heterologous gene expression by infectious and replicon vectors derived from tick-borne encephalitis virus and direct comparison of this flavivirus system with an alphavirus replicon. *J Gen Virol* 86: 1045-1053.
33. Schlick P, Taucher C, Schittl B, Tran JL, Kofler RM, et al. (2009) Helices α_2 and α_3 of WNV Capsid Protein are Dispensable for the Assembly of Infectious Virions. *J Virol*.
34. Kofler RM, Hoenninger VM, Thurner C, Mandl CW (2006) Functional analysis of the tick-borne encephalitis virus cyclization elements indicates major differences between mosquito-borne and tick-borne flaviviruses. *J Virol* 80: 4099-4113.
35. Orlinger KK, Hoenninger VM, Kofler RM, Mandl CW (2006) Construction and mutagenesis of an artificial bicistronic tick-borne encephalitis virus genome

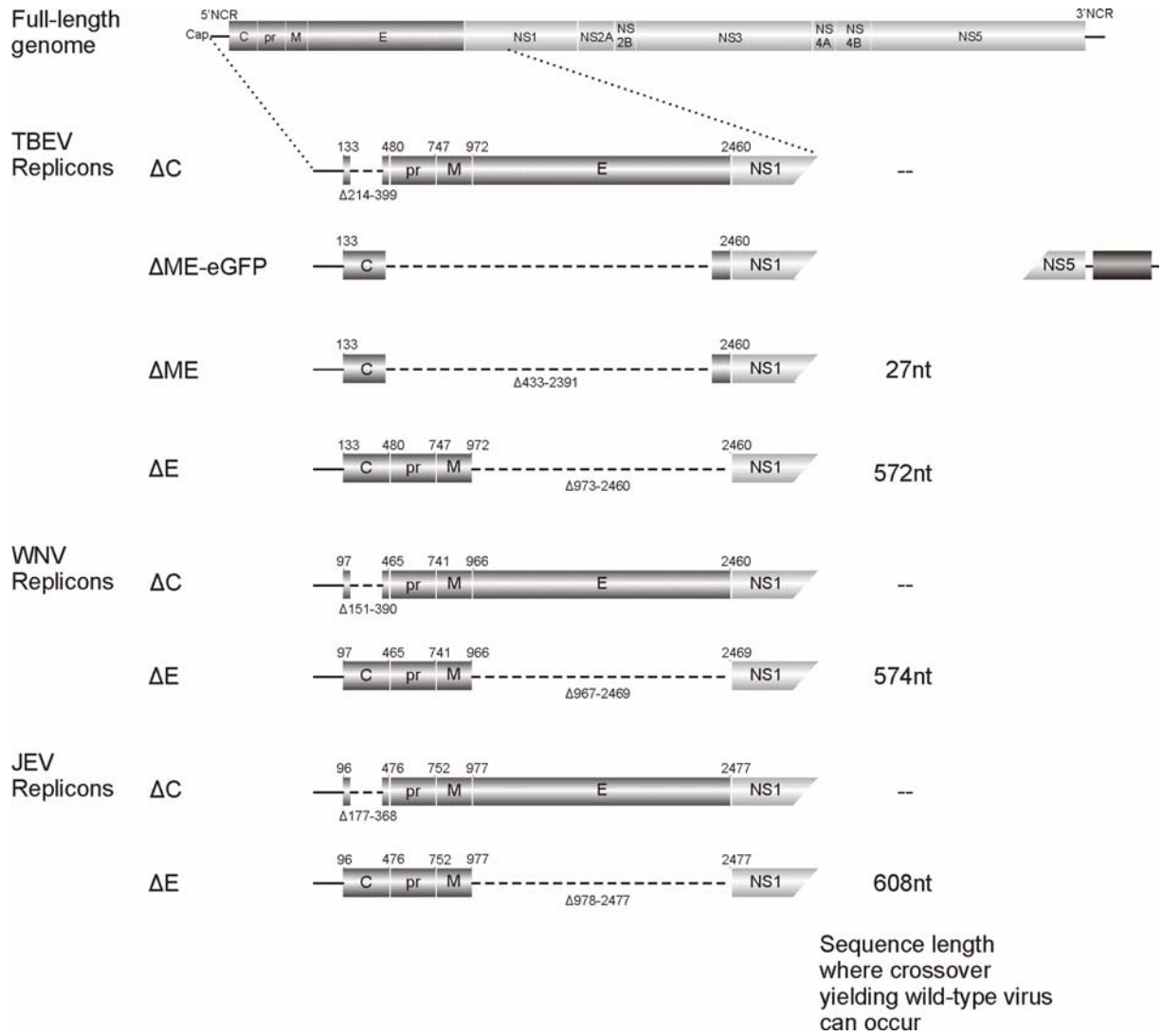
- reveals an essential function of the second transmembrane region of protein e in flavivirus assembly. *J Virol* 80: 12197-12208.
36. Guirakhoo F, Heinz FX, Kunz C (1989) Epitope model of tick-borne encephalitis virus envelope glycoprotein E: analysis of structural properties, role of carbohydrate side chain, and conformational changes occurring at acidic pH. *Virology* 169: 90-99.
37. Heinz FX, Tuma W, Guirakhoo F, Kunz C (1986) A model study of the use of monoclonal antibodies in capture enzyme immunoassays for antigen quantification exploiting the epitope map of tick-borne encephalitis virus. *J Biol Stand* 14: 133-141.
38. Kofler RM, Heinz FX, Mandl CW (2004) A novel principle of attenuation for the development of new generation live flavivirus vaccines. *Arch Virol Suppl*: 191-200.
39. Holmes EC, Twiddy SS (2003) The origin, emergence and evolutionary genetics of dengue virus. *Infect Genet Evol* 3: 19-28.
40. Schrauf S, Schlick P, Skern T, Mandl CW (2008) Functional analysis of potential carboxy-terminal cleavage sites of tick-borne encephalitis virus capsid protein. *J Virol* 82: 2218-2229.
41. Guirakhoo F, Pugachev K, Zhang Z, Myers G, Levenbook I, et al. (2004) Safety and efficacy of chimeric yellow Fever-dengue virus tetravalent vaccine formulations in nonhuman primates. *J Virol* 78: 4761-4775.
42. Higgs S, Vanlandingham DL, Klingler KA, McElroy KL, McGee CE, et al. (2006) Growth characteristics of ChimeriVax-Den vaccine viruses in *Aedes aegypti* and *Aedes albopictus* from Thailand. *Am J Trop Med Hyg* 75: 986-993.

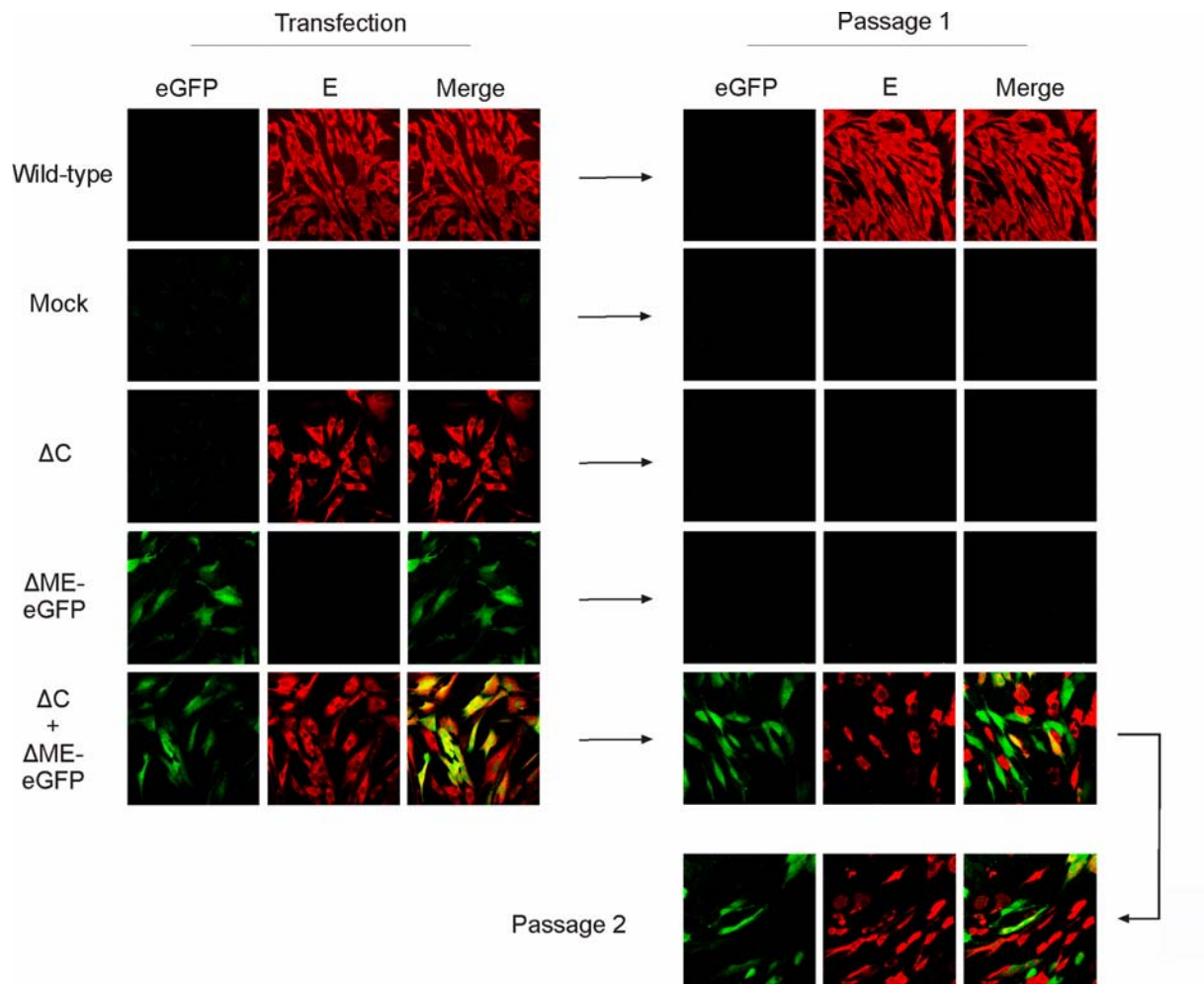
43. Huang CY, Butrapet S, Tsuchiya KR, Bhamarapravati N, Gubler DJ, et al. (2003) Dengue 2 PDK-53 virus as a chimeric carrier for tetravalent dengue vaccine development. *J Virol* 77: 11436-11447.
44. Monath TP, Guirakhoo F, Nichols R, Yoksan S, Schrader R, et al. (2003) Chimeric live, attenuated vaccine against Japanese encephalitis (ChimeriVax-JE): phase 2 clinical trials for safety and immunogenicity, effect of vaccine dose and schedule, and memory response to challenge with inactivated Japanese encephalitis antigen. *J Infect Dis* 188: 1213-1230.
45. Monath TP, Levenbook I, Soike K, Zhang ZX, Ratterree M, et al. (2000) Chimeric yellow fever virus 17D-Japanese encephalitis virus vaccine: dose-response effectiveness and extended safety testing in rhesus monkeys. *J Virol* 74: 1742-1751.
46. Liao CL, Lai MM (1992) RNA recombination in a coronavirus: recombination between viral genomic RNA and transfected RNA fragments. *J Virol* 66: 6117-6124.
47. Minor PD, John A, Ferguson M, Icenogle JP (1986) Antigenic and molecular evolution of the vaccine strain of type 3 poliovirus during the period of excretion by a primary vaccinee. *J Gen Virol* 67 (Pt 4): 693-706.
48. Hu WS, Temin HM (1990) Retroviral recombination and reverse transcription. *Science* 250: 1227-1233.
49. Stuhlmann H, Berg P (1992) Homologous recombination of copackaged retrovirus RNAs during reverse transcription. *J Virol* 66: 2378-2388.
50. Raju R, Subramaniam SV, Hajjou M (1995) Genesis of Sindbis virus by in vivo recombination of nonreplicative RNA precursors. *J Virol* 69: 7391-7401.
51. Becher P, Orlich M, Thiel HJ (1998) Ribosomal S27a coding sequences upstream of ubiquitin coding sequences in the genome of a pestivirus. *J Virol* 72: 8697-8704.

52. Becher P, Orlich M, Thiel HJ (2000) Mutations in the 5' nontranslated region of bovine viral diarrhoea virus result in altered growth characteristics. *J Virol* 74: 7884-7894.
53. Meyers G, Tautz N, Dubovi EJ, Thiel HJ (1991) Viral cytopathogenicity correlated with integration of ubiquitin-coding sequences. *Virology* 180: 602-616.
54. Meyers G, Thiel HJ (1996) Molecular characterization of pestiviruses. *Adv Virus Res* 47: 53-118.
55. Becher P, Thiel HJ, Collins M, Brownlie J, Orlich M (2002) Cellular sequences in pestivirus genomes encoding gamma-aminobutyric acid (A) receptor-associated protein and Golgi-associated ATPase enhancer of 16 kilodaltons. *J Virol* 76: 13069-13076.
56. Gallei A, Rumenapf T, Thiel HJ, Becher P (2005) Characterization of helper virus-independent cytopathogenic classical swine fever virus generated by an in vivo RNA recombination system. *J Virol* 79: 2440-2448.
57. Cascone PJ, Carpenter CD, Li XH, Simon AE (1990) Recombination between satellite RNAs of turnip crinkle virus. *Embo J* 9: 1709-1715.
58. Lazzarini RA, Keene JD, Schubert M (1981) The origins of defective interfering particles of the negative-strand RNA viruses. *Cell* 26: 145-154.
59. Kofler RM, Leitner A, O'Riordain G, Heinz FX, Mandl CW (2003) Spontaneous mutations restore the viability of tick-borne encephalitis virus mutants with large deletions in protein C. *J Virol* 77: 443-451.
60. Kopek BG, Perkins G, Miller DJ, Ellisman MH, Ahlquist P (2007) Three-dimensional analysis of a viral RNA replication complex reveals a virus-induced mini-organelle. *PLoS Biol* 5: e220.

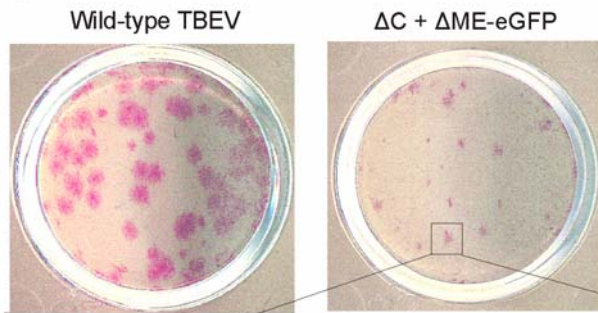
61. Welsch S, Miller S, Romero-Brey I, Merz A, Bleck CK, et al. (2009) Composition and three-dimensional architecture of the dengue virus replication and assembly sites. Cell Host Microbe 5: 365-375.

Figures

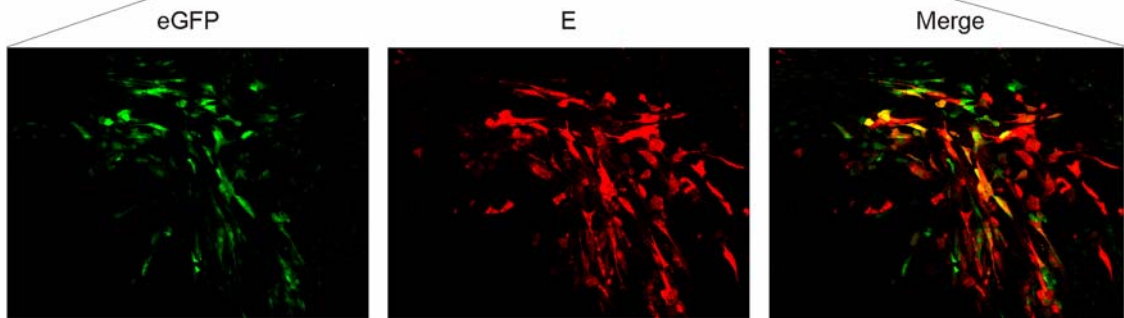




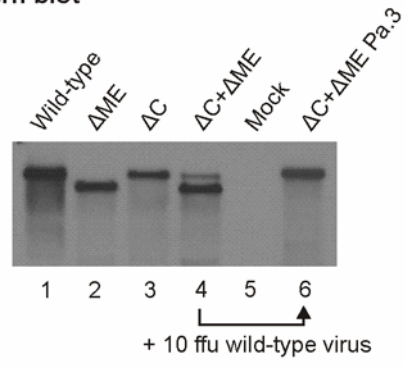
A Focus Assay



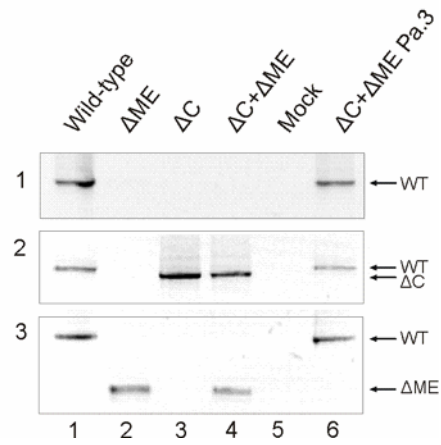
B Immunofluorescence



A Northern blot



B RT-PCRs

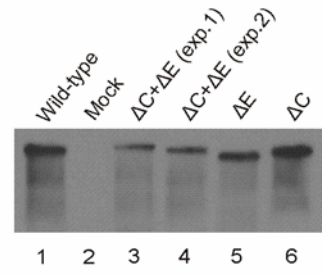
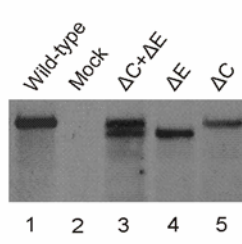
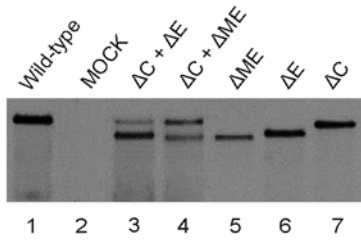


Tick-borne encephalitis virus

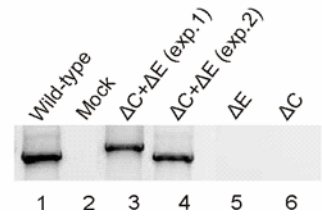
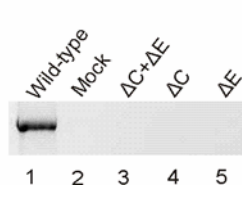
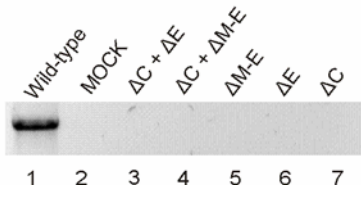
West Nile virus

Japanese encephalitis virus

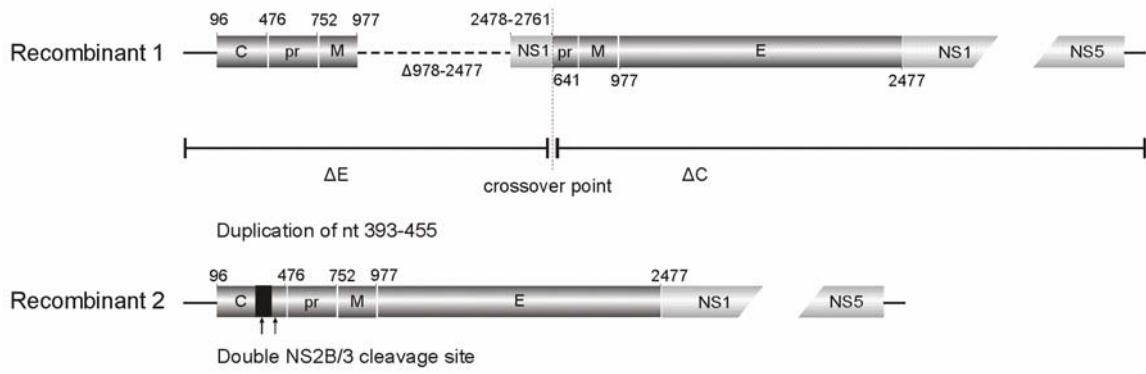
A Northern blot



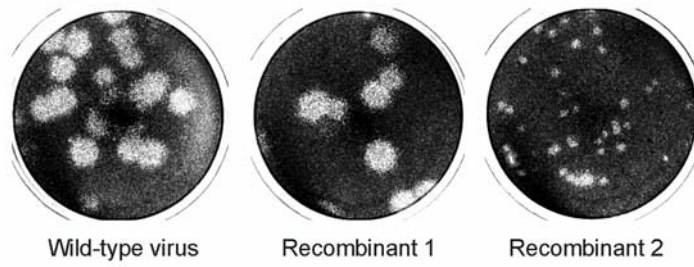
B RT-PCR



A JEV Recombinant full-length viruses



B Plaque assay



C Growth curves

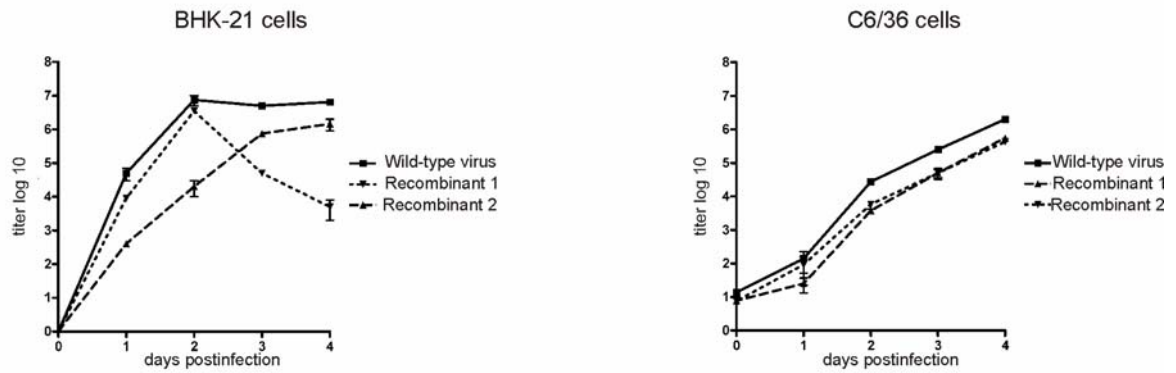


Figure Legends

Figure 1. Structural organization of flavivirus genomes and replicons. *Top:* Schematic drawing of a full-length flavivirus genome. *Below:* Expanded view of the structural region of each replicon. Deletions are indicated by dotted lines, and the missing nucleotides are indicated after the " Δ " symbol. Nucleotide numbers refer to the position in the corresponding wild-type virus sequence. The length of the homologous region that would allow recombination to yield a full-length virus is indicated on the right. C, capsid protein; pr, N-terminal part of prM; M, C-terminal part of prM corresponding to the mature M protein; E, protein E; NS, nonstructural protein; NCR, noncoding region; IRES, internal ribosome entry site; eGFP, enhanced green fluorescent protein.

Figure 2. Packaging and propagation of complementing TBEV replicons. *Left:* Fluorescence micrographs showing eGFP and E protein expression in BHK-21 cells 24 hours after transfection with *in vitro*-transcribed full-length genomic RNA or replicon RNA. From top to bottom: cells transfected with wild-type RNA, mock-transfected control without RNA, cells transfected with Δ C alone, cells transfected with Δ ME-eGFP alone, and cells cotransfected with both Δ C and Δ ME-eGFP. Green fluorescence indicates eGFP expression, and red fluorescence indicates viral E protein expression. In the merged images shown at the right, cells expressing both proteins appear yellow. *Right:* Cell culture passage 1. Supernatants from the transfected cells shown in the left panel were used to inoculate fresh BHK-21 cells, and expression of eGFP and E protein was again detected by immunofluorescence staining. *Bottom:* Cell culture passage 2. Supernatants from passage 1 containing both packaged replicons were again transferred to fresh BHK-21 cells, and these cells were likewise examined by immunofluorescence staining.

Figure 3. Analysis of foci. **A.** Typical foci produced in BHK-21 cells after infection with culture supernatants containing wild-type TBEV (left) or a mixture of packaged TBEV replicons ΔC and ΔME -eGFP (right). **B.** Immunofluorescence staining of a single focus observed after coinfection with packaged TBEV replicons ΔC and ΔME -eGFP. Cells were processed in the same way as for the focus assay shown in A except that instead of an immunoenzymatic reaction, immunofluorescence staining was used to detect eGFP and E protein expression as in Fig. 2.

Figure 4. Spiking experiment to examine competition between replicons and full-length virus genomes. **A.** Northern blot analysis of total intracellular RNA extracted from BHK-21 cells transfected with full-length TBEV genomic RNA (lane 1), TBEV replicon ΔME (lane 2), TBEV replicon ΔC (lane 3), or both replicons simultaneously (lane 4). After transfection, 10 focus-forming units (ffu) of TBEV wild-type virus was added to the supernatant of cells cotransfected with replicons ΔME and ΔC , and fresh cells were infected with this mixture. Three endpoint passages later, intracellular RNA was examined again, revealing the presence of a single RNA species corresponding in size to the viral genome (lane 6). Mock = mock-infected control. **B.** RT-PCR performed with the same intracellular RNA samples used for the northern blot analysis in A and the TBEV-specific primers listed in Table 1. cDNA synthesis was performed using a reverse primer that allowed the synthesis of the 5' terminal part of TBEV genome, extending to the middle of the region coding for NS1. *RT-PCR 1*: PCR with primers binding to sequences in the region coding for the capsid protein (forward) and protein E (reverse), allowing detection of the wild-type genome but not replicon ΔC or ΔME , which lack the forward and reverse primer-binding site, respectively. This PCR confirmed the presence of a full-length viral genome three endpoint passages after spiking the replicon mixture with a small amount of wild-type TBEV. *RT-PCR 2*: PCR with primers binding to the 5'NCR (forward) and to the sequence coding for protein E (reverse), allowing detection of

wild-type virus (lane 1) and replicon ΔC (lane 3) but not ΔME . Note the absence of the ΔC -specific PCR product three endpoint passages after spiking with wild-type virus (lane 6). *RT-PCR 3*: PCR with primers binding to the regions coding for the capsid protein (forward) and the NS1 protein (reverse), allowing detection of wild-type virus (lane 1) and replicon ΔME (lane 3), but not ΔC . Again, note the absence of the ΔME -specific product three endpoint passages after spiking with wild-type virus (lane 6).

Figure 5. Detection of recombinants using the recombination trap. **A.** Northern blot analysis of intracellular RNA. *Left:* Total cellular RNA was isolated from BHK-21 cells infected with wild-type TBEV (lane 1), mock-transfected cells (lane 2), cells infected using supernatants from the tenth passage after cotransfection with TBEV replicons $\Delta C + \Delta E$ (lane 3) or $\Delta C + \Delta ME$ (lane 4), and control cells that were transfected separately with TBEV replicon ΔME (lane 5), ΔE (lane 6), or ΔC (lane 7). *Middle:* The RNA was isolated from BHK-21 cells infected with wild-type WNV (lane 1), mock-transfected cells (lane 2), cells infected using supernatants from the tenth passage after cotransfection with WNV replicons $\Delta C + \Delta E$ (lane 3), and control cells that were transfected separately with WNV replicon ΔE (lane 4) or ΔC (lane 5). *Right:* The RNA was isolated from BHK-21 cells infected with wild-type JEV (lane 1), mock-transfected cells (lane 2), cells that were infected using supernatants from the tenth passage after cotransfection with JEV replicons $\Delta C + \Delta E$ in two separate experiments (lanes 3 and 4), and control cells that were transfected separately with JEV replicon ΔE (lane 5) or ΔC (lane 6). **B.** RT-PCR for detection of recombinants. Lane designations are the same as in A. RT-PCR assays analogous to RT-PCR 1 in Fig. 4B were carried out using the same cellular RNA preparations used for the northern blot shown in A and the appropriate virus-specific "RT-PCR1" primers shown in Table 1. The forward and reverse primers in this assay bind to the missing regions of the ΔC and ΔE replicons, respectively, and an amplification product is

therefore only obtained when both of these sites are present on the same RNA molecule, as was observed with two JEV recombinants (lanes 3 and 4 of the right panel).

Figure 6. Growth properties of JEV recombinants **A.** Schematic diagram of the JEV recombinants selected in experiments 1 and 2 (Fig. 5), named recombinant 1 and recombinant 2, respectively. The 5' part of the genome of recombinant 1 was derived from replicon ΔE and retained the original deletion. The crossover point is after the deletion, in the middle of the sequence coding for NS1. The 3' part of recombinant 1 begins with nucleotide 641 of the ΔC replicon (numbering corresponds to wild-type TBEV) and continues to the 3' end of the genome. The resulting genome thus contains two copies of most of the prM region. The genome of recombinant 2 differs from the wild-type genome by a short duplication in the C-terminal portion of the capsid protein gene, resulting in a duplication of the cleavage site for the viral NS2B/3 protease. **B.** Morphology of plaques produced in Vero cells infected with the cloned recombinants. Recombinant 1 produced plaques similar to those of wild-type virus, whereas recombinant 2 produced only small plaques. **C.** Growth curves. *Left:* Growth kinetics of wild-type virus and recombinant viruses in BHK-21 cells after infection at an MOI of 0.1. *Right:* Growth kinetics of wild-type JEV and recombinant viruses in C6/36 mosquito cells after infection at an MOI of 0.1

TABLE 1. Primers used for RT-PCR

Forward primer			Reverse primer			
	Position in full-length genome	in	Sequence (5'→3')	Position in full-length genome	Sequence (5'→3')	Possible amplicons
TBEV						
cDNA synthesis				NS-1 (nt 3700-3679)	ccaccacatagcgcaccagg	
RT-PCR 1	Capsid (214-235)	(nt)	caaccagagtccaaatgcaa	E (nt 2100-2081)	cagctgcatctctatgaagc	full-length: 1887 nt, ΔC: none, ΔME: none, ΔE: none
RT-PCR 2	5'NCR (nt 1-21)		gcagcgggttggttgaagag	E (nt 2100-2081)	cagctgcatctctatgaagc	full-length: 2100 nt, ΔC: 1915nts, ΔME: none, ΔE: none
RT-PCR 3	Capsid (214-235)	(nt)	caaccagagtccaaatgcaa	NS-1 (nt 3300-3279)	tccagttatcagagaggag	full-length: 3087 nt, ΔC: none, ΔME: 589 nt, ΔE: 1600 nt
WNV						
cDNA synthesis				NS-1 (nt 3700-3680)	tgacatagcgtaacacatcag	
RT-PCR 1	Capsid (164-187)	(nt)	gcgtgttgctcttgattgactga	E (nt 2100-2080)	gggtggtccaattcaatcag	full-length: 1937 nt, ΔC: none, ΔE: none
RT-PCR 2	5'NCR (nt 1-20)		agtagtgcctgtgtgagc	E (nt 2100-2080)	gggtggtccaattcaatcag	full-length: 2100 nt, ΔC: 1860 nt, ΔE: none
RT-PCR 3	Capsid (164-187)	(nt)	gcgtgttgctcttgattgactga	NS-1 (nt 3300-3280)	gaagtcaatctctaccggcc	full-length: 3137 nt, ΔC: none, ΔE: 1636 nt
JEV						
cDNA synthesis				NS-1 (nt 3407-3381)	ccagtcagtgatcaacttcca ctgtcag	
RT-PCR 1	Capsid (166-190)	(nt)	tattcccactagtgggagtgaag ag	E (nt 2130-2110)	ctacgatgtaggagtctccga	full-length: 1995 nt, ΔC: none, ΔE: none
RT-PCR 2	5'NCR (nt 48-67)		tcgagagattagtcagttt	E (nt 2130-2110)	ctacgatgtaggagtctccga	full-length: 2082 nt, ΔC: 1860 nt, ΔE: none
RT-PCR 3	Capsid (166-190)	(nt)	tattcccactagtgggagtgaag ag	NS-1 (nt 3079-3057)	ccagtcagacaagtactatg gac	full-length: 2913 nt, ΔC: none, ΔE: 2722 nt

Trans-complementing replicon pairs of TBEV evolve by the acquisition of spontaneous deletions but not recombination to infectious virus

Abstract

Many RNA viruses show high levels of genetic diversity and recombination can be frequently observed. Flaviviruses seem to exhibit an unusually low propensity for homologous recombination as demonstrated in a recent study. Among three different flaviviruses (tick-borne encephalitis virus, TBEV, West Nile virus, WNV, Japanese encephalitis virus, JEV) tested in a ‘recombination trap’ consisting of pairs of overlapping replicons, none underwent homologous recombination which would have generated infectious wild-type genomes. Only JEV yielded infectious genomes with unnatural genome organization by an aberrant recombination process. To further investigate the evolution of such trans-complementing replicon pairs upon repeated passages, we designed TBEV replicons which shared an exceptionally long (2kb) sequence overlap between the deletions in the genes encoding protein C or E, respectively. The two replicons could complement each other in the production of virus particles and could be serially passaged. As observed with shorter overlap regions, no recombination generating infectious full-length genomes was observed. Surprisingly, however, the replicon carrying a deletion in the E gene spontaneously extended this deletion to reach into the NS1 gene. These new mutants were incapable to replicate by themselves, but in the presence of the other replicon or wild-type virus, they were efficiently replicated and packaged. Cotransfection with wildtype virus proved that they behaved functionally as defective interfering particles. This represents the first characterization of DI RNAs of TBEV. Taken together our data demonstrate the ability of TBEV to undergo

intramolecular recombination but suggests that intermolecular recombination between different TBEV genomes is an unlikely event.

Introduction

TBEV belongs to the tick borne group of the genus flavivirus. Both experimental (Manuscript 1) and phylogenetic studies (147) on RNA recombination of tick-borne viruses failed to provide evidence for recombination to occur with this virus.. The close antigenic and phylogenetic relationships and the characteristics of their geographic distribution led to the proposal that viruses of this group had evolved in a gradual manner by the acquisition of point mutations (40). This contrasts with mosquito-borne flaviviruses which appeared to have evolved in a more discontinuous fashion which is demonstrated by the identification of recombinant genomes of JEV, all four dengue viruses and St.Louis encephalitis virus (Manuscript 1)(57, 143, 147, 148). In addition to recombination to full-length viruses, RNA viruses can generate recombinant subgenomic deletion RNAs designated defective interfering RNA (DI RNA). Such DI RNAs have been found in cell cultures persistently infected with west Nile virus (WNV), murray valley virus and JEV (15, 30, 86, 145, 155) but not with TBEV. It has been suggested that DI RNAs are generated according to the copy choice model of RNA recombination (17, 87, 116) (King, A.M.Q. 1988. Genetic recombination in positive strand RNA viruses, p150-185. In E. Domingo, J.J. Holland, and P. Ahlquist (ed.), RNA genetics II. CRC Press, Inc., Boca Raton Fla.) in which the viral RNA dependent RNA polymerase (RdRp) jumps either within (intramolecular) or between (intermolecular) templates during RNA replication. DI RNA genomes contain large internal deletions but retain all cis-acting regulatory sequences required for replication and packaging of the RNA. Their RNA replication depends on enzymes and structural proteins, provided by infectious

helper virus. Importantly, DI RNA can interfere with the replication of viruses able to act as helpers (121) and are most efficiently generated under conditions in which many infectious virus genomes simultaneously infect the same cell (55)

TBEV is a single stranded positive-sensed RNA virus. Its genome encodes only a single open reading frame which is translated into a polyprotein. Posttranslational cleavages by viral and host proteases yield three structural proteins: the capsid (C) protein, membrane (M) and envelope (E), as well as seven non-structural proteins that are essential for viral replication. Replicons, defined as a self-replicating, non-infectious RNA molecules, can be generated by deleting parts or all of the region coding for the structural proteins C, prM and E. In contrast to DI RNA genomes, replicons are capable of autonomous RNA replication. Recently, we have developed a recombination trap that favors the selection and sensitive detection of recombination products (Manuscript 1). This system involves two different replicons with reciprocal deletions of different parts of the structural region. Upon introduction of both replicons into the same host cell, each replicon provides the structural protein(s) that are missing in the other one. Complementation leads to packaging of both defective RNA genomes in two different viral particles and further rounds of infection are possible at a multiplicity of infection that allows sufficient coinfection. Possible recombinant full-length infectious viruses were shown to outgrow complementing replicons in limiting dilution passages, because they do not depend on coinfection (Manuscript 1). Using this system, we could demonstrate that replicons of JEV were able to recombine to full-length viruses by aberrant homologous recombination. In contrast replicons of TBEV and WNV sharing the same length of homologous sequence did not show evidence of recombination. In the here described study we wanted to further explore the evolutionary boundaries of tick-borne encephalitis virus in this experimental setting. Two replicons which shared almost 2kb homologous sequence where crossover yielding wild-type virus could occur were constructed and tested for their propensity for recombination. Despite selecting conditions for full-length

virus, one of the complementing replicons evolved by the acquisition of large internal deletions. These results provide evidence that TBEV exhibits a greater propensity for intramolecular adaptation than for recombination between different RNA genomes.

Materials and Methods

Cells. BHK-21 cells were grown in Eagle's minimal essential medium (Sigma) supplemented with 5% fetal calf serum (FCS), 1% glutamine and 0.5% neomycin (growth medium) and maintained in Eagle's minimal essential medium supplemented with 1% FCS, 1% glutamine, 0.5% neomycin and 15 mM HEPES, pH 7.4 (maintenance medium).

Plasmids and cloning procedures. Plasmid pTNd/c, used for generating infectious TBEV, contains a full-length genomic cDNA insert of TBEV strain Neudoerfl (GenBank accession number U27495) cloned in plasmid pBR322 (96). RNA transcribed from this plasmid was used as the TBEV wild-type virus control. Plasmid pTNd/5' contains a 5' cDNA fragment of the same viral genome (96). Full-length DNA templates for *in vitro* transcription of TBEV plasmids were generated as described previously (77). Plasmid pTNd/ Δ DIII was constructed using the following primers: tttcTACGTAacccaagaagcatagaaagac (SnaBI restriction site) and gcattATCGATtagtgtgactagcaggccatg (ClaI restriction site). pTNd/5' was used as template for the PCR, generating a SnaBI – ClaI fragment lacking domain III of the E protein. This fragment was cloned into plasmid pTNd/c generating a full-length replicon lacking the sequence coding for domain III of E (aa302-395) as well as additional 10 aa of the stem region of protein E (or nucleotides Δ 1884-2187 respectively). pTNd/c- Δ M-E-Ns1 and pTNd/c- Δ E-Ns1 were cloned using the amplicon of the RT-PCR-3 of RNA isolated after 6 serial passages of infectious combination Δ C + Δ DIII at limiting dilution. The PCR was carried out with primers that excluded the amplification of Δ C (see RT-PCR). The resulting

amplicons were digested with MluI and ClaI and cloned into pTNd/5'. E. coli colonies were screened for TBEV virus sequences with the following primers: forward primer corresponding to nucleotides 43-63, reverse primer corresponding to complementary nucleotides of 3170-3150. Positive clones were subjected to sequence analysis and revealed that of 40 positive clones 1 clone contained the original Δ DIII deletion, 4 contained a deletion of Δ E-Ns1 (nucleotides 986-3097) and the remaining 35 contained a deletion of Δ M-E-Ns1 (nucleotides 690-2999). One of Δ E-Ns1 and one of Δ M-E-Ns1 positive pTNd/5' clones were further digested with Sall and ClaI and the resulting fragment was cloned into pTNd/c generating pTNd/c- Δ E-Ns1 and pTNd/c- Δ E-Ns1 or into pTNd/c- Δ M-E-eGFP(42) resulting in pTNd/c- Δ E-Ns1-eGFP and pTNd/c- Δ E-Ns1-eGFP respectively.

RNA transfection. *In vitro* transcription and transfection of BHK-21 cells by electroporation were performed as described previously (79, 96, 114). RNA was synthesized (80)reagents of the T7 Megascript kit (Ambion) according to manufacturer's protocol. The template DNA was digested by incubation with DNase I, and the quality of the RNA was checked by electrophoresis in a 1% agarose gel containing 6% formalin. RNA was purified using an RNeasy Mini kit (Qiagen) and quantified spectrophotometrically. Equimolar amounts of RNA were then introduced into BHK-21 cells by electroporation using a Bio-Rad Gene Pulser (1.8kV, 25 μ F, 200 Ω). For cotransfections, equal amounts of RNA ($\sim 1.1 \cdot 10^{12}$ copies) of each construct were mixed before electroporation.

Immunofluorescence assays. Twenty-four hours after transfection or infection, BHK-21 cells were fixed for 20 min with 4% paraformaldehyde in PBS (pH 7.4) and then washed two times for 5 min with PBS (pH 7.4) and permeabilized with ice-cold methanol for 6 min at -20°C. After three washes with PBS (pH 7.4) and blocking with 3% BSA in PBS (pH 7.4) for 30 min at room temperature, intracellular E protein was visualized by sequential incubation

with a monoclonal mouse antibody against E (1E9) (48) and a Rhodamine-Red-X-conjugated anti-mouse IgG antibody (Jackson Immune Research Laboratory). Simultaneously, eGFP fluorescence was enhanced with a polyclonal rabbit-antibody against GFP (Abcam: ab6556) and successive incubation with fluorescein-isothiocyanate (FITC)-conjugated anti-rabbit IgG antibody (Jackson Immune Research Laboratory).

Endpoint passages. Supernatants of infected cells were sequentially diluted, and 200 μ l of each dilution was applied to fresh BHK-21 cells grown in 24-well plates (Nunc). After three days, half of the medium was replaced by fresh medium, and after six days, protein E released into the supernatant was detected using a four-layer enzyme-linked immunosorbent assay (ELISA)(53). After six days, the highest dilution yielding a positive signal in ELISA was cleared of cell debris, sequentially diluted and used for infection of fresh BHK-21 cells. Intracellular RNA genomes were analyzed at different passage numbers by northern blotting and RT-PCR (see below)

Northern blot analysis. Template DNA for synthesis of RNA probes for northern blotting was generated using the following primers and templates: TBEV: template pTNd/c and primers agagagcagaagggattga and tacttaatacgaactcactataggtgtgcaagacacccttg generated a probe binding to nucleotides 4093-4773 in wild-type virus. After phenol-chloroform purification of the template DNA, the T7 promoter sequence (underlined) fused to each reverse primer allowed RNA synthesis using a T7 MAXIscript In Vitro Transcription Kit (Ambion). The probe RNA was labeled by using 0.4 μ l of 10 mM Bio-11-UTP (Ambion) instead of UTP. Probe RNA was separated from free nucleotides using Micro Bio-Spin 30 columns (BioRad).

Cytoplasmic RNA was extracted from BHK-21 cells 24 hours after transfection or infection. Ten μ g of total RNA was applied to a 1% Agarose gel and northern blotting was

carried out according to the instructions of the NorthernMax-Gly Kit (Ambion), blotted RNA was detected using a BrightStar BioDetect Kit (Ambion).

RT-PCR. BHK-21 cells were seeded into 25-cm² tissue culture flasks. The monolayer of cells was infected with 2 ml supernatant of wild-type virus or infectious combination of replicons. After 24 hours post infection cytoplasmic RNA was extracted using RNeasy ® Mini Kit (Qiagen). Further cDNA was synthesized using a specific primer to TBEV (sequence reverse complementary to nucleotides 3700-3679 of plasmid pTNd/c) with the cDNA Synthesis system of ROCHE. Wild-type, replicon or possible recombinant genomes were detected using primers binding to a sequences present only in wild-type virus (RT-PCR 1) or replicon ΔC (RT-PCR) or replicon ΔDIII (RT-PCR 3) (see table 1) using the Advantage® HF2 PCR Kit (Clontech). As size control separately transfected control RNA of wild-type virus and each replicon RNA was used. Further, each obtained amplicon was subjected to sequence analysis (as described before (79)).

Table. 1. Primers used for RT-PCR analysis.

TBEV	Position in full-length genome	Forward (5'→3')	Position in full-length genome	Reverse (5'→3')	possible amplicons
cDNA synthesis			NS-1 (nt 3700-3679)	ccaccacatagcgcaccagg	
RT-PCR 1	Capsid (nt 214-235)	caaccagagtcctcaaatgcaa	E (nt 2100-2081)	cagctgcattctctatgaagc	full-length: 1887 nts ΔC: none ΔDIII: none
RT-PCR 2	5'NCR (nt 1-21)	gcagcgggttggttgaaagag	E (nt 2100-2081)	cagctgcattctctatgaagc	full-length: 2100 nts ΔC: 1915nts ΔDIII: none
RT-PCR 3	Capsid (nt 214-235)	caaccagagtcctcaaatgcaa	NS-1 (nt 3300-3279)	tccgagttatcagagaggag	full-length: 3087 nts ΔC: none ΔDIII: 2784 nts

Quantitative PCR. RNA replication and export kinetics were analyzed by quantitative real-time PCR (qPCR). For the determination of intracellular RNA copy numbers,

cells were collected at individual time points and counted in a Casy TT cell counter (Schärfe Systems). Cytoplasmic RNA was purified from a defined number of cells using an RNeasy Mini kit and subjected to qPCR. Primer and probes of each qPCR are listed in table 2. The same conditions were used for each qPCR as described in a previous study (79). For the measurement of viral RNA export, aliquots of supernatants were harvested at the same time points as those used for intracellular RNA levels and were cleared from cell debris and insoluble material by centrifugation. Next, 140 μ l of the supernatant was incubated with 35 μ l 5x RLN lysis buffer (250 mM Tris-Cl, pH 8.0, 700 mM NaCl, 7.5 mM MgCl₂, 2.5% [vol/vol] Nonidet P-40, 5 mM DTT) for 1 min on ice to break up the viral membrane. Viral RNA was further isolated from one-fifth of each lysate, again using an RNeasy Mini kit by following the protocol utilized for intracellular RNA purification. One-fifth of the isolated RNA then was used as a template for cDNA synthesis using an iScript cDNA synthesis kit (Bio-Rad) according to the manufacturer's protocol. An aliquot corresponding to 7 μ l of the original cell culture supernatant was subjected to qPCR using the same conditions as those for the quantification of intracellular RNA (79). The amounts of intra- and extracellular RNA were quantified by the comparison of the results to a standard curve. The standard curve was prepared by using a serial 10-fold dilution of spectrophotometrically quantified, purified, in vitro-synthesized RNA. The total amount of RNA present in each culture flask (intra- and extracellular) was further calculated from the measured RNA concentrations to determine the percentage of total RNA exported into the supernatant.

Table. 2. Primers used for qPCR analysis.

qPCR in NS5	5' → 3'	Position in wild-type sequence
forward Primer	GAAGCGGAGGCTGAACAACT	nt 7701-7720
reverse Primer	TTGTCACGTTCCGTCTCCAG	nt 7781-7762
Probe	TGTGTACAGGCGCACCCGCA	nt 7740-7759
qPCR in Capsid		

forward Primer	CAAATGGGCTTGTGTTGATG	nt 233-252
reverse Primer	GCACTCACCGTCCTTTTGAT	nt 383-364
Probe	GAAGGCGTTCTGGA ACTCAG	nt 309-328
qPCR in DIII of protein E		
forward Primer	CAGTGGGCATGATACAGTGG	nt 1932-1951
reverse Primer	AATTGTTGGGTTTGGCGTTA	nt 2064-2045
Probe	AAGCCCTGTAGGATCCCAGT	nt 1978-1997

Results

TBEV replicons with long redundant sequences can complement each other.

Earlier studies have shown that two replicons with deletions of different structural proteins (protein C or E) can produce infectious virus particles when they are present in the same cell. In this study, we further exploited this approach by constructing two replicons with different deletions in the region coding for the structural proteins and a 2kb long overlapping region between the respective deletions where recombination would generate full-length viral genomes. Replicon ΔC contained a large deletion (62aa) in the region coding for the capsid protein (78)(figure 1) and replicon $\Delta DIII$ contained a small deletion in protein E comprising the region coding for domain III (figure 1). The sequences between the two engineered deletions are present on both replicons and could potentially comprise sequence elements that facilitate template switch for intermolecular recombination to full-length virus. Although each replicon lacked an essential part of the structural region, all three structural proteins could be provided when both replicons were present in the same cell: Capsid (encoded on replicon $\Delta DIII$), prM (on both replicons) and E (only on replicon ΔC). To test this hypothesis, both mutants were cotransfected into BHK-21 cells and a first passage was discarded out with undiluted supernatant. The observation of infected cells stained with polyclonal TBEV serum

indicated that trans-complementation between replicon ΔC and $\Delta DIII$ took place and infectious virus particles were produced (data not shown).

Selection of recombination products. ComPLEMENTING replicons of TBEV were shown to be outgrown by few infectious units of full-length infectious virus in limiting passages (data not shown). Hence, to select for infectious full-length viruses, the following passages of complementing replicons ΔC and $\Delta DIII$ were done by serial dilution of supernatants of infected cells and determination of the endpoint dilution by ELISA after 6 days post infection. Typically, wild-type virus under these conditions grew to titers 10^6 to 10^7 whereas the replicon pairs achieved titers of only 10^2 to 10^3 . This can easily be explained by the fact that in the case of the replicons producing cells must be double infected. Upon passages, recombination to full length genome would have been expected to lead to growth to higher virus titers. However, over a course of 10 passages, no such shift to higher virus titers was observed suggesting that no recombination had occurred. To confirm this assumption, intracellular viral RNA was analyzed by northern blot analysis and RT-PCR. In the northern blot analysis wild-type virus (figure 2a lane 1) or separately transfected control RNA of replicon ΔC (figure 2a lane 4) and $\Delta DIII$ (figure 2a lane 5) produced a single band. As expected, only one band was visible after cotransfection of the two replicons ΔC and $\Delta DIII$ (figure 2a lane 2) because of almost equal genome size of the two constructs. Surprisingly, after 6 passages with these complementing replicons, northern blot analysis revealed two bands (figure 2a lane 3). This indicated that a new RNA genome smaller than the two original replicons had emerged. Interestingly, the smaller band was more prominent than the larger, indicating a selective advantage of the smaller genome.

Complementing TBE replicons evolve by intramolecular recombination. As a more sensitive and precise means of assessing which recombinant RNA molecules were present in the population, we devised a RT-PCR assay for detecting sequence rearrangement in the structural regions of the original complementing replicons ΔC and $\Delta DIII$. This was

accomplished by first making a cDNA copy of approximately the 5' half of the isolated intracellular RNA (extending to the middle of the NS1 gene) and then attempting to amplify a portion of this cDNA using different combinations of primers (for details see material and methods). First, the absence of RNA genomes encoding all three structural proteins on one molecule was confirmed. RT-PCR 1 with primers binding to sequences absent on both replicons (in the capsid and e genes) yielded a product only for cells infected with wild-type virus (figure 2b lane 1) but not for any replicon RNA (figure 2b lanes 2 and 3). The lack of amplicons from cells infected with complementing replicons ΔC and $\Delta DIII$ showed that no full-length virus genome were present even after repeated copassages (figure 2b lane 4).

Subsequently, each replicon was specifically identified with appropriately designed PCR assays. RT-PCR-2 with primers not binding to replicon $\Delta DIII$ (reverse primer in E gene) yielded the expected product of replicon ΔC (figure 2b lane 3) which is smaller than that of wild-type virus (figure 2b lane 1). After copassages replicon ΔC was still present (figure 2b lane 4). To specifically detect replicon $\Delta DIII$ RT-PCR-3 was designed with primers not binding to replicon ΔC . Again, amplicons of this replicons (figure 2b, lane2) were smaller than that of wild-type virus (lane 1). Interestingly, after co-passages of ΔC and $\Delta DIII$ (figure 2b lane 4) products were obtained that were smaller than the expected size for replicon $\Delta DIII$. Cloning and sequencing of these PCR products (for details see material and methods) revealed that the originally designed deletion within $\Delta DIII$ had been significantly extended in these emerged mutants: These new mutants were designated $\Delta E-NS1$ and $\Delta ME-NS1$ and their organization is shown in figure 1. Mutant $\Delta E-NS1$ contained an internal deletion lacking nucleotides 986 to 3097. The deleted sequence comprised the whole sequence coding for protein E and part of the non-structural protein NS1 and was therefore designated $\Delta E-NS1$ (figure 1). Mutant $\Delta ME-NS1$ contained an internal deletion of nucleotides 690 to 2999. The deletion comprised the mature protein M as well as the whole sequence coding for protein E as well as part of NS1 (figure 1). In summary, both emerged RNAs contained an enlarged

deletion compared to the original replicon Δ DIII. Both deletions affected the sequences coding for protein NS-1.

Emerged RNAs show characteristics of defective interfering RNAs. To examine whether the emerged mutants exhibit characteristics of DI RNA the deletions were introduced into the cDNA clone of full-length TBE virus (see materials and methods and figure 1). Then, the replication competence of each mutant in the absence of the complementing replicon Δ C was analyzed. BHK cells were transfected with full-length mutant RNA and intracellular RNA was quantified by quantitative PCR analysis.

As shown in figure 3a, transfected RNA of Δ E-NS1 and Δ ME-NS1 as well as of a replication deficient mutant Δ NS5 which contained a deletion in the region coding for the viral polymerase (79) were shown to decrease over time. In contrast, replicon Δ DIII and a replicon Δ R88 which exhibits a RNA replication level like wild-type virus (32) were capable of accumulating viral RNA within transfected cells. This confirmed that the two emerged mutants were incapable of autonomous RNA replication.

Furthermore, the effect of the emerged mutants on the replication of infectious wild-type virus was monitored (figure 3b). Equal amounts of wild-type virus RNA were co-transfected with each mutant. Viral titers were determined by focus assay and revealed that co-transfection of wild-type virus with either mutant resulted in a reduced titer. These results demonstrated that both emerged mutants could not!!! replicate without enzymes provided by helper virus and interfered with replication of infectious virus, both of which are characteristics of DI RNA.

DI RNAs are infectious by complementation with replicon Δ C. To analyze whether the observed DI RNAs Δ E-NS1 and Δ ME-NS1 can complement replicon Δ C and produce infectious virus particles the mutants were cotransfected with replicon Δ C. To allow separate detection of mutant RNA genomes and replicon Δ C DI RNAs were tagged with eGFP encoded in a second open reading frame in the 3'NCR as described previously (figure 1). Then, each GFP tagged DI RNA was co-transfected with replicon Δ C. Replication of DI

RNAs was monitored by the expression of eGFP and replication of replicon ΔC by the expression of protein E. As expected, transfection of replicon ΔC yielded cells expressing protein E (figure 4) and transfection of DI RNA genomes ΔE -NS1-eGFP and ΔME -NS1-eGFP resulted in cells negative for eGFP expression which further confirmed the replication deficiency of these mutants. However, co-transfection of replicon ΔC and either ΔE -NS1-eGFP or ΔME -NS1-eGFP yielded cells not only expressing protein E but also eGFP. This indicated that replicon ΔC could restore replication of the DI RNAs when both were present in the same cells.

Interestingly, after transfer of supernatants onto fresh cells, cells expressing only protein E but not eGFP, as well as cells expressing E and eGFP could be observed (figure 4). However, as expected, there were no cells expressing eGFP in the absence of protein E expression confirming that the eGFP expressing deletion mutants were not capable of self-replication in the absence of a helper replicon or virus. In addition, cells expressing both proteins indicated that both genomes were packaged into viral particles and coinfection with two viral particles containing different viral genomes resulted in another round of trans-complementation.

RNA replication and packaging of DI RNAs is complemented by replicon ΔC . To confirm that replicon ΔC is able to restore the replication of the DI RNAs which is required for trans-complementation, a quantitative PCR analysis was established. Primers and probes directed to the region absent on replicon ΔC allowed exclusive monitoring of replication and packaging of replicon $\Delta DIII$ or DI RNA genomes. Analysis of intracellular RNA revealed that RNA replication of DI RNA mutants ΔE -NS1 and ΔME -NS1 was restored to the level of the original replicon $\Delta DIII$ after cotransfection with replicon ΔC (figure 5a). Further, quantification of RNA released from cotransfected cells showed that DI RNAs were exported as efficiently as replicon $\Delta DIII$ after cotransfection with replicon ΔC (figure 5c). Concluding, replicon ΔC was able to restore RNA replication of DI RNA genomes, probably by providing a functional NS-1 protein. This again led to the presence of two replicating genomes coding

for all three necessary structural proteins and thus packaging of the DI RNAs ΔE -NS1 and ΔME -NS1.

DI RNAs interfere with RNA replication of replicon ΔC but increase its packaging efficiency. DI RNAs replicate by means of enzymes provided by infectious helper virus with which they interfere. To assess a possible inhibiting effect of DI RNAs on the replication of replicon ΔC a quantitative PCR analysis with primers and probe directed to the region coding for domain III of protein E was designed. This allowed the specific detection of replicon ΔC excluding all other mutant genomes. As shown in figure 5b, transfection of replicon ΔC alone or together with $\Delta DIII$ resulted in similar replication efficiencies, indicating that replicon $\Delta DIII$ did not interfere with the replication of replicon ΔC . In contrast cotransfection of replicon ΔC with one of the emerged DI RNAs, led to a decreased replication of replicon ΔC by at least one log (figure 5b). This result showed that mutants ΔE -NS1 and ΔME -NS1 not only interfered with replication of infectious full-length genomes but also with RNA replication of replicon ΔC . Despite the decreased replication, analysis of exported RNA revealed that almost equal amount of replicon ΔC was exported disregarding if the complementing partner was replicon $\Delta DIII$ or one of the emerged DI RNAs (figure 5d). Calculation of the export efficiency showed that RNA of replicon ΔC was exported more efficiently when the complementing partner was one of the emerged DI RNAs (figure 6). This means, that although DI RNA interfere with RNA replication of replicon ΔC , the overall efficiency of trans-complementation is not inhibited because of better packaging of replicon ΔC . Taken together, despite the presence of two viral genomes with long homologous sequences replicating in the same cell and the low efficiency of trans-complementation between the two replicons, an infectious full-length virus generated by intermolecular recombination was not detected in any passage. On the contrary, one of the two complementing replicons evolved by acquisition of large internal deletions, possibly by an intramolecular recombination process. The emerged mutants ΔE -NS1 and ΔME -NS1

exhibited classical DI RNA properties meaning they interfered not only with replication of infectious wildtype virus but also with RNA replication of replicon ΔC . However, in the trans-complementation system, this was compensated by an increased packaging efficiency of replicon ΔC . In summary, our data presents the first characterization of DI RNA of TBEV and suggests that TBEV has an extremely low propensity for intermolecular recombination.

Discussion

Unlike other RNA viruses, flaviviruses seem to have a low propensity for intermolecular recombination. Only recently we were able to provide the first direct proof for RNA recombination between two flavivirus genomes. Using a recombination trap designed to detect even rare recombination events we obtained two recombinants generated by intermolecular recombination between two complementing replicons of JEV. The established recombination trap consisted of pairs of self-replicating subgenomic RNAs (replicons) that, lacked different portions of the structural proteins. Individually, replicons can not produce infectious virions but in this system they could complement each other *in trans* and thus be propagated together in cell culture over multiple passages. Any infectious viruses with intact, full-length genomes that were generated by possible recombination of the two replicons would be selected and enriched by endpoint-dilution passage, as was demonstrated in spiking experiments. Interestingly, no viable recombinants were detected between replicons of WNV or TBEV despite the presence of 0,5kb homologous sequences where crossover could have occurred. To allow more detailed investigation of the types of recombination events that TBEV is capable of undergoing as well as their relative frequencies a similar approach was taken in this analysis: To provide optimal conditions for intermolecular recombination, we constructed two replicons of TBEV that shared 2kb long homologous sequences and only poorly complemented each other in virus particle production which would favor the selection

of recombinant full-length genomes even with reduced growth properties. Surprisingly, despite our extensive efforts we could not detect intermolecular recombination to infectious full-length viruses.

On the contrary, one of the two analyzed complementing replicons of TBEV adapted by the acquisition of large internal deletions. The loss of sequences not required for complementation in-cis resulted in two subgenomic RNAs that contained in frame deletions of the entire E gene and different portions of the flanking regions including the region coding for the N-terminal NS-1 protein. Strikingly, the lack of protein E and N-terminal part of NS-1 are features shared by all DI RNAs described for flaviviruses. Of 43 different DI RNAs described for JEV and MVE, the majority contained deletions affecting the regions coding for prM, E and NS-1 while only few also affected the region coding for protein C(145, 155). Interestingly, the deletions never affected the C-terminal part of NS-1. This is in good agreement with the observation that NS-1 can only be complemented in-trans efficiently if the C-terminal part is retained (69). This overall similar molecular organization of DI RNA of different flaviviruses and the fact that all deletions are in-frame suggests that DI RNAs are not generated by recombination hot spots but are selected because of their properties including their ability to be complemented in-trans.

Generally, DI RNAs emerge in association with infectious wild-type virus and interfere with its infectivity while depending on the help of the wild-type virus for RNA replication. Here, the observed RNA genomes Δ ME-NS-1 and Δ E-NS-1 showed classical DI RNA properties in association with wild-type virus. However in the two component trans-complementation system, infectivity depended on the presence of these mutants. Even though they interfered with the RNA replication of the non-infectious helper genome of replicon Δ C, the loss of sequences on the mutants not essentially required for complementation seemed to be advantageous. One possible reason is that the remaining part of protein E encoded by replicon Δ DIII is impedimental in assembly or when packaged into virions.

The generation of DI RNAs is believed to follow a similar or identical mechanism as true intermolecular recombination. One obvious example is the generation of DI RNA of Sindbis virus, in which tRNA sequences are incorporated at the 5' terminus of the virion RNA (146). Another example is provided by structural analysis of a DI RNA of influenza virus (34). The analyzed RNA has been shown to consist of several discontinuous regions, some of which were derived from influenza virus RNA-1 and others from RNA-3. Thus, it may represent a true recombinant RNA between two different RNA molecules, although both RNAs belong to the same virus. Moreover, in Coronavirus it was shown that recombination occurred more frequently within a hypervariable region (5), in which deletions commonly occur after virus passage in tissue culture or animals. Therefore we hypothesize that intermolecular recombination, the acquisition of internal deletions or the generation of DI RNAs are related. However, considering that in this study DI RNAs were generated despite conditions favoring the selection of full-length viruses generated by intermolecular recombination suggests that TBEV polymerase exhibits a lower propensity for inter- than for intramolecular recombination. This assumption is supported by the fact that under experimental conditions true intermolecular recombination has only been demonstrated for JEV (Manuscript 1). In contrast, DI RNAs were identified not only in cells persistently infected with JEV (145, 155) but also with MVE (86) and WNV(15). In addition, infectious West Nile or TBE viruses can quickly acquire large internal deletions or duplications (80, 127) probably by a mechanism similar to intramolecular recombination.

One possible explanation for this different propensity of inter- or intra-molecular recombination may be provided by the organization of the flavivirus replication complex. For flaviviruses RNA replication occurs in association with ~50–70 nm diameter membranous vesicles or spherules (151). It has been speculated that a single spherule contains only one or few (–) RNA templates for replication (81, 151) which would explain the low probability for template switches between different viral genomes. Another explanation may be that the

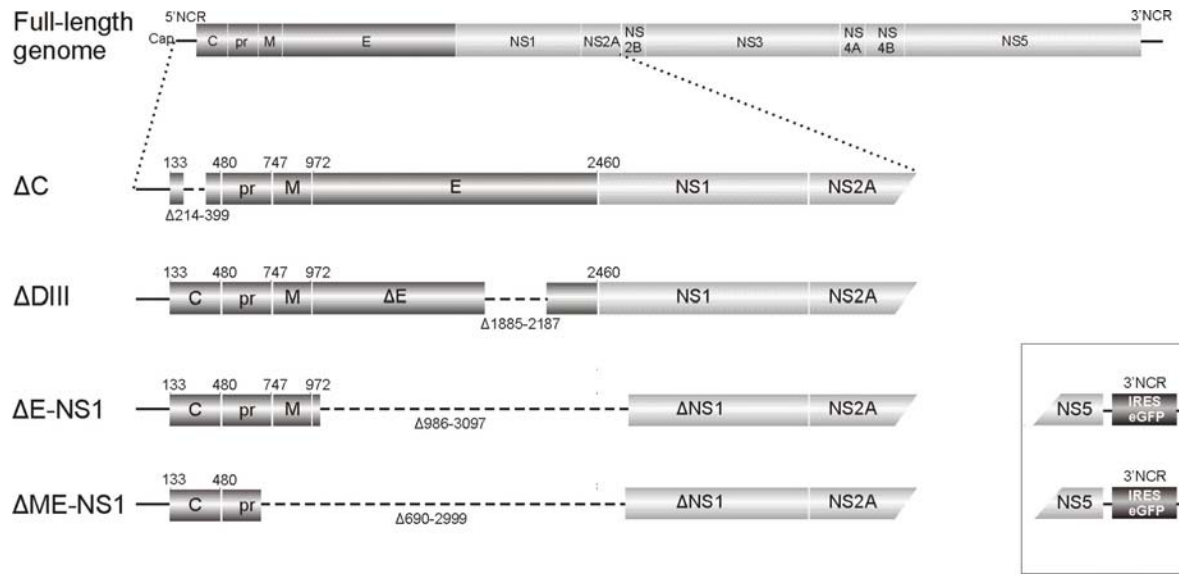
flavivirus replication complex itself accounts for the low propensity for template switches by a strong association to negative-sense template RNA.

In addition to RNA recombination, the described trans-complementation system allowed insights into flavivirus packaging. Separate detection of both involved viral RNAs and calculation of export efficiencies revealed that no direct correlation between RNA replication and packaging efficiency existed in this trans-complementation system. Although mutants ΔE -NS1 and ΔME -NS1 diminished the RNA replication of replicon ΔC , it was exported to similar levels as when the complementing partner was replicon $\Delta DIII$. This means that the packaging efficiency of replicon ΔC was not determined by sequences in-cis but by the in-trans complementing helper RNA suggesting that no RNA sequences but the way the three structural proteins are provided determined the packaging efficiency in this trans-complementation system. Notably, replicon $\Delta DIII$ did not affect the RNA replication of replicon ΔC . This suggests that two flaviviruses do not compete with each other on the level of RNA replication when both are capable of autonomous replication and that the interfering effect of DI RNA rests on the limited access of functional protein NS-1. In summary, we provide the first characterization of DI RNAs of TBEV and confirm that flaviviruses have an extremely low – if any – propensity for intermolecular recombination and show that TBEV has a higher propensity for intramolecular recombination. It will be interesting to determine what constraints are responsible for this discrepancy. Nevertheless, the general low propensity of TBEV to generate recombinants by intermolecular recombination makes this virus a reliable tool for vector development or live vaccines.

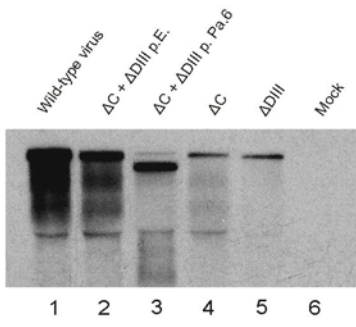
References

1. **Banner, L. R., J. G. Keck, and M. M. Lai.** 1990. A clustering of RNA recombination sites adjacent to a hypervariable region of the peplomer gene of murine coronavirus. *Virology* **175**:548-55.
2. **Brinton, M. A.** 1983. Analysis of extracellular West Nile virus particles produced by cell cultures from genetically resistant and susceptible mice indicates enhanced amplification of defective interfering particles by resistant cultures. *J Virol* **46**:860-70.
3. **Cascone, P. J., C. D. Carpenter, X. H. Li, and A. E. Simon.** 1990. Recombination between satellite RNAs of turnip crinkle virus. *Embo J* **9**:1709-15.
4. **Debnath, N. C., R. Tiernery, B. K. Sil, M. R. Wills, and A. D. Barrett.** 1991. In vitro homotypic and heterotypic interference by defective interfering particles of West Nile virus. *J Gen Virol* **72 (Pt 11)**:2705-11.
5. **Elshuber, S., S. L. Allison, F. X. Heinz, and C. W. Mandl.** 2003. Cleavage of protein prM is necessary for infection of BHK-21 cells by tick-borne encephalitis virus. *J Gen Virol* **84**:183-91.
6. **Fields, S., and G. Winter.** 1982. Nucleotide sequences of influenza virus segments 1 and 3 reveal mosaic structure of a small viral RNA segment. *Cell* **28**:303-13.
7. **Gao, G. F., W. R. Jiang, M. H. Hussain, K. Venugopal, T. S. Gritsun, H. W. Reid, and E. A. Gould.** 1993. Sequencing and antigenic studies of a Norwegian virus isolated from encephalomyelitic sheep confirm the existence of louping ill virus outside Great Britain and Ireland. *J Gen Virol* **74 (Pt 1)**:109-14.
8. **Gehrke, R., F. X. Heinz, N. L. Davis, and C. W. Mandl.** 2005. Heterologous gene expression by infectious and replicon vectors derived from tick-borne encephalitis virus and direct comparison of this flavivirus system with an alphavirus replicon. *J Gen Virol* **86**:1045-53.
9. **Guirakhoo, F., F. X. Heinz, and C. Kunz.** 1989. Epitope model of tick-borne encephalitis virus envelope glycoprotein E: analysis of structural properties, role of carbohydrate side chain, and conformational changes occurring at acidic pH. *Virology* **169**:90-9.
10. **Heinz, F. X., W. Tuma, F. Guirakhoo, and C. Kunz.** 1986. A model study of the use of monoclonal antibodies in capture enzyme immunoassays for antigen quantification exploiting the epitope map of tick-borne encephalitis virus. *J Biol Stand* **14**:133-41.
11. **Holland, J., K. Spindler, F. Horodyski, E. Grabau, S. Nichol, and S. VandePol.** 1982. Rapid evolution of RNA genomes. *Science* **215**:1577-85.
12. **Holmes, E. C., M. Worobey, and A. Rambaut.** 1999. Phylogenetic evidence for recombination in dengue virus. *Mol Biol Evol* **16**:405-9.
13. **Khromykh, A. A., P. L. Sedlak, and E. G. Westaway.** 2000. cis- and trans-acting elements in flavivirus RNA replication. *J Virol* **74**:3253-63.
14. **Kofler, R. M., J. H. Aberle, S. W. Aberle, S. L. Allison, F. X. Heinz, and C. W. Mandl.** 2004. Mimicking live flavivirus immunization with a noninfectious RNA vaccine. *Proc Natl Acad Sci U S A* **101**:1951-6.
15. **Kofler, R. M., F. X. Heinz, and C. W. Mandl.** 2002. Capsid protein C of tick-borne encephalitis virus tolerates large internal deletions and is a favorable target for attenuation of virulence. *J Virol* **76**:3534-43.
16. **Kofler, R. M., F. X. Heinz, and C. W. Mandl.** 2004. A novel principle of attenuation for the development of new generation live flavivirus vaccines. *Arch Virol Suppl*:191-200.

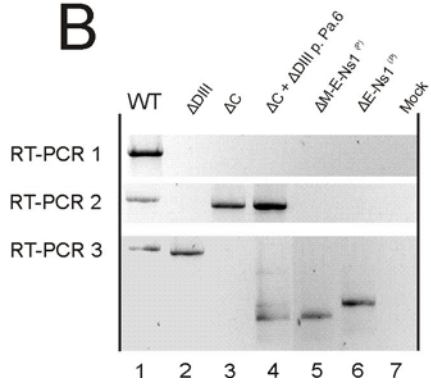
17. **Kofler, R. M., V. M. Hoenninger, C. Thurner, and C. W. Mandl.** 2006. Functional analysis of the tick-borne encephalitis virus cyclization elements indicates major differences between mosquito-borne and tick-borne flaviviruses. *J Virol* **80**:4099-113.
18. **Kofler, R. M., A. Leitner, G. O'Riordain, F. X. Heinz, and C. W. Mandl.** 2003. Spontaneous mutations restore the viability of tick-borne encephalitis virus mutants with large deletions in protein C. *J Virol* **77**:443-51.
19. **Kopek, B. G., G. Perkins, D. J. Miller, M. H. Ellisman, and P. Ahlquist.** 2007. Three-dimensional analysis of a viral RNA replication complex reveals a virus-induced mini-organelle. *PLoS Biol* **5**:e220.
20. **Lancaster, M. U., S. I. Hodgetts, J. S. Mackenzie, and N. Urosevic.** 1998. Characterization of defective viral RNA produced during persistent infection of Vero cells with Murray Valley encephalitis virus. *J Virol* **72**:2474-82.
21. **Lazzarini, R. A., J. D. Keene, and M. Schubert.** 1981. The origins of defective interfering particles of the negative-strand RNA viruses. *Cell* **26**:145-54.
22. **Mandl, C. W., M. Ecker, H. Holzmann, C. Kunz, and F. X. Heinz.** 1997. Infectious cDNA clones of tick-borne encephalitis virus European subtype prototypic strain Neudoerfl and high virulence strain Hypr. *J Gen Virol* **78 (Pt 5)**:1049-57.
23. **Orlinger, K. K., V. M. Hoenninger, R. M. Kofler, and C. W. Mandl.** 2006. Construction and mutagenesis of an artificial bicistronic tick-borne encephalitis virus genome reveals an essential function of the second transmembrane region of protein e in flavivirus assembly. *J Virol* **80**:12197-208.
24. **Perrault, J.** 1981. Origin and replication of defective interfering particles. *Curr Top Microbiol Immunol* **93**:151-207.
25. **Reichmann, M. E., and W. M. Schnitzlein.** 1979. Defective interfering particles of rhabdoviruses. *Curr Top Microbiol Immunol* **86**:123-68.
26. **Schlick, P., C. Taucher, B. Schittl, J. L. Tran, R. M. Kofler, W. Schueler, A. von Gabain, A. Meinke, and C. W. Mandl.** 2009. Helices $\{\alpha\}_2$ and $\{\alpha\}_3$ of WNV Capsid Protein are Dispensable for the Assembly of Infectious Virions. *J Virol*.
27. **Tolou, H. J., P. Couissinier-Paris, J. P. Durand, V. Mercier, J. J. de Pina, P. de Micco, F. Billoir, R. N. Charrel, and X. de Lamballerie.** 2001. Evidence for recombination in natural populations of dengue virus type 1 based on the analysis of complete genome sequences. *J Gen Virol* **82**:1283-90.
28. **Tsai, K. N., S. F. Tsang, C. H. Huang, and R. Y. Chang.** 2007. Defective interfering RNAs of Japanese encephalitis virus found in mosquito cells and correlation with persistent infection. *Virus Res* **124**:139-50.
29. **Tsiang, M., S. S. Monroe, and S. Schlesinger.** 1985. Studies of defective interfering RNAs of Sindbis virus with and without tRNA^{Asp} sequences at their 5' termini. *J Virol* **54**:38-44.
30. **Twiddy, S. S., and E. C. Holmes.** 2003. The extent of homologous recombination in members of the genus *Flavivirus*. *J Gen Virol* **84**:429-40.
31. **Uzcategui, N. Y., D. Camacho, G. Comach, R. Cuello de Uzcategui, E. C. Holmes, and E. A. Gould.** 2001. Molecular epidemiology of dengue type 2 virus in Venezuela: evidence for in situ virus evolution and recombination. *J Gen Virol* **82**:2945-53.
32. **Welsch, S., S. Miller, I. Romero-Brey, A. Merz, C. K. Bleck, P. Walther, S. D. Fuller, C. Antony, J. Krijnse-Locker, and R. Bartenschlager.** 2009. Composition and three-dimensional architecture of the dengue virus replication and assembly sites. *Cell Host Microbe* **5**:365-75.
33. **Yoon, S. W., S. Y. Lee, S. Y. Won, S. H. Park, S. Y. Park, and Y. S. Jeong.** 2006. Characterization of homologous defective interfering RNA during persistent infection of Vero cells with Japanese encephalitis virus. *Mol Cells* **21**:112-20.

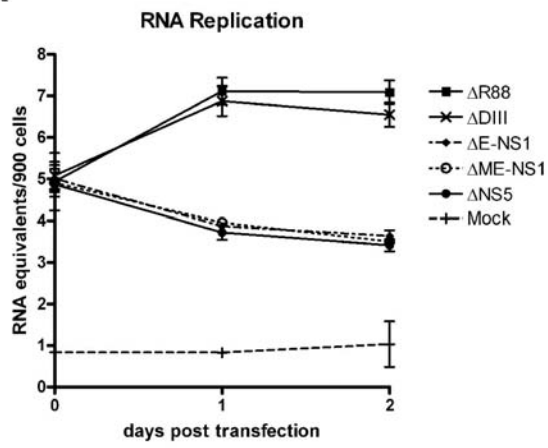
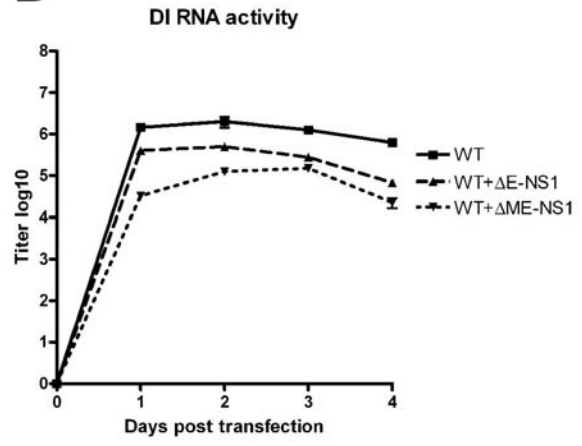


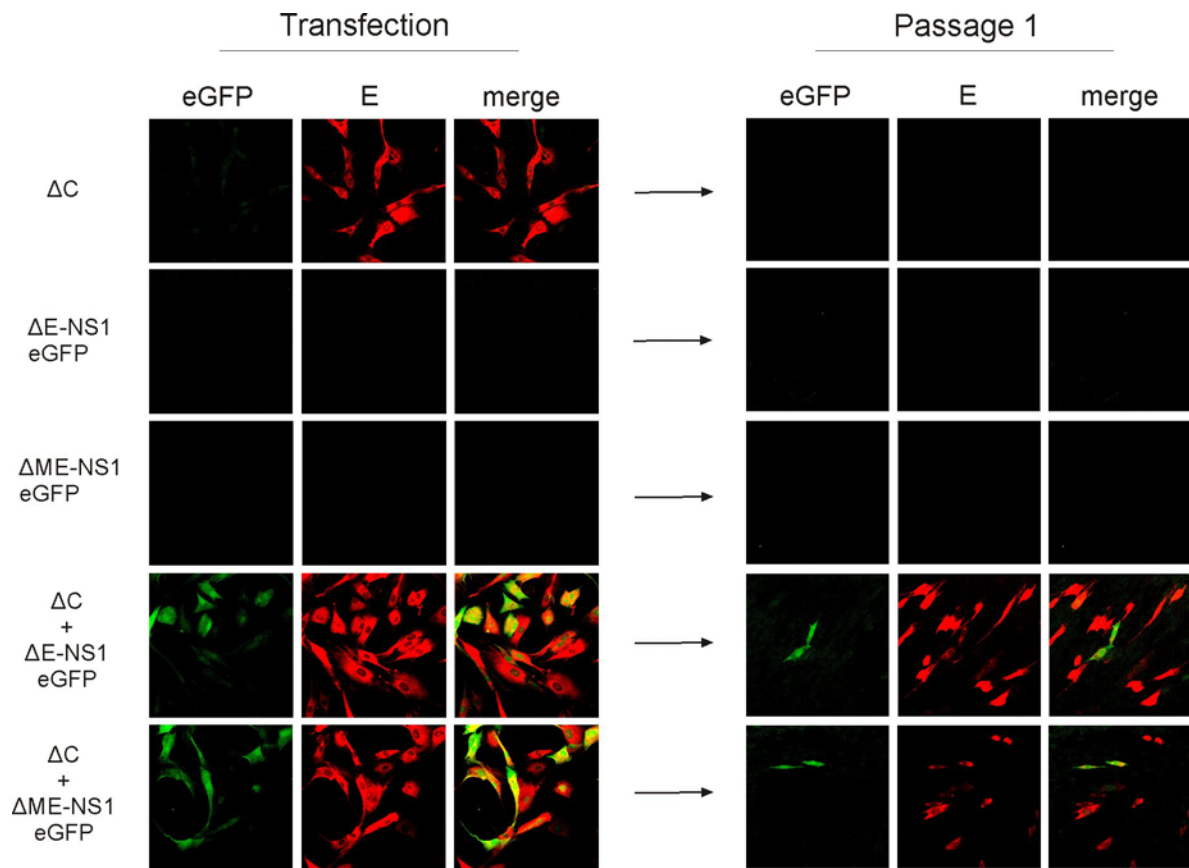
A

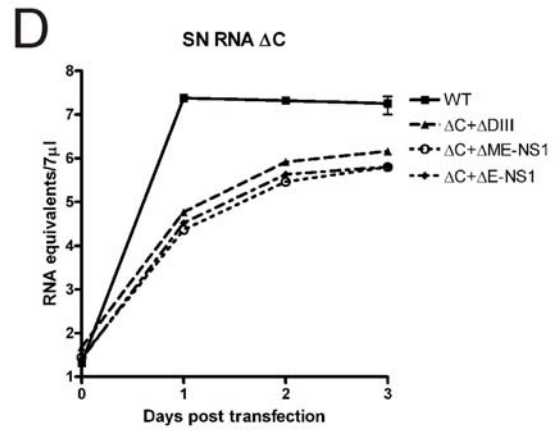
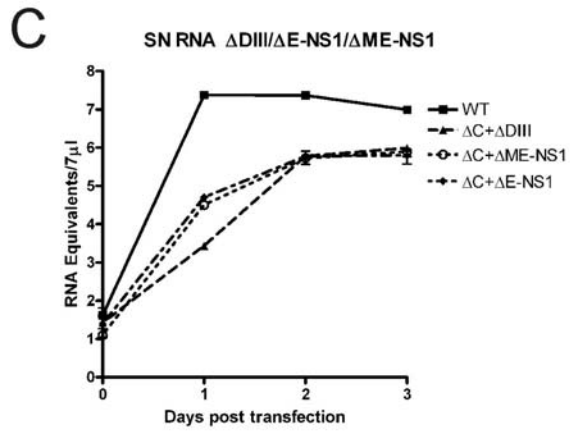
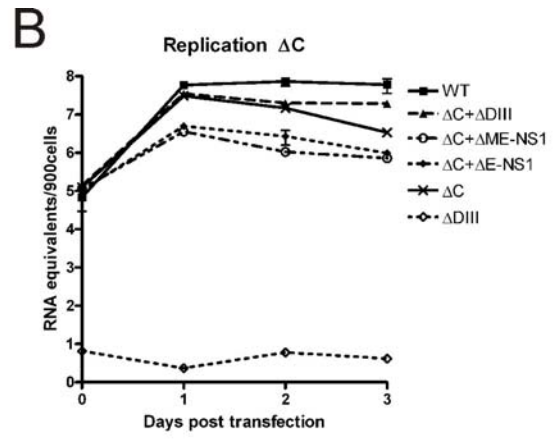
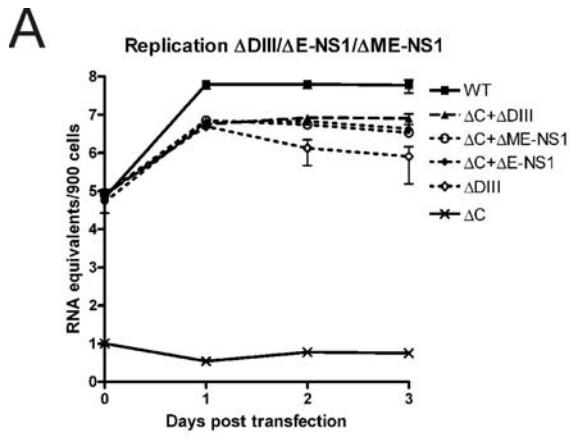


B



A**B**





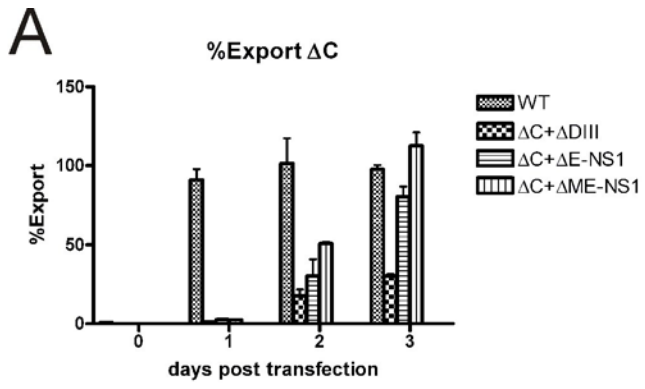


Figure Legends

Figure 1. *Top:* Schematic drawing of a full-length flavivirus genome. *Below:* Schematic blow up of the structural region of TBEV replicons ΔC (76), and replicon $\Delta DIII$ as well as DI RNA genomes $\Delta E-NS1$ and $\Delta ME-NS1$. *Box.* An internal ribosomal entry site (IRES) driven translation element of eGFP was cloned in the 3' noncoding region of the emerged DI RNAs. Deletions are indicated by dotted lines and the missing nucleotides are indicated within each deletion. Nucleotide numbers refer to the position in each respective wild-type virus sequence. The length of homologous sequences allowing recombination yielding full-length virus is indicated at left. C: capsid protein; pr: pr part of protein prM; M: mature protein prM; E: protein E, NS: non-structural protein; NCR: non coding region

Figure 2. A. Northern blot analysis of intracellular viral RNA: Lane 1. RNA of cells infected with wild-type virus. Lane 2: RNA of cells transfected with replicon ΔC as well as $\Delta DIII$. Lane 3: RNA of cells infected with supernatant containing replicons ΔC and $\Delta DIII$ after 6 passages. Lane 4: RNA of cells transfected with replicon ΔC alone. Lane 5: RNA of cells transfected with replicon $\Delta DIII$ alone. Lane 6: mock transfected cells. **B.** RT-PCR analysis of intracellular RNA. RT-PCR-1 was performed with primers binding to sequences absent on both replicons. RT-PCR-2 was performed with primers allowing amplification of replicon ΔC . RT-PCR 3 was performed with primers binding to sequences absent of replicon ΔC . Lane 1. RNA of cells infected with wild-type virus. Lane 2: RNA of cells transfected with replicon $\Delta DIII$. Lane 3: RNA of cells transfected with replicon ΔC alone. Lane 4: RNA from cells infected with supernatant containing replicons ΔC and $\Delta DIII$ after 6 passages. Lane 5: RNA of cells transfected with cloned RNA of $\Delta E-NS-1$. Lane 6: RNA of cells transfected with cloned RNA of $\Delta ME-NS-1$. Lane 7: RNA of mock transfected cells.

Figure 3. A. Quantitative PCR with primer and probes binding to sequences coding for NS-5 of intra-cellular RNA after RNA transfection. $\Delta R88$ is a non-infectious TBE virus with a single amino acid deletion which replicates to wild-type virus levels. $\Delta NS5$ lacks the 3' terminal part of the TBEV genome including the sequences coding for NS5 and serves as a control for a non-replicating viral genome. **B.** Analysis of the interfering effect of the emerged RNAs on wild-type virus. Cells were transfected with wild-type virus and equal amounts of $\Delta E-NS-1$ or $\Delta ME-NS-1$. Infectious units were quantified by focus assay.

Figure 4. Co-immunofluorescence staining with antibody against eGFP and protein E. Cells were transfected with the respective constructs and protein expression was monitored 24 hours post-transfection. Due the secondary antibodies cells expressing eGFP appear in green (FITC) and cells expressing protein E in red (rodhamine red). After 3 days post transfection supernatant was harvested and used to transfect fresh cells. Again, cells were stained 24 hours post infection.

Figure 5. A. Quantitative PCR of intracellular RNA of cells transfected with viral RNA as indicated. Primers and probes bound to sequences coding for the capsid protein which excluded the detection of replicon ΔC . **B.** Quantitative PCR of intracellular RNA of cells transfected with viral RNA as indicated. Primers and probes bound to sequences coding for domain III of protein E which excluded the detection of all mutant RNAs except replicon ΔC . **C.** Quantitative PCR of RNA in the supernatant of cells transfected with viral RNAs as indicated. Primer and probes as in A. **D.** Quantitative PCR of RNA in the supernatant of cells transfected with viral RNAs as indicated. Primer and probes as in B.

Figure 6. Export efficiencies of replicon ΔC calculated by the percentage of extra cellular RNA in relation to intra-cellular RNA.

Manuscript 3

**Helices $\alpha 2$ and $\alpha 3$ of WNV capsid protein are dispensable for the assembly
of infectious virions**

Helices $\alpha 2$ and $\alpha 3$ of West Nile Virus Capsid Protein Are Dispensable for Assembly of Infectious Virions[∇]

Petra Schlick,^{1*} Christian Taucher,^{2†} Beate Schittl,^{1‡} Janina L. Tran,^{1§} Regina M. Kofler,^{2¶} Wolfgang Schueler,¹ Alexander von Gabain,¹ Andreas Meinke,¹ and Christian W. Mandl^{2||}

Intercell AG, Campus Vienna Biocenter, Vienna, Austria,¹ and Clinical Institute of Virology, Medical University of Vienna, Vienna, Austria²

Received 24 December 2008/Accepted 13 March 2009

The internal hydrophobic sequence within the flaviviral capsid protein (protein C) plays an important role in the assembly of infectious virions. Here, this sequence was analyzed in a West Nile virus lineage I isolate (crow V76/1). An infectious cDNA clone was constructed and used to introduce deletions into the internal hydrophobic domain which comprises helix $\alpha 2$ and part of the loop intervening helices $\alpha 2$ and $\alpha 3$. In total, nine capsid deletion mutants (4 to 14 amino acids long) were constructed and tested for virus viability. Some of the short deletions did not significantly affect growth in cell culture, whereas larger deletions removing almost the entire hydrophobic region significantly impaired viral growth. Efficient growth of the majority of mutants could, however, be restored by the acquisition of second-site mutations. In most cases, these resuscitating mutations were point mutations within protein C changing individual amino acids into more hydrophobic residues, reminiscent of what had been observed previously for another flavivirus, tick-borne encephalitis virus. However, we also identified viable spontaneous pseudorevertants with more than one-third of the capsid protein removed, i.e., 36 or 37 of a total of 105 residues, including all of helix $\alpha 3$ and a hydrophilic segment connecting $\alpha 3$ and $\alpha 4$. These large deletions are predicted to induce formation of large, predominantly hydrophobic fusion helices which may substitute for the loss of the internal hydrophobic domain, underlining the unrivaled structural and functional flexibility of protein C.

The genus *Flavivirus* within the family *Flaviviridae* comprises important human pathogens such as Japanese encephalitis virus (JEV), the dengue viruses (DENV), yellow fever virus (YFV), tick-borne encephalitis virus (TBEV) and West Nile virus (WNV) (28). The ~50-nm flavivirus virion is composed of two surface proteins, envelope (E) and membrane (M, derived from its precursor protein prM by furin-mediated cleavage), and the nucleocapsid consisting of the capsid protein (protein C) and the 11-kb positive-stranded RNA genome. In addition to the three structural proteins C, prM, and E, the genome encodes seven nonstructural proteins (NS1, NS2A, NS2B, NS3, NS4A, NS4B, and NS5), which are necessary for replication of the RNA genome (28). Structural and nonstructural proteins are derived from a single polyprotein, which is co- and posttranslationally processed into mature proteins by viral and cellular proteases (6, 28).

The assembly of the virions is thought to occur at the membrane of the rough endoplasmic reticulum (ER) (28, 32). Protein C, which is the protein located at the very N terminus of the polyprotein, facilitates translocation of the subsequent pro-

tein prM into the lumen of the ER via an internal signal sequence located at its C terminus. Proteins prM and E remain attached to the host-derived membrane by spanning the lipid bilayer twice via their C-terminal anchor regions (38, 47, 48). Protein C is originally also anchored to the ER membrane via the C-terminal internal signal sequence. However, this signal sequence is cleaved off by the viral NS2B/3 protease, thereby producing the mature, cytoplasmic form of the protein (4, 30, 40). Multiple copies of protein C and one copy of the RNA genome form the nucleocapsid. In the virion, the nucleocapsid appears not to directly interact with the surrounding membrane and the embedded surface proteins prM and E (47) and furthermore lacks, in contrast to the icosahedrally arranged surface proteins, a well-ordered structure (25, 49). Instead, the nucleocapsid may nonspecifically interact with the ER membrane during budding by virtue of a hydrophobic, mostly helical sequence element which is present at a conserved position in all of the flavivirus protein C sequences (31, 35).

The recently solved three-dimensional (3D) structures of the DENV-2 and Kunjin virus C proteins (Kunjin virus is an Australian strain of WNV) (11, 31) support this notion. The nuclear magnetic resonance 3D structure of DENV-2 protein C indicates that the protein, composed of four α helices, forms a dimer in solution (31). The contact surfaces for dimerization are provided by helices $\alpha 2$ and $\alpha 4$. Helix $\alpha 2$ comprises most of the internal hydrophobic sequence within protein C. After dimerization, the interacting helices $\alpha 2$ form the bottom of a hydrophobic cleft. The highest density of positively charged residues is found on the opposite side of the dimer, on the surfaces of helices $\alpha 4$, which interact by forming a coiled coil. Accordingly, a model suggesting that the hydrophobic cleft

* Corresponding author. Mailing address: Intercell AG, Campus Vienna Biocenter 3, A-1030 Vienna, Austria. Phone: 43-1-20620-1305. Fax: 43-1-20620-81305. E-mail: pschlick@intercell.com.

† These authors contributed equally to the study.

‡ Present address: Institute of Virology, Helmholtz Center Munich, Neuherberg, Germany.

§ Present address: Veterinary Centre Departments of the Municipal District Office, Vienna, Austria.

¶ Present address: Lambda GmbH, Freistadt, Austria.

|| Present address: Novartis Vaccines and Diagnostics, Inc., Cambridge, MA.

∇ Published ahead of print on 18 March 2009.

presumably enables the nucleocapsid to attach to the membrane and that helices $\alpha 4$ play a potential role in interaction with the negatively charged RNA genome has been established (31).

The functional importance of the conserved internal hydrophobic domain in virus assembly and/or dimerization of protein C is supported by studies with a variety of flaviviruses. For instance, removal of major parts of this sequence element in TBEV resulted in an increased formation of capsidless subviral particles (19), the secretion of which is also observed in the course of natural infection or by expression of proteins prM and E only (1, 22–24, 36). Large deletions were tolerated only upon the acquisition of additional mutations increasing the hydrophobicity of the protein (21). These results are in good accordance with studies of YFV protein C (42) and WNV, in which case removal of the entire helix $\alpha 2$ produced a noninfectious phenotype (44). Furthermore, in DENV, removing large parts of the hydrophobic domain abolished both the ability to dimerize in vitro (46) and the ability to associate with the ER membrane (35). Taken together, these studies underlined the important roles of the conserved internal hydrophobic sequence in dimerization of protein C and virion assembly.

In the present study, we set out to systematically test the functional role of the hydrophobic sequence of WNV protein C for viral infectivity by introducing deletions ranging from 4 to 14 amino acids. Some of the smaller deletions were well tolerated, whereas growth with others was, consistent with previous findings with TBEV (21), dependent on the acquisition of second-site point mutations. Surprisingly, two well-replicating pseudorevertants were shown to have restored growth capability through spontaneously enlarged deletions. These mutants lacked more than one-third of the protein C sequence. The spontaneously deleted sequences included all of helix $\alpha 3$ and a hydrophilic loop connecting helices $\alpha 3$ and $\alpha 4$. Our data provide evidence that although removal of large parts or the entire internal hydrophobic domain usually causes severe defects in viral growth, truncating protein C even further can largely revert this impairment. A viable WNV mutant with capsid proteins less than two-thirds of the size of the natural protein was generated by reverse genetics, and its growth properties were analyzed in comparison to those of the wild-type virus. Secondary-structure predictions suggest that in these mutants, the formation of large, hydrophobic fusion helices might compensate for the loss of the conserved hydrophobic domain.

MATERIALS AND METHODS

Cells and virus. Vero (ATCC CCL-81) cells were grown in Eagle's minimal essential medium (EMEM) supplemented with 10% fetal bovine serum (FBS; PAA Laboratories), 1.5% glutamine (200 mM; Cambrex), 1% penicillin-streptomycin (10,000 U/ml penicillin and 10 mg/ml streptomycin; Sigma), and 15 mM HEPES, pH 7.4. Infections were performed in the presence of 2% instead of 10% FBS, and after infection, cells were maintained in medium lacking FBS. For virus stock production, FBS was replaced with 1% (wt/vol) bovine serum albumin (BSA). BHK-21 cells used for introduction of in vitro-transcribed RNA were handled in growth medium (EMEM supplemented with 5% FBS, 1% glutamine, 0.5% [10 mg/ml] neomycin, and 15 mM HEPES, pH 7.4) and maintenance medium (EMEM supplemented with 1% FBS, 1% glutamine, 0.5% neomycin, and 15 mM HEPES, pH 7.4) as described earlier (19, 33, 41).

The WNV strain used in this study was originally isolated from a dead crow collected during the summer of 1999 in New York City (crow V76/1). The virus was passaged three times in Vero cells and once in suckling mouse brain prior to the construction of the infectious cDNA clone.

Cloning procedures. The two partial cDNA clones pWNV-K1 and pWNV-K4 were constructed as described in previous studies (7, 33, 45), with the exception that pBR322 (5) had been modified by replacing the tetracycline resistance gene with a multiple-cloning site (BspEI-SwaI-PacI-NotI-SwaI-AatII). For the introduction of deletions into the capsid protein within plasmid pWNV-K1, the Gene Tailor site-directed mutagenesis system (Invitrogen) was used. Detailed primer sequences for all constructs are available from the authors upon request.

All constructs were amplified in *Escherichia coli* strain DH5 α cells and characterized by complete sequencing of both strands of the entire inserts.

In vitro RNA transcription and transfection. In vitro transcription with T7 RNA polymerase (Ambion T7 Megascript transcription kit) and transfection of BHK-21 cells by electroporation were performed as described in previous studies (12, 19). In the case of transcription reactions required as standards in real-time PCR analysis, the pWNV-K1 template DNA was degraded by incubation with DNase I for 15 min at 37°C, and the RNA was purified and separated from unincorporated nucleotides by using an RNeasy Mini kit (Qiagen). RNA concentrations were estimated from band intensities or, for determination of the RNA standard concentration, measured spectrophotometrically.

Immunofluorescence staining. Intracellular expression of WNV specific proteins was determined by indirect immunofluorescence staining of the envelope protein E. Accordingly, RNA-transfected BHK-21 cells were seeded into 24-well plates and supplied with growth medium (EMEM with supplements and 5% FBS), which was exchanged for maintenance medium (EMEM with supplements and 1% FBS) at 20 h posttransfection. After 24 or 48 h, cells were treated with 1:1 acetone-methanol for fixation and permeabilization. To specifically detect WNV protein E, a cross-reactive polyclonal antibody directed against JEV protein E was used (dilution, 1:50). Staining was performed with a secondary fluorescein isothiocyanate-conjugated anti-rabbit antibody (Jackson ImmunoResearch Laboratories) as suggested by the manufacturer.

Hemagglutination assay (HA). For the detection of WNV viral and/or subviral particles in supernatants of infected cells, a rapid assay based on the agglutination of erythrocytes, which is induced by the interaction with viral particles, was applied (8, 13). Briefly, virus supernatants were diluted 1:1 in borate-buffered saline (120 mM sodium chloride, 50 mM sodium borate, pH 9.0) containing 0.4% BSA for particle stabilization. Subsequently, this mixture was further diluted to produce a geometrical dilution row. Fifty microliters of each of the diluted samples was mixed with the same amount of a 0.5% solution of goose erythrocytes in round-bottom 96-well plates and incubated for 3 h at room temperature. Virus-induced agglutination of erythrocytes was visible by the lack of sedimented erythrocytes; the examination of plates was performed by visual inspection.

Mutant stability. To assay the genetic stability of transfected mutants, supernatants of transfected cells were diluted until the end point of infectivity was reached. The supernatant corresponding to the end point was then transferred onto fresh cells, and these passages were repeated at least twice. Subsequently, RNA was isolated and sequence analysis was performed by using the cDNA synthesis system of Roche Applied Science and standard PCR and sequencing protocols.

RNA replication and export. Intracellular RNA replication was monitored by real-time PCR as described previously (20, 41) with minor modifications. Briefly, Vero cells grown in six-well plates were incubated with wild-type and mutant WNV stock preparations at a multiplicity of infection (MOI) of 1. After 1 h, the cell monolayer was washed and supplied with growth medium which contained 1% BSA and 15 mM HEPES instead of FBS. At selected time points, cells were detached by trypsin incubation and washed twice in phosphate-buffered saline (PBS) (pH 7.4) containing 1% BSA. Cytoplasmic RNA was purified from these cells (RNeasy Mini kit; Qiagen) and was subjected to real-time PCR (PE Applied Biosystems) quantification as described previously (20, 41). The primers (5'-TC AGCGATCTCTCCACCAAAG-3' and 5'-GGGTCAGCACGTTTGTTCATTG-3') and probe (5'-Fam-TGCCCGACCATGGGAGAAGCT-Tamra-3') targeted a region within the envelope gene of the WNV genomic RNA. RNA equivalents were finally determined from a standard curve based on an RNA preparation of known concentration which was serially diluted in cell lysates of negative control cells and purified according to the same protocol.

The RNA content in supernatants of transfected cells was measured as published recently (41). Accordingly, prior to quantification by real-time PCR, aliquots of supernatants were cleared by low-speed centrifugation and RNA was purified by using the QIAamp viral RNA Mini kit (Qiagen) as suggested by the manufacturer. RNA export was finally calculated by determining the percentage of total RNA (intracellular and extracellular) in the supernatant fraction.

Cytotoxicity assay. Similar to the RNA replication and export experiments, Vero cells were seeded into six-well plates and infected with WNV stock preparations at an MOI of 1, but the growth medium did not contain BSA. Aliquots of supernatants were transferred into 96-well plates, and cytotoxicity was as-

TABLE 1. WNV V76/1 isolate-specific genomic sequence differences

Nucleotide no. ^a	Nucleotide in:		Amino acid difference	Location
	NY99-flamingo382-99 (GenBank accession no. AF196835) ^b	WNV V76/1 (GenBank accession no. FJ151394)		
1118	C	U	A → V	E
1285	C	U	Silent	E
3138	U	C	Silent	NS1
6735	C	A	Silent	NS4A
7015	U	C	Silent	NS4B
7491	G	U	Silent	NS4B
8811	U	C	Silent	NS5
10851	A	G	NA ^c	3' noncoding region

^a Genome position numbers are the same for both isolates.

^b The genomic sequence of the isolate used for sequence comparison (GenBank accession no. AF196835) is published in reference 27.

^c NA, not applicable.

essed by measuring the release of lactate dehydrogenase (LDH) using the CytoTox 96 nonradioactive cytotoxicity assay (Promega) according to the manufacturer's instructions.

Plaque morphology and immunocytochemistry. Vero cells were grown to 80% confluence in 12-well plates and incubated for 1 h with virus suspensions serially diluted in infection medium. The cells were subsequently overlaid with EMEM containing 5% FBS (PAA Laboratories), 1.5% glutamine (200 mM; Cambrex), 1% penicillin-streptomycin (10,000 U/ml penicillin and 10 mg/ml streptomycin; Sigma), 15 mM HEPES, and 0.25% agarose (Sigma). The plaque morphology was determined following an incubation period ranging from 6 to 9 days postinfection. Accordingly, cells were fixed and stained with a solution containing 4% formaldehyde and 0.1% crystal violet.

Focus-forming units (FFU) were determined by immunocytochemistry. After incubation for 6 days, the agarose overlay was removed and cells were fixed with 1:1 acetone-methanol. The cells were rehydrated with PBS (pH 7.4) containing 5% sheep serum for 30 min at room temperature. Subsequently, the cells were incubated for 1 h at 37°C with a WNV-specific polyclonal antiserum (gamma-WN/KIS/2) diluted 1:3,000 in PBS (pH 7.4) with 0.2% Tween and 3% sheep serum. Cells were washed twice with PBS (pH 7.4) containing 0.2% Tween and 3% sheep serum and once with TBS buffer (137 mM sodium chloride, 3 mM potassium chloride, 25 mM Tris, pH 8.0) containing 0.2% Tween and 3% sheep serum. The incubation with a 1:400 dilution of an anti-rabbit alkaline phosphatase-conjugated secondary antibody was performed in TBS buffer with 0.2% Tween and 3% sheep serum for 45 min at room temperature. Following two washes with the same buffer, WNV-specific foci were detected by incubating with Sigma Fast Red TR/naphthol AS-MX for 10 min.

Computer-assisted sequence analysis. Secondary-structure predictions were performed using PsiPred (15). Hydrophobicity plots were generated according to the algorithm of Kyte and Doolittle (26) using PROTEAN (DNASTAR, Inc.) and a window size of 11.

Nucleotide sequence accession number. The sequence of the WNV isolate (crow 76/1) was deposited under GenBank accession no. FJ151394.

RESULTS

Establishment of a two-component infectious cDNA clone for WNV isolate V76/1. To generate a tool for WNV reverse genetics, the genome of a previously uncharacterized lineage I isolate (see Materials and Methods) (Table 1) was reverse transcribed, sequenced, and assembled into two plasmids from which, after *in vitro* ligation, full-length genomic RNA could be transcribed (Fig. 1A). To verify the functionality of the infectious cDNA clone, full-length RNAs were transcribed in several independent experiments and introduced into BHK-21 cells by electroporation. An apparent cytopathic effect (CPE) was observed in cells at day 2 posttransfection, indicating virus

replication. The supernatants of transfected BHK-21 cells were harvested and used to inoculate Vero cells, which are more susceptible to infection by WNV than BHK-21 cells (unpublished observation). At day 2 postinoculation, the release of infectious virions into the supernatant was tested by plaque assays on fresh Vero cells, indicating that virus had grown to high titers of typically 5×10^8 PFU/ml. Thus, the growth properties of the recombinant virus were virtually indistinguishable from those of the parental wild-type virus, which was furthermore confirmed by repeated growth curve analyses (data not shown).

Deletions within helix $\alpha 2$ of WNV protein impair viral growth to various degrees. To better characterize the functional importance of the hydrophobic helix $\alpha 2$ in WNV protein C, a set of nine deletions (Fig. 1B) was introduced into the infectious cDNA clone. Genomic RNAs were transcribed *in vitro* and used to transfect BHK-21 cells. Intracellular protein E expression was determined by immunofluorescence staining, using wild-type RNA and untransfected cells as positive and negative controls, respectively. At 24 h posttransfection, all of the samples presented a very similar picture, with approximately 10% of the cells being stained by immunofluorescence (data not shown). At 48 h posttransfection, the number of positive cells, however, had increased to 100% for deletion mutants $\Delta 4/1$, $\Delta 4/3$, and $\Delta 4/4$, thus being indistinguishable from wild-type-RNA-transfected cells (Fig. 2A). In contrast, cell culture spreading was reduced in all other mutants, with the most significant effect observed for mutants $\Delta 7/2$, $\Delta 10$, and

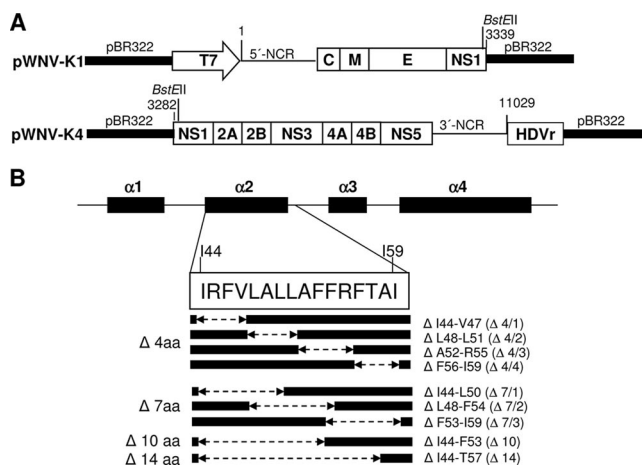


FIG. 1. Capsid deletion mutants of WNV. (A) Schematic drawing of the two partial WNV cDNA clones (not to scale). The WNV genome was engineered as two partial cDNA clones into pBR322 using 5' PacI and 3' NotI restriction sites. pWNV-K1 contains the T7 promoter sequence (open arrow) and bp 1 to 3339 of the WNV genomic sequence. The second plasmid, pWNV-K4, contains the sequence corresponding to WNV bp 3282 to 11029 and the hepatitis δ virus ribozyme sequence (HDVr). To generate full-length DNA templates for *in vitro* transcription, the two clones are ligated *in vitro* subsequent to cleavage at the BstEII site at nucleotide position 3321/3326. *In vitro* transcription is driven by the T7 promoter, and the HDVr sequence ensures the production of an authentic 3' end. (B) Schematic drawing of the positions and sizes of the engineered deletions. Deletions of 4, 7, 10, or 14 amino acids (aa) were introduced into helix $\alpha 2$ of WNV protein C as indicated by the broken arrows. The respective amino acid positions are indicated, as well as the nomenclature used for mutants throughout the study. NCR, noncoding region.

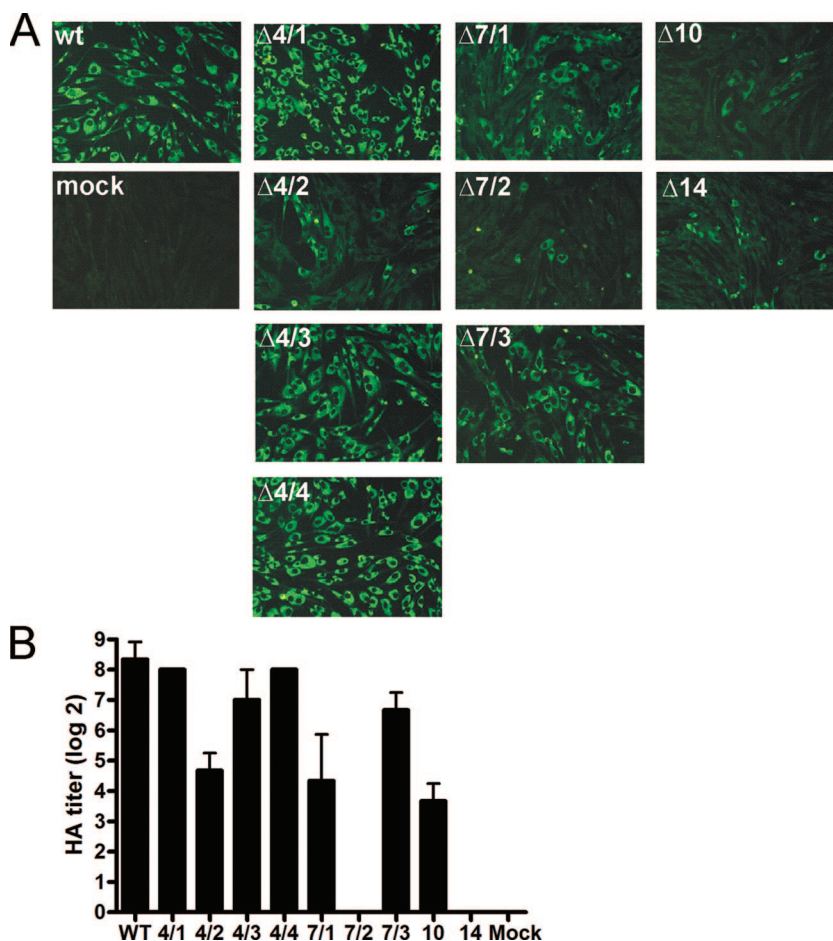


FIG. 2. Infectious properties of WNV protein C deletion mutants. (A) Viral spread in cell culture. BHK-21 cells were transfected with wild-type (wt) or mutant in vitro-transcribed RNAs as indicated. As a control, mock-transfected cells were used. At 48 h posttransfection, intracellular protein E expression was visualized by immunofluorescence staining using a polyclonal antibody directed against JEV protein E which is cross-reactive to WNV protein E. As secondary antibody, an anti-rabbit fluorescein isothiocyanate conjugate was used. (B) Cell culture passage. Supernatants of transfected cells were used to inoculate fresh Vero cells. At 6 days postinoculation, the release of virus particles was assessed by subjecting aliquots of the supernatants to HA. Twofold serial dilutions of supernatants were tested, and the titers (indicated on the left) are expressed on a log₂ scale (samples were measured in duplicate). Error bars indicate standard deviations.

$\Delta 14$ (Fig. 2A). Notably, deletions $\Delta 4/2$ and $\Delta 7/2$ exhibited a more distinct defect than the other deletions of the same length. Sequence inspection (Fig. 1B) indicates that both of these deletions are located within the most hydrophobic section of the helix (LALL-AFF) suggesting that the loss of hydrophobicity even more than the length of the deletion may cause the observed defect in cell culture spreading.

To further evaluate the production of infectious virions and to assess the export of viral particles by the infected cells, we inoculated a monolayer of fresh Vero cells with supernatants of transfected cells. At day 6 postinoculation, virus particles in supernatants were quantified by HAs (Fig. 2B). Cells infected with mutants $\Delta 4/1$, $\Delta 4/3$, and $\Delta 4/4$ were capable of exporting viral particles as much as wild-type virus. In comparison, mutants $\Delta 4/2$, $\Delta 7/1$, $\Delta 7/3$, and $\Delta 10$ exhibited some degree of impairment, whereas mutants $\Delta 7/2$ and $\Delta 14$ were found to be incapable of producing infectious particles under these experimental conditions. Whereas these data mostly correlated well with the above-described immunofluorescence results, there are also discrepancies (such as with mutant $\Delta 4/2$, which pro-

duced more HA-reactive particles than one would have expected from the immunofluorescence data). This can be explained by the selection of pseudorevertants already in this first passage, a phenomenon which is analyzed in detail in a later section.

The supernatants tested in HA were also subjected to plaque and focus formation assays to quantify the infectious titers of the various mutants. However, only wild-type virus, but none of the mutants, formed visible plaques on Vero cells at 6 days postinfection. Infectious titers obtained by focus assay amounted to 1×10^6 FFU/ml for mutants $\Delta 4/4$ and $\Delta 7/3$, 5×10^5 FFU/ml for mutants $\Delta 4/1$ and $\Delta 4/3$, and 1×10^5 FFU/ml for mutants $\Delta 4/2$, $\Delta 7/1$, and $\Delta 10$, whereas no infectious particles were detected for mutants $\Delta 7/2$ and $\Delta 14$, in good agreement with the above-described HA data. Thus, the titers for all mutants were significantly lower than that obtained for wild-type virus (5×10^8 FFU/ml), suggesting that a large percentage of the particles produced by these mutants (as detected by HA) were not infectious or did not initiate the formation of visible foci.

TABLE 2. Spontaneous mutations as determined by sequence analysis

Mutant ^b	Mutation(s) at passage ^a :				
	1	2	5	8	11
Δ4/1	None	None	ND ^c	ND	ND
Δ4/2	P61L	P61L	ND	ND	ND
Δ4/3	None	None	ND	ND	ND
Δ4/4	None	None	ND	ND	ND
Δ7/1	P22L	P22L	P22L/M34L	P22L/M34L	ND
Δ7/2	ND ^c	ND ^c	P22L	K31M	K31M
Δ7/3	None	Δ L51-E87	R45L	R45L	ND
Δ10	D39E/ΔG40-Q75	D39E/ΔG40-Q75	D39E/ΔG40-Q75	D39E/ΔG40-Q75	ND

^a For the first two passages, concentrated samples were used. Subsequently, supernatants were diluted until the end point of infectivity was reached, and these samples were subjected to further end point passages.

^b The 4-amino-acid deletion mutants were passaged only twice.

^c ND, not done (sequence analysis was not performed).

Spontaneous mutations are selected during cell culture passages. In order to test whether some of the WNV protein C mutants might revert to a better growth phenotype, end point dilution passages on Vero cells were performed and viral titers were monitored. Improved growth properties were indeed observed for mutants Δ4/2, Δ7/1, Δ7/2, Δ7/3, and Δ10 at different passage numbers, whereas several rounds of blind passaging of mutant Δ14 failed to produce a viable revertant. To investigate if these changes in phenotype were a direct result of additional alterations within the protein C sequence, viral RNA was isolated from supernatants of infected cells and subjected to reverse transcription-PCR and sequence analysis. Notably, sequencing of the protein C-coding region indeed verified the appearance of second-site mutations (Table 2). In most of the cases, and consistent with previous findings obtained with TBEV (21), point mutations that represented amino acid changes to more hydrophobic residues had evolved; however, most of these amino acid changes were, in contrast to findings with TBEV, located upstream of the original deletion (Fig. 3A). In total, five different point mutations were identified, with one of the point mutations, P22L, appearing more frequently than others and in the sequence context of two different engineered deletions.

Furthermore, and much to our surprise, we also identified mutations in which the original deletions were enlarged to lengths of 36 and 37 residues, respectively (Fig. 3B). Passaging of mutants Δ10 and Δ7/3 resulted in the appearance of large deletions removing more than one-third of the entire amino acid sequence of protein C. Mutant Δ10 evolved into a deletion of residues G40 to Q75 (termed Δ36) and furthermore contains a conservative D-to-E exchange at the deletion border (position 39). This deletion removed all residues of helices α2 and α3 as well as flanking residues, thus producing a capsid protein lacking the entire internal hydrophobic sequence (31). The second large deletion mutant (termed Δ37) originated from mutant Δ7/3 and had residues L51 to E87 and thus part of helix α2, all of helix α3, and part of helix α4 removed. This mutant was predominant in the sequence pattern obtained after two cell culture passages (Table 2). However, apparently another pseudorevertant, which contained the original 7/3 deletion in combination with a single point mutation, R45L, arose in the same passaging experiment and outgrew the large deletion mutant during subsequent passages (Table 2, passage

5). A similar phenomenon was observed with mutant Δ7/2, in which case the original P22L mutation was replaced by a K31M mutation at later passages. In contrast, the same P22L mutation was also observed to arise in mutant Δ7/1 but there was complemented by a second amino acid change (M34L) at a later passage. These observations illustrate the competition of pseudorevertants with presumably variable evolutionary fitness during these cell culture passages.

Recombinant mutants Δ36 and Δ37 can be readily passaged in cell culture. The unexpected tolerance of protein C toward deletions comprising 36 and 37 amino acids encouraged us to investigate these mutations in more detail. To ensure that the observed phenotypes were indeed a direct consequence of the identified alterations, the Δ36 and Δ37 deletions were engineered into the WNV wild-type backbone using the infectious cDNA clone. Immunofluorescence staining at 48 h posttransfection of in vitro-transcribed RNA (Fig. 3C) suggested that mutants Δ36 and Δ37 were indeed viable.

To further characterize the growth of these mutants, plaque and focus assays were performed on Vero cells. Even after incubation for 6 days, no plaques could be identified for both mutants, whereas wild-type plaques reached a size of between 8 and 15 mm (12.6 ± 2.4 mm) (Table 3). In contrast, both mutants were capable of forming foci on Vero cells, thus confirming their infectivity. These were, however, at least four times smaller than wild-type foci, indicating their reduced ability to spread in cell culture (Table 3). Nevertheless, both mutants achieved significantly higher titers (1×10^7 FFU/ml) than their respective parental mutants Δ10 (1×10^5 FFU/ml) and Δ7/3 (1×10^6 FFU/ml), thus confirming the notion that extension of the original deletions to 36 and 37 amino acids within protein C indeed caused improved cell culture growth properties.

Subsequently, we tested whether mutants Δ36 and Δ37 could be serially passaged in Vero cells and if that would provoke additional genetic alterations. A single passage using undiluted supernatant and three subsequent end point passages were performed, followed by sequence analysis of the entire genomes. No further sequence alterations were identified after the passages. These data indicated that the large deletion mutations present in mutants Δ36 and Δ37 are sufficient for providing efficient growth properties in cell culture and remain genetically stable.

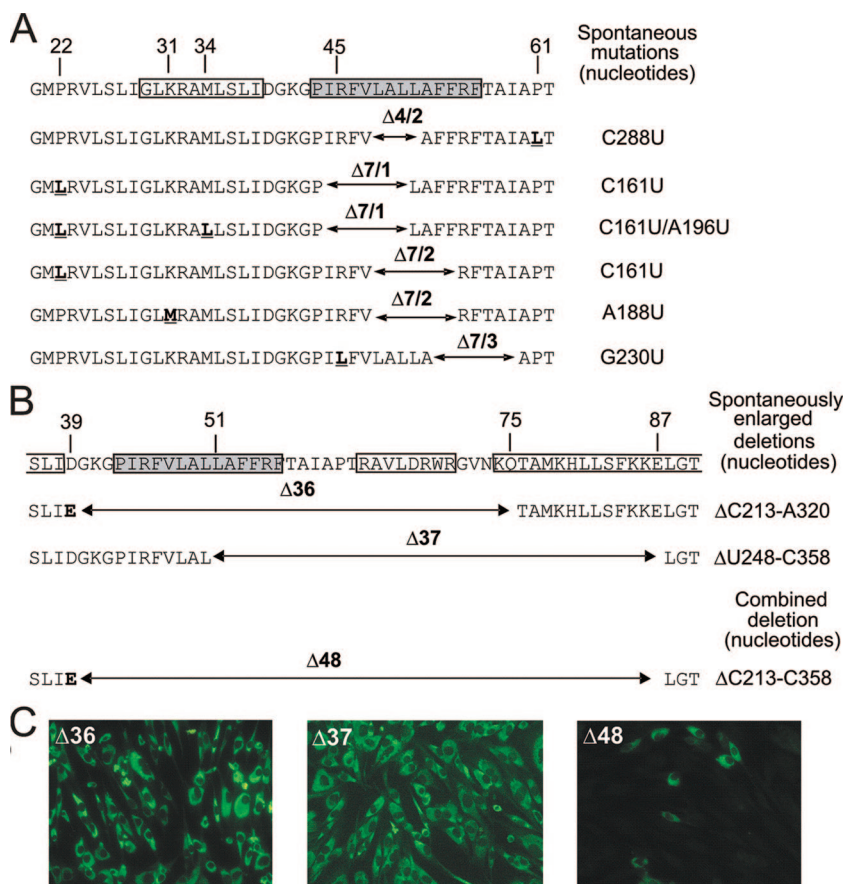


FIG. 3. Spontaneous mutations in the WNV capsid protein. (A) Second-site point mutations identified after passaging in Vero cells. The point mutations were identified at the indicated amino acid positions (marked on top) within a region corresponding to helix $\alpha 1$ (open box), helix $\alpha 2$ (gray box), and surrounding residues. The originally engineered deletions are shown by arrows, and the second-site point mutations are marked in bold and underlined. On the right, the corresponding nucleotide exchanges are listed. (B) Large deletions $\Delta 36$ and $\Delta 37$, identified after passaging of mutants $\Delta 10$ and $\Delta 7/3$, respectively. The helical parts of the capsid protein are indicated by boxes, and helix $\alpha 2$ is highlighted in gray. The positions of the large deletions are indicated by arrows. Furthermore, an artificial large deletion mutant (i.e., $\Delta 48$) was constructed, lacking all residues which had been spontaneously deleted in both $\Delta 36$ and $\Delta 37$. The precise nucleotide deletions are shown on the right. (C) Immunofluorescence analysis of large deletion mutants. The large deletions (i.e., $\Delta 36$, $\Delta 37$, and $\Delta 48$) were engineered into the infectious cDNA clone, and mutants were tested as described for Fig. 2A.

A combined deletion mutant ($\Delta 48$) is severely impaired and genetically unstable. The deletions present in mutants $\Delta 36$ and $\Delta 37$ affect overlapping but different regions of protein C. We wanted to investigate whether removal of the entire region extending from the 5' border of the $\Delta 36$ deletion to the 3' border of the $\Delta 37$ deletion would still yield a viable phenotype. To this end, mutant $\Delta 48$, including the D39E mutation and lacking residues G40 to E87 (Fig. 3B), was constructed and

analyzed. Immunofluorescence analysis indicated a strongly impaired phenotype of mutant $\Delta 48$ (Fig. 3C), and no plaque or focus formation was observed with this mutant (not shown). However, a single blind passage was sufficient to rescue a viable phenotype in Vero cells. Sequence analysis after subsequent end point passages revealed a duplication of the residues flanking the 48-amino-acid deletion (i.e., DuM16-D39E+L88-A94), but the growth properties of this pseudorevertant remained restricted, achieving a titer of only 10^4 FFU/ml.

RNA export and specific infectivity of mutants $\Delta 36$ and $\Delta 37$ are moderately reduced compared to those of wild-type WNV. To characterize in detail the capacity of mutants $\Delta 36$ and $\Delta 37$ to replicate, export, and infect, quantitative tests were performed in comparison to wild-type virus. As shown in Fig. 4A, intracellular RNA replication of both mutants was similar to that of the wild type at 24 and 48 h postinfection. At 72 and 96 h postinfection, intracellular RNA values of mutant $\Delta 37$ were still at wild-type levels, whereas those of mutant $\Delta 36$ decreased. This decrease was accompanied by strong CPE, causing a strong reduction of cell numbers at these time points.

TABLE 3. Growth properties of mutants $\Delta 36$ and $\Delta 37$

Virus	mm (mean \pm SD)		Titer (FFU/ml)
	Plaque size ^a	Focus size ^b	
Wild type	12.6 \pm 2.4	19.8 \pm 2.86	5 \times 10 ⁸
$\Delta 36$		2.85 \pm 0.63	1 \times 10 ⁷
$\Delta 37$		5.05 \pm 1.07	1 \times 10 ⁷

^a Mean plaque size was determined at day 6 postinfection. None of the capsid deletion mutants induced plaque formation, even when incubation was prolonged to 9 days postinfection.

^b Mean focus size was determined at day 6 postinfection.

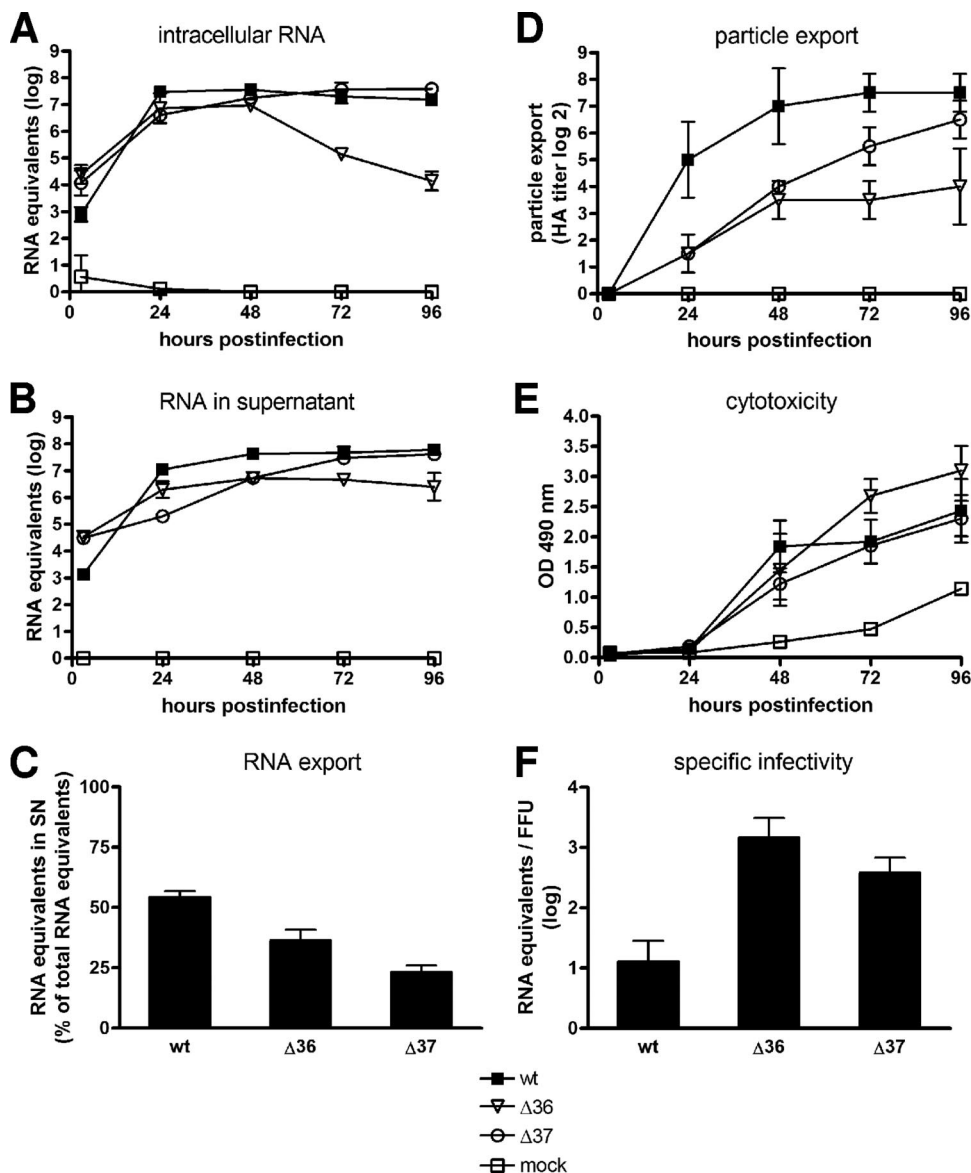


FIG. 4. Characterization of mutants $\Delta 36$ and $\Delta 37$. Approximately 10^6 Vero cells were infected at an MOI of 1 with the indicated virus preparation. Wild-type virus and infection medium were used as the respective positive and negative controls. (A) RNA replication (intracellular RNA) was measured by real-time PCR at the indicated time points. (B) The RNA export kinetics (RNA in supernatant) of mutants $\Delta 36$ and $\Delta 37$ was monitored by real-time PCR. (C) The percentage of exported relative to total RNA (intra- plus extracellular RNA) was calculated for the 48-h time point. (D) Release of viral particles into the supernatant was assessed by HA. (E) Cytotoxicity was assessed by CytoTox 96 nonradioactive cytotoxicity assay (Promega) using supernatants of the same samples. The respective optical density at 490 nm (OD_{490}) values, representing LDH release of disintegrating cells, are shown. (F) Specific infectivity of mutants $\Delta 36$ and $\Delta 37$ and wild-type virus. The specific infectivity was calculated by determining the ratio of RNA (real-time PCR) to infectious units (focus assay) in virus stock preparations. Mean values from two independent experiments with error bars indicating standard deviations are shown. wt, wild-type.

To confirm the visually observed CPE, cytotoxicity was quantitatively assessed by measuring the release of LDH into the supernatants of infected cells. As shown in Fig. 4E, LDH release from cells infected with mutant $\Delta 36$ was in the same range as for the wild type and mutant $\Delta 37$ until 48 h postinfection. In contrast, at the later time points, LDH levels in supernatants of $\Delta 36$ -infected cells were significantly higher than others thus confirming its high cytotoxicity and suggesting that the decreased intracellular RNA values for $\Delta 36$ at 72 and

96 h postinfection were indeed a consequence of excessive cell deaths (compare Fig. 4A and E).

Quantification of RNA release into the supernatants revealed moderate differences between protein C deletion mutants and wild-type virus. Mutants $\Delta 36$ and, particularly, $\Delta 37$ released less viral RNA into the supernatant than the wild type at 24 h postinfection (Fig. 4B). Mutant $\Delta 37$ achieved wild-type levels at later time points; however, $\Delta 36$ remained approximately one order of magnitude below the wild-type control at

all times. The decreasing values after 48 h (i.e., at 72 and 96 h) presumably reflect the loss of producing cells caused by the mutant's prominent cytotoxicity, thus calling into question the accuracy of the quantitative data at the later time points. To better compare the export efficiencies of mutant and wild-type RNAs, the percentage of total (extracellular and intracellular) RNA equivalents in the supernatant was calculated for the 48-h time point, at which time effects of cytotoxicity were still low and comparable among the samples. As illustrated in Fig. 4C, export efficiencies of mutants $\Delta 36$ and $\Delta 37$ were about two-thirds and half of the wild-type value, indicating that the mutated capsid proteins, although clearly less efficient in packaging of RNA and/or assembly of virions, were still able to facilitate the export of a significant percentage of the total RNA from infected cells. To further determine the export of viral particles, the same supernatants as used for the quantification of viral RNA were subjected to HA. As shown in Fig. 4D, the results of this analysis were in good agreement with the RNA data shown in Fig. 4B. For mutant $\Delta 37$, the release of viral particles was delayed but reached nearly the wild-type level at the latest time point. In contrast, the level for mutant $\Delta 36$ remained below that of the wild type by approximately 3 log₂ dilutions (i.e., approximately 8-fold) at all times, similar to the approximately 10-fold difference observed in the RNA values.

To quantitatively compare the specific infectivities of mutant and wild-type viruses, virus preparations were subjected to quantitative PCR to determine the number of RNA equivalents (presumed to correlate to the number of virions) and to focus assays to quantify infectious units in these preparations. The ratio of RNA equivalents to FFU was then calculated, and results are plotted in Fig. 4F. Whereas this ratio was approximately 10 for wild-type virus (i.e., 1 out of 10 RNA equivalents/virions caused an infectious focus), it was between 10- and 100-fold higher in the case of the two deletion mutants, indicating reduced specific infectivity.

In conclusion, the quantitative comparisons indicated moderate but significant impairments of both viral export and entry caused by the deletion mutations.

Large deletions are predicted to cause complex rearrangements of the overall helical composition of protein C. Notably, protein C deletion mutants $\Delta 36$ and $\Delta 37$ are capable of producing infectious virions, whereas mutants with deletions of fewer amino acids are much more severely impaired (i.e., $\Delta 4/2$, $\Delta 7/1$, $\Delta 7/2$, $\Delta 7/3$, and $\Delta 10$) or noninfectious in cell culture (i.e., $\Delta 14$). To obtain further insight into the structural consequences of deletions $\Delta 36$ and $\Delta 37$, the protein C sequences of these pseudorevertants were subjected to secondary-structure prediction analysis (PsiPred) (15) and compared to the wild-type sequence. In Fig. 5A, the secondary-structure prediction for the WNV V76/1 sequence is presented, with positions of helices being almost identical to those defined in the crystal structure (11). In addition, we determined the Kyte-Doolittle hydrophobicity profile (26). The spontaneous enlargements of the deletions apparently removed a hydrophilic region extending from $\alpha 3$ to the beginning of $\alpha 4$ (Fig. 5A, lower panel). This suggests that the spontaneous deletions compensate for the loss of the hydrophobic helical structure as represented by helix $\alpha 2$ by removing another, more hydrophilic region (Fig. 5A). Subsequently, the sequences of protein C deletion mu-

tants (i.e., $\Delta 36$, and $\Delta 37$) were analyzed. As illustrated in the WNV crystal structure (11), the spontaneous deletion of 36 amino acids resulted in complete removal of helices $\alpha 2$ and $\alpha 3$ (Fig. 5B, lower panel). The secondary-structure prediction suggested the formation of a large single α helix (Fig. 5B, upper panel) by fusion of helices $\alpha 1$ and $\alpha 4$. Whether the mutant protein (i.e., a polypeptide of only 61 amino acids) is likely to adopt a stable conformation in solution remains elusive, and it will be interesting to investigate this using recombinant proteins. However, it is certainly conceivable that such a long fusion helix might form upon insertion of protein C into the ER membrane. Similarly, the formation of a fusion helix was predicted in the analysis of the second large deletion mutant (i.e., $\Delta 37$, illustrated in Fig. 5C). Notably, in the crystal structure, the remainders of helices $\alpha 2$ and $\alpha 4$ are oriented toward each other, thus suggesting, albeit not proving, that the formation of a large fusion helix might indeed be possible.

DISCUSSION

The internal hydrophobic domain of the flaviviral protein C is a functionally important region involved in protein dimerization and membrane interaction during assembly of the virion (19, 31, 34, 46). In earlier reports, it had been demonstrated that mutants lacking the entire internal hydrophobic sequence of protein C are either severely impaired or not viable at all (21, 42, 44). Although this was also observed with some of the WNV deletion mutants analyzed in this study, the pseudorevertant $\Delta 36$, lacking amino acids G40 to Q75 and thus the entire conserved hydrophobic domain, surprisingly demonstrates that efficient virion assembly and cell culture growth are in fact possible even in the complete absence of this region. $\Delta 37$, the second large, spontaneously emerged WNV capsid deletion mutant, lacks residues L51 to E87 and thus also large parts of this domain. Both mutants grew well in cell culture, indicating that highly truncated capsid proteins can be functional.

A remarkable flexibility of protein C toward deletions and sequence alterations has already been observed in earlier studies (19, 21, 42, 43, 50). Protein C is essential for binding and packaging of genomic RNA and contributes to particle assembly and stability (reviewed in reference 38). RNA binding has been assigned to the highly basic N- and C-terminal parts of the protein (17). Notably, as tested in a YFV *trans*-packaging system, one intact terminus is sufficient for the encapsidation of genomic RNA (42). Thus, nearly 40 residues of the N terminus of YFV protein C could be removed while the ability to package RNA was retained. Similarly, 27 residues of its C terminus, including the entire helix $\alpha 4$, were dispensable for packaging. Based on their observations with mutants containing deletions in both termini, Patkar et al. proposed a mechanism in which the N terminus is involved in initial binding of the genomic RNA, followed by binding of the C terminus (42). The capacity to bind and package viral RNA is largely preserved in both mutant $\Delta 36$ and mutant $\Delta 37$ proteins, as measured by their capacity to export RNA into the supernatants of infected cells. Another functional requirement of protein C is to mediate interaction with the ER membrane during budding (19, 35). It is believed that this interaction involves the hydrophobic cleft present on the surface of dimeric protein C (31).

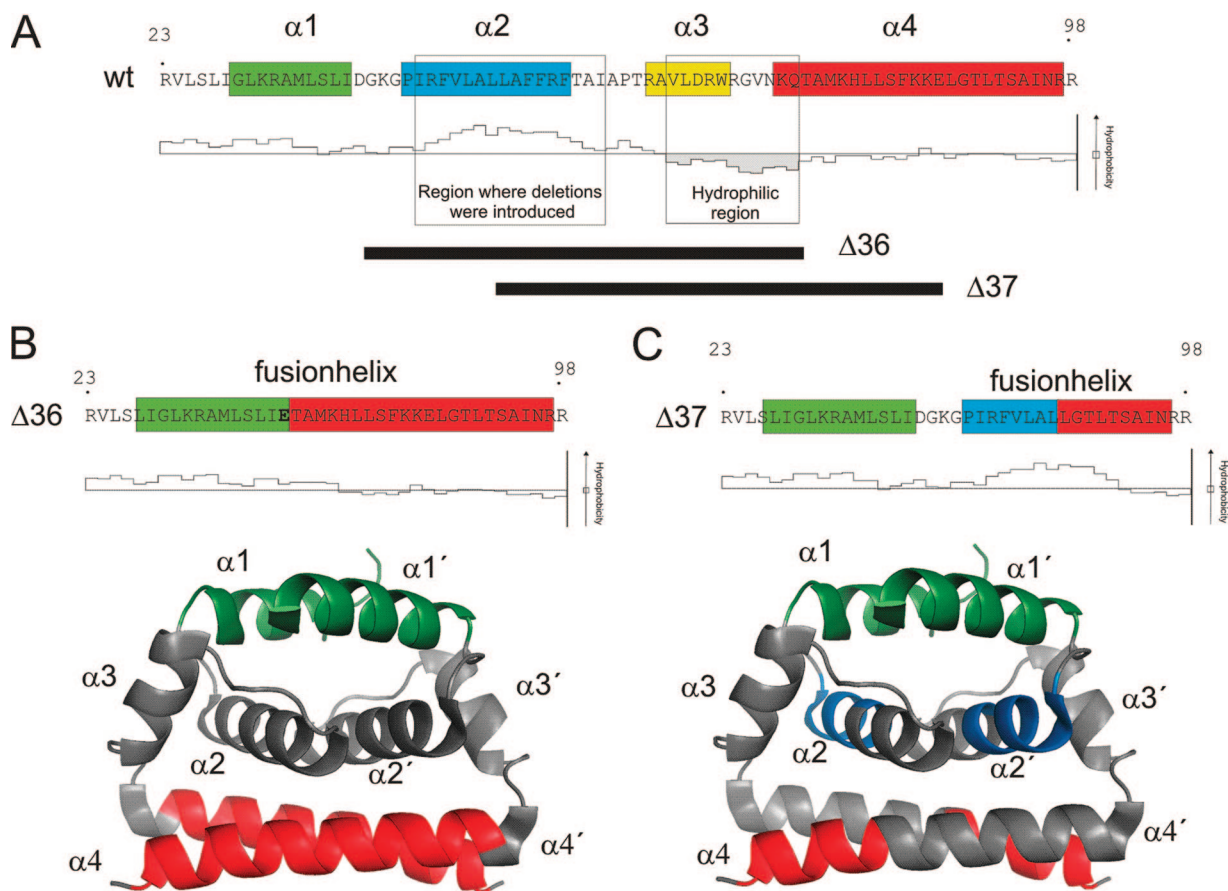


FIG. 5. Structure predictions for sequences of the wild type (A), deletion mutation $\Delta 36$ (B), and deletion mutation $\Delta 37$ (C). (A) Secondary-structure prediction and hydrophobicity blot for the WNV V76/1 sequence. Residues R23 to R98, which are also present in the Kunjin protein C crystal structure (11), are shown. The positions of the introduced deletions and the most hydrophilic part of the protein are shown by open boxes. The spontaneous deletions $\Delta 36$ and $\Delta 37$ are illustrated by black bars below. (B and C) Upper panels, secondary-structure predictions for mutant protein C sequences and corresponding hydrophobicity blots. Lower panels, deletions on the Kunjin protein C dimer (11). The four helices are shown, where present, with the same coloring in all three panels (i.e., $\alpha 1$ in green, $\alpha 2$ in blue, $\alpha 3$ in yellow, and $\alpha 4$ in red); the spontaneous large deletions (i.e., $\Delta 36$ and $\Delta 37$) are shown in gray. All secondary-structure predictions were performed using PsiPred (15), and the hydrophobicity blots were generated according to the algorithm of Kyte and Doolittle (26). The protein C 3D structure was adapted from the Protein Data Bank (accession no. 1SFK) using PyMOL software (10). wt, wild-type.

In the dimer of protein C, helices $\alpha 2$ from each monomer interact with each other, thus forming the bottom of this cleft. It is puzzling that mutants $\Delta 36$ and $\Delta 37$ still produced infectious particles even though the entire or large parts of helix $\alpha 2$ were missing. Secondary-structure predictions and hydrophobicity plots suggested the formation of new large, hydrophobic α helices in both of these mutants, whereas a hydrophilic stretch of residues was lost from both of these proteins. Taken together, these findings support the idea that the newly formed fusion helices might functionally substitute for the loss of helix $\alpha 2$. In addition, the protein C dimer serves as the basic building block in the assembly of the flaviviral nucleocapsid (18). In the 3D structures of flaviviral protein C (11, 31), the dimers resemble a three-layer structure with helices $\alpha 1$ on top, helices $\alpha 2$ in the middle, and helices $\alpha 4$ at the bottom. In contrast, helix $\alpha 3$ is not organized pairwise and seems to serve as a spacer. Mutant $\Delta 36$ lacks helices $\alpha 2$ and $\alpha 3$ and, as a consequence, the middle part of the three-layer structure is completely removed whereas the top layer of helices $\alpha 1$ and the bottom layer of helices $\alpha 4$ remain more or less unaffected (Fig.

5B). Similarly, mutant $\Delta 37$ lacks approximately half of helix $\alpha 2$, the entire helix $\alpha 3$, and approximately half of helix $\alpha 4$ (Fig. 5C). One might assume that the formation of a fusion helix (composed of the remainders of helices $\alpha 2$ and $\alpha 4$) results in the formation of two layers instead of three. Stacking of such two-layer structures might nevertheless enable multimer formation and nucleocapsid assembly, which has been shown as an intrinsic property of WNV C and DENV C proteins (11, 31). Therefore, it will be interesting to explore the oligomeric properties and the atomic structures of the mutant proteins in future experiments. Mutants $\Delta 36$ and $\Delta 37$, however, had a significantly reduced specific infectivity and formed only small foci and no plaques, indicating a significantly attenuated phenotype. This attenuation may be caused not only by an assembly defect but also by an impairment during entry and uncoating and/or a reduced physico-chemical stability of the mutant particles. Indeed, a decreased thermal stability of particles containing C-terminal deletions [C($\Delta 77-96$)] or deletions within the internal hydrophobic sequence [C($\Delta 43-48$)] had recently been observed (42). The impairment of export and,

potentially connected with this observation, an altered cytotoxicity (i.e., for mutant $\Delta 36$) are likely caused by a partial defect in particle assembly.

In this study, we also identified spontaneous mutations which resembled those described previously for TBEV (21), i.e., exchanges of individual amino acids to more hydrophobic residues and duplication mutations. In the TBEV study, the residue changes were, without exception, located downstream of the originally engineered deletion, whereas this was the case for only a single mutation in the WNV system. The P61L mutation in mutant $\Delta 4/2$ resembles a P57L mutation identified in TBEV mutant C($\Delta 28-46$). Both of these mutations of P to L are located in the loop between the helix $\alpha 2$ containing the hydrophobic domain and the subsequent helix $\alpha 3$. All other WNV second-site point mutations, however, appeared upstream of the original deletion and affected residues preceding or located within helix $\alpha 1$. In addition, the TBEV study (21) identified two duplications as rescuing mutations. Similarly, WNV mutant $\Delta 48$ was rescued by the emergence of a duplication mutation, DuM16-D39E+L88-A94, although growth of the resulting mutant was still highly restricted. Taken together, these findings suggest that similar mechanisms can work to compensate for deletion mutations in both TBEV and WNV and possibly flaviviruses in general.

Flaviviral RNA replication is dependent on the cyclization of the positive-stranded RNA genome, which is mediated via 5' and 3' cyclization sequences (reviewed in reference 34). In mosquito-borne flaviviruses, the 5' cyclization sequence is located within the amino-terminal coding region of protein C (2, 3, 9, 14, 16, 20, 29, 39). The WNV 5' cyclization sequence comprises nucleotides 137 to 144, encoding amino acids V14 to M16 of protein C. In good agreement with the functional importance of this region, none of the second-site mutations including also the large deletions affected this part of the sequence. Thus, intracellular RNA replication should not be impaired, and indeed, quantitative assessment showed no significant differences between mutants $\Delta 36$ and $\Delta 37$ and wild-type virus.

In conclusion, our data support a functional importance of the internal hydrophobic domain of the WNV protein C but demonstrate that this functionality can be substituted for in dramatically truncated forms of this protein. Deletions of more than one-third of the protein in the absence of additional mutations, which would increase hydrophobicity, can generate functional protein C. As suggested by secondary-structure predictions for WNV protein C deletion mutants $\Delta 36$ and $\Delta 37$, the loss of functional elements contained in the hydrophobic helix $\alpha 2$ was presumably compensated for by the formation of hydrophobic fusion helices and the extrusion of an intermittent hydrophilic loop region. The high immunogenicity of mutant flaviviruses containing deletions within protein C has been successfully demonstrated (19, 21, 37, 44). Taking into account the delayed growth kinetics together with the fact that high titers can be achieved with mutants $\Delta 36$ and $\Delta 37$ in cell culture, we propose that these large deletion mutants might be particularly useful vaccine candidates.

ACKNOWLEDGMENTS

We thank Ernest Gould, Bob Shope, Bob Tesh, Eileen N. Oslund, and Franz X. Heinz for kindly providing the virus isolate WNV V76/1

and Paul Breit for photographic artwork. We are especially grateful to Franz X. Heinz for very helpful discussions.

This project was funded by the Wiener Wirtschafts Förderungs Fonds ("Co operate Vienna 2003").

We declare a potential conflict of financial interests as employees of InterCell AG (P.S., W.S., A.V.G., and A.M.), a biotechnology company.

REFERENCES

- Allison, S. L., K. Stadler, C. W. Mandl, C. Kunz, and F. X. Heinz. 1995. Synthesis and secretion of recombinant tick-borne encephalitis virus protein E in soluble and particulate form. *J. Virol.* **69**:5816–5820.
- Alvarez, D. E., M. F. Lodeiro, C. V. Filomatoris, S. Fucito, J. A. Mondotte, and A. V. Gamarnik. 2006. Structural and functional analysis of dengue virus RNA. *Novartis Found. Symp.* **277**:120–132. (Discussion, **277**:132–135, 251–253.)
- Alvarez, D. E., M. F. Lodeiro, S. J. Luduena, L. I. Pietrasanta, and A. V. Gamarnik. 2005. Long-range RNA-RNA interactions circularize the dengue virus genome. *J. Virol.* **79**:6631–6643.
- Amberg, S. M., A. Nestorowicz, D. W. McCourt, and C. M. Rice. 1994. NS2B-3 proteinase-mediated processing in the yellow fever virus structural region: in vitro and in vivo studies. *J. Virol.* **68**:3794–3802.
- Bolivar, F., R. L. Rodriguez, P. J. Greene, M. C. Betlach, H. L. Heyneker, and H. W. Boyer. 1977. Construction and characterization of new cloning vehicles. II. A multipurpose cloning system. *Gene* **2**:95–113.
- Chambers, T. J., C. S. Hahn, R. Galler, and C. M. Rice. 1990. Flavivirus genome organization, expression, and replication. *Annu. Rev. Microbiol.* **44**:649–688.
- Chowrira, B. M., P. A. Pavco, and J. A. McSwiggen. 1994. In vitro and in vivo comparison of hammerhead, hairpin, and hepatitis delta virus self-processing ribozyme cassettes. *J. Biol. Chem.* **269**:25856–25864.
- Clarke, D. H., and J. Casals. 1958. Techniques for hemagglutination and hemagglutination-inhibition with arthropod-borne viruses. *Am. J. Trop. Med. Hyg.* **7**:561–573.
- Corver, J., E. Lenches, K. Smith, R. A. Robison, T. Sando, E. G. Strauss, and J. H. Strauss. 2003. Fine mapping of a *cis*-acting sequence element in yellow fever virus RNA that is required for RNA replication and cyclization. *J. Virol.* **77**:2265–2270.
- DeLano, W. L. 2002. The PyMOL molecular graphics system. DeLano Scientific, San Carlos, CA.
- Dokland, T., M. Walsh, J. M. Mackenzie, A. A. Khromykh, K. H. Ee, and S. Wang. 2004. West Nile virus core protein; tetramer structure and ribbon formation. *Structure* **12**:1157–1163.
- Elshuber, S., S. L. Allison, F. X. Heinz, and C. W. Mandl. 2003. Cleavage of protein prM is necessary for infection of BHK-21 cells by tick-borne encephalitis virus. *J. Gen. Virol.* **84**:183–191.
- Guirakhoo, F., F. X. Heinz, and C. Kunz. 1989. Epitope model of tick-borne encephalitis virus envelope glycoprotein E: analysis of structural properties, role of carbohydrate side chain, and conformational changes occurring at acidic pH. *Virology* **169**:90–99.
- Hahn, C. S., Y. S. Hahn, C. M. Rice, E. Lee, L. Dalgarno, E. G. Strauss, and J. H. Strauss. 1987. Conserved elements in the 3' untranslated region of flavivirus RNAs and potential cyclization sequences. *J. Mol. Biol.* **198**:33–41.
- Jones, D. T. 1999. Protein secondary structure prediction based on position-specific scoring matrices. *J. Mol. Biol.* **292**:195–202.
- Khromykh, A. A., H. Meka, K. J. Guyatt, and E. G. Westaway. 2001. Essential role of cyclization sequences in flavivirus RNA replication. *J. Virol.* **75**:6719–6728.
- Khromykh, A. A., and E. G. Westaway. 1996. RNA binding properties of core protein of the flavivirus Kunjin. *Arch. Virol.* **141**:685–699.
- Kiermayr, S., R. M. Kofler, C. W. Mandl, P. Messner, and F. X. Heinz. 2004. Isolation of capsid protein dimers from the tick-borne encephalitis flavivirus and in vitro assembly of capsid-like particles. *J. Virol.* **78**:8078–8084.
- Kofler, R. M., F. X. Heinz, and C. W. Mandl. 2002. Capsid protein C of tick-borne encephalitis virus tolerates large internal deletions and is a favorable target for attenuation of virulence. *J. Virol.* **76**:3534–3543.
- Kofler, R. M., V. M. Hoenninger, C. Thurner, and C. W. Mandl. 2006. Functional analysis of the tick-borne encephalitis virus cyclization elements indicates major differences between mosquito-borne and tick-borne flaviviruses. *J. Virol.* **80**:4099–4113.
- Kofler, R. M., A. Leitner, G. O'Riordain, F. X. Heinz, and C. W. Mandl. 2003. Spontaneous mutations restore the viability of tick-borne encephalitis virus mutants with large deletions in protein C. *J. Virol.* **77**:443–451.
- Konishi, E., and A. Fujii. 2002. Dengue type 2 virus subviral extracellular particles produced by a stably transfected mammalian cell line and their evaluation for a subunit vaccine. *Vaccine* **20**:1058–1067.
- Konishi, E., A. Fujii, and P. W. Mason. 2001. Generation and characterization of a mammalian cell line continuously expressing Japanese encephalitis virus subviral particles. *J. Virol.* **75**:2204–2212.
- Konishi, E., and P. W. Mason. 1993. Proper maturation of the Japanese

- encephalitis virus envelope glycoprotein requires cosynthesis with the pre-membrane protein. *J. Virol.* **67**:1672–1675.
25. **Kuhn, R. J., W. Zhang, M. G. Rossmann, S. V. Pletnev, J. Corver, E. Lenches, C. T. Jones, S. Mukhopadhyay, P. R. Chipman, E. G. Strauss, T. S. Baker, and J. H. Strauss.** 2002. Structure of dengue virus: implications for flavivirus organization, maturation, and fusion. *Cell* **108**:717–725.
 26. **Kyte, J., and R. F. Doolittle.** 1982. A simple method for displaying the hydropathic character of a protein. *J. Mol. Biol.* **157**:105–132.
 27. **Lanciotti, R. S., J. T. Roehrig, V. Deubel, J. Smith, M. Parker, K. Steele, B. Crise, K. E. Volpe, M. B. Crabtree, J. H. Scherret, R. A. Hall, J. S. Mackenzie, C. B. Cropp, B. Panigrahy, E. Ostlund, B. Schmitt, M. Malkinson, C. Banet, J. Weissman, N. Komar, H. M. Savage, W. Stone, T. McNamara, and D. J. Gubler.** 1999. Origin of the West Nile virus responsible for an outbreak of encephalitis in the northeastern United States. *Science* **286**:2333–2337.
 28. **Lindenbach, B. D., and C. M. Rice.** 2001. Flaviviridae: the viruses and their replication, p. 991–1041. *In* D. M. Knipe and P. M. Howley (ed.), *Fields virology*, 4th ed. Lippincott Williams & Wilkins, Philadelphia, PA.
 29. **Lo, M. K., M. Tilgner, K. A. Bernard, and P. Y. Shi.** 2003. Functional analysis of mosquito-borne flavivirus conserved sequence elements within 3' untranslated region of West Nile virus by use of a reporting replicon that differentiates between viral translation and RNA replication. *J. Virol.* **77**:10004–10014.
 30. **Lobigs, M.** 1993. Flavivirus pre-membrane protein cleavage and spike heterodimer secretion require the function of the viral proteinase NS3. *Proc. Natl. Acad. Sci. USA* **90**:6218–6222.
 31. **Ma, L., C. T. Jones, T. D. Groesch, R. J. Kuhn, and C. B. Post.** 2004. Solution structure of dengue virus capsid protein reveals another fold. *Proc. Natl. Acad. Sci. USA* **101**:3414–3419.
 32. **Mackenzie, J. M., and E. G. Westaway.** 2001. Assembly and maturation of the flavivirus Kunjin virus appear to occur in the rough endoplasmic reticulum and along the secretory pathway, respectively. *J. Virol.* **75**:10787–10799.
 33. **Mandl, C. W., M. Ecker, H. Holzmann, C. Kunz, and F. X. Heinz.** 1997. Infectious cDNA clones of tick-borne encephalitis virus European subtype prototypic strain Neudoerfl and high virulence strain Hypr. *J. Gen. Virol.* **78**:1049–1057.
 34. **Markoff, L.** 2003. 5'- and 3'-noncoding regions in flavivirus RNA. *Adv. Virus Res.* **59**:177–228.
 35. **Markoff, L., B. Falgout, and A. Chang.** 1997. A conserved internal hydrophobic domain mediates the stable membrane integration of the dengue virus capsid protein. *Virology* **233**:105–117.
 36. **Mason, P. W., S. Pincus, M. J. Fournier, T. L. Mason, R. E. Shope, and E. Paoletti.** 1991. Japanese encephalitis virus-vaccinia recombinants produce particulate forms of the structural membrane proteins and induce high levels of protection against lethal JEV infection. *Virology* **180**:294–305.
 37. **Mason, P. W., A. V. Shustov, and I. Frolov.** 2006. Production and characterization of vaccines based on flaviviruses defective in replication. *Virology* **351**:432–443.
 38. **Mukhopadhyay, S., R. J. Kuhn, and M. G. Rossmann.** 2005. A structural perspective of the flavivirus life cycle. *Nat. Rev. Microbiol.* **3**:13–22.
 39. **Nomaguchi, M., T. Teramoto, L. Yu, L. Markoff, and R. Padmanabhan.** 2004. Requirements for West Nile virus (–) and (+)-strand subgenomic RNA synthesis in vitro by the viral RNA-dependent RNA polymerase expressed in *Escherichia coli*. *J. Biol. Chem.* **279**:12141–12151.
 40. **Nowak, T., P. M. Farber, G. Wengler, and G. Wengler.** 1989. Analyses of the terminal sequences of West Nile virus structural proteins and of the in vitro translation of these proteins allow the proposal of a complete scheme of the proteolytic cleavages involved in their synthesis. *Virology* **169**:365–376.
 41. **Orlinger, K. K., V. M. Hoenninger, R. M. Kofler, and C. W. Mandl.** 2006. Construction and mutagenesis of an artificial bicistronic tick-borne encephalitis virus genome reveals an essential function of the second transmembrane region of protein e in flavivirus assembly. *J. Virol.* **80**:12197–12208.
 42. **Patkar, C. G., C. T. Jones, Y. H. Chang, R. Warriar, and R. J. Kuhn.** 2007. Functional requirements of the yellow fever virus capsid protein. *J. Virol.* **81**:6471–6481.
 43. **Schrauf, S., P. Schlick, T. Skern, and C. W. Mandl.** 2008. Functional analysis of potential carboxy-terminal cleavage sites of tick-borne encephalitis virus capsid protein. *J. Virol.* **82**:2218–2229.
 44. **Seregin, A., R. Nistler, V. Borisevich, G. Yamshchikov, E. Chaporgina, C. W. Kwok, and V. Yamshchikov.** 2006. Immunogenicity of West Nile virus infectious DNA and its noninfectious derivatives. *Virology* **356**:115–125.
 45. **Varnavski, A. N., P. R. Young, and A. A. Khromykh.** 2000. Stable high-level expression of heterologous genes in vitro and in vivo by noncytopathic DNA-based Kunjin virus replicon vectors. *J. Virol.* **74**:4394–4403.
 46. **Wang, S. H., W. J. Syu, and S. T. Hu.** 2004. Identification of the homotypic interaction domain of the core protein of dengue virus type 2. *J. Gen. Virol.* **85**:2307–2314.
 47. **Zhang, W., P. R. Chipman, J. Corver, P. R. Johnson, Y. Zhang, S. Mukhopadhyay, T. S. Baker, J. H. Strauss, M. G. Rossmann, and R. J. Kuhn.** 2003. Visualization of membrane protein domains by cryo-electron microscopy of dengue virus. *Nat. Struct. Biol.* **10**:907–912.
 48. **Zhang, W., S. Mukhopadhyay, S. V. Pletnev, T. S. Baker, R. J. Kuhn, and M. G. Rossmann.** 2002. Placement of the structural proteins in Sindbis virus. *J. Virol.* **76**:11645–11658.
 49. **Zhang, Y., B. Kaufmann, P. R. Chipman, R. J. Kuhn, and M. G. Rossmann.** 2007. Structure of immature West Nile virus. *J. Virol.* **81**:6141–6145.
 50. **Zhu, W., C. Qin, S. Chen, T. Jiang, M. Yu, X. Yu, and E. Qin.** 2007. Attenuated dengue 2 viruses with deletions in capsid protein derived from an infectious full-length cDNA clone. *Virus Res.* **126**:226–232.

References

1. **Aaskov, J., K. Buzacott, E. Field, K. Lowry, A. Berlioz-Arthaud, and E. C. Holmes.** 2007. Multiple recombinant dengue type 1 viruses in an isolate from a dengue patient. *J Gen Virol* **88**:3334-40.
2. **Allison, S. L., C. W. Mandl, C. Kunz, and F. X. Heinz.** 1994. Expression of cloned envelope protein genes from the flavivirus tick-borne encephalitis virus in mammalian cells and random mutagenesis by PCR. *Virus Genes* **8**:187-98.
3. **Allison, S. L., Y. J. Tao, G. O'Riordain, C. W. Mandl, S. C. Harrison, and F. X. Heinz.** 2003. Two distinct size classes of immature and mature subviral particles from tick-borne encephalitis virus. *J Virol* **77**:11357-66.
4. **Archer, A. M., and R. Rico-Hesse.** 2002. High genetic divergence and recombination in Arenaviruses from the Americas. *Virology* **304**:274-81.
5. **Banner, L. R., J. G. Keck, and M. M. Lai.** 1990. A clustering of RNA recombination sites adjacent to a hypervariable region of the peplomer gene of murine coronavirus. *Virology* **175**:548-55.
6. **Baric, R. S., K. Fu, M. C. Schaad, and S. A. Stohlman.** 1990. Establishing a genetic recombination map for murine coronavirus strain A59 complementation groups. *Virology* **177**:646-56.
7. **Baroth, M., M. Orlich, H. J. Thiel, and P. Becher.** 2000. Insertion of cellular NEDD8 coding sequences in a pestivirus. *Virology* **278**:456-66.
8. **Becher, P., M. Orlich, M. Konig, and H. J. Thiel.** 1999. Nonhomologous RNA recombination in bovine viral diarrhea virus: molecular characterization of a variety of subgenomic RNAs isolated during an outbreak of fatal mucosal disease. *J Virol* **73**:5646-53.
9. **Becher, P., M. Orlich, and H. J. Thiel.** 2000. Mutations in the 5' nontranslated region of bovine viral diarrhea virus result in altered growth characteristics. *J Virol* **74**:7884-94.
10. **Becher, P., M. Orlich, and H. J. Thiel.** 1998. Ribosomal S27a coding sequences upstream of ubiquitin coding sequences in the genome of a pestivirus. *J Virol* **72**:8697-704.
11. **Becher, P., M. Orlich, and H. J. Thiel.** 2001. RNA recombination between persisting pestivirus and a vaccine strain: generation of cytopathogenic virus and induction of lethal disease. *J Virol* **75**:6256-64.
12. **Becher, P., H. J. Thiel, M. Collins, J. Brownlie, and M. Orlich.** 2002. Cellular sequences in pestivirus genomes encoding gamma-aminobutyric acid (A) receptor-associated protein and Golgi-associated ATPase enhancer of 16 kilodaltons. *J Virol* **76**:13069-76.
13. **Bernardin, F., B. Herring, K. Page-Shafer, C. Kuiken, and E. Delwart.** 2006. Absence of HCV viral recombination following superinfection. *J Viral Hepat* **13**:532-7.
14. **Bolin, S. R., A. W. McClurkin, R. C. Cutlip, and M. F. Coria.** 1985. Severe clinical disease induced in cattle persistently infected with noncytopathic bovine viral diarrhea virus by superinfection with cytopathic bovine viral diarrhea virus. *Am J Vet Res* **46**:573-6.
15. **Brinton, M. A.** 1983. Analysis of extracellular West Nile virus particles produced by cell cultures from genetically resistant and susceptible mice indicates enhanced amplification of defective interfering particles by resistant cultures. *J Virol* **46**:860-70.

16. **Cammack, N., A. Phillips, G. Dunn, V. Patel, and P. D. Minor.** 1988. Intertypic genomic rearrangements of poliovirus strains in vaccinees. *Virology* **167**:507-14.
17. **Cascone, P. J., C. D. Carpenter, X. H. Li, and A. E. Simon.** 1990. Recombination between satellite RNAs of turnip crinkle virus. *Embo J* **9**:1709-15.
18. **Chang, G. J., G. Kuno, D. E. Purdy, and B. S. Davis.** 2004. Recent advancement in flavivirus vaccine development. *Expert Rev Vaccines* **3**:199-220.
19. **Chare, E. R., E. A. Gould, and E. C. Holmes.** 2003. Phylogenetic analysis reveals a low rate of homologous recombination in negative-sense RNA viruses. *J Gen Virol* **84**:2691-703.
20. **Charrel, R. N., X. de Lamballerie, and C. F. Fulhorst.** 2001. The Whitewater Arroyo virus: natural evidence for genetic recombination among Tacaribe serocomplex viruses (family Arenaviridae). *Virology* **283**:161-6.
21. **Cheng, C. P., E. Serviene, and P. D. Nagy.** 2006. Suppression of viral RNA recombination by a host exoribonuclease. *J Virol* **80**:2631-40.
22. **Chetverin, A. B.** 1999. The puzzle of RNA recombination. *FEBS Lett* **460**:1-5.
23. **Chetverin, A. B., H. V. Chetverina, A. A. Demidenko, and V. I. Ugarov.** 1997. Nonhomologous RNA recombination in a cell-free system: evidence for a transesterification mechanism guided by secondary structure. *Cell* **88**:503-13.
24. **Chu, J. J., and M. L. Ng.** 2004. Infectious entry of West Nile virus occurs through a clathrin-mediated endocytic pathway. *J Virol* **78**:10543-55.
25. **Cleaves, G. R., T. E. Ryan, and R. W. Schlesinger.** 1981. Identification and characterization of type 2 dengue virus replicative intermediate and replicative form RNAs. *Virology* **111**:73-83.
26. **Colina, R., D. Casane, S. Vasquez, L. Garcia-Aguirre, A. Chunga, H. Romero, B. Khan, and J. Cristina.** 2004. Evidence of intratypic recombination in natural populations of hepatitis C virus. *J Gen Virol* **85**:31-7.
27. **Cristina, J., and R. Colina.** 2006. Evidence of structural genomic region recombination in Hepatitis C virus. *Virol J* **3**:53.
28. **Cuervo, N. S., S. Guillot, N. Romanenkova, M. Combiescu, A. Aubert-Combiescu, M. Seghier, V. Caro, R. Crainic, and F. Delpeyroux.** 2001. Genomic features of intertypic recombinant sabin poliovirus strains excreted by primary vaccinees. *J Virol* **75**:5740-51.
29. **De Socio, G. V., D. Francisci, F. Mecozzi, A. Sensini, M. Polidori, R. Castronari, S. Pauluzzi, and G. Stagni.** 1996. Hepatitis C virus genotypes in the liver and serum of patients with chronic hepatitis C. *Clin Microbiol Infect* **2**:20-24.
30. **Debnath, N. C., R. Tiernery, B. K. Sil, M. R. Wills, and A. D. Barrett.** 1991. In vitro homotypic and heterotypic interference by defective interfering particles of West Nile virus. *J Gen Virol* **72 (Pt 11)**:2705-11.
31. **Ecker, M., S. L. Allison, T. Meixner, and F. X. Heinz.** 1999. Sequence analysis and genetic classification of tick-borne encephalitis viruses from Europe and Asia. *J Gen Virol* **80 (Pt 1)**:179-85.
32. **Elshuber, S., S. L. Allison, F. X. Heinz, and C. W. Mandl.** 2003. Cleavage of protein prM is necessary for infection of BHK-21 cells by tick-borne encephalitis virus. *J Gen Virol* **84**:183-91.
33. **Elshuber, S., and C. W. Mandl.** 2005. Resuscitating mutations in a furin cleavage-deficient mutant of the flavivirus tick-borne encephalitis virus. *J Virol* **79**:11813-23.
34. **Fields, S., and G. Winter.** 1982. Nucleotide sequences of influenza virus segments 1 and 3 reveal mosaic structure of a small viral RNA segment. *Cell* **28**:303-13.
35. **Figlerowicz, M., P. D. Nagy, and J. J. Bujarski.** 1997. A mutation in the putative RNA polymerase gene inhibits nonhomologous, but not homologous, genetic recombination in an RNA virus. *Proc Natl Acad Sci U S A* **94**:2073-8.

36. **Fu, K., and R. S. Baric.** 1992. Evidence for variable rates of recombination in the MHV genome. *Virology* **189**:88-102.
37. **Fu, K., and R. S. Baric.** 1994. Map locations of mouse hepatitis virus temperature-sensitive mutants: confirmation of variable rates of recombination. *J Virol* **68**:7458-66.
38. **Gallei, A., A. Pankraz, H. J. Thiel, and P. Becher.** 2004. RNA recombination in vivo in the absence of viral replication. *J Virol* **78**:6271-81.
39. **Gallei, A., T. Rumenapf, H. J. Thiel, and P. Becher.** 2005. Characterization of helper virus-independent cytopathogenic classical swine fever virus generated by an in vivo RNA recombination system. *J Virol* **79**:2440-8.
40. **Gao, G. F., W. R. Jiang, M. H. Hussain, K. Venugopal, T. S. Gritsun, H. W. Reid, and E. A. Gould.** 1993. Sequencing and antigenic studies of a Norwegian virus isolated from encephalomyelitic sheep confirm the existence of louping ill virus outside Great Britain and Ireland. *J Gen Virol* **74 (Pt 1)**:109-14.
41. **Gehrke, R., M. Ecker, S. W. Aberle, S. L. Allison, F. X. Heinz, and C. W. Mandl.** 2003. Incorporation of tick-borne encephalitis virus replicons into virus-like particles by a packaging cell line. *J Virol* **77**:8924-33.
42. **Gehrke, R., F. X. Heinz, N. L. Davis, and C. W. Mandl.** 2005. Heterologous gene expression by infectious and replicon vectors derived from tick-borne encephalitis virus and direct comparison of this flavivirus system with an alphavirus replicon. *J Gen Virol* **86**:1045-53.
43. **Giangaspero, M., R. Harasawa, and A. Zanetti.** 2008. Taxonomy of genus Hepacivirus. Application of palindromic nucleotide substitutions for the determination of genotypes of human hepatitis C virus species. *J Virol Methods* **153**:280-99.
44. **Gibbs, M. J., J. S. Armstrong, and A. J. Gibbs.** 2001. Recombination in the hemagglutinin gene of the 1918 "Spanish flu". *Science* **293**:1842-5.
45. **Gmyl, A. P., E. V. Belousov, S. V. Maslova, E. V. Khitrina, A. B. Chetverin, and V. I. Agol.** 1999. Nonreplicative RNA recombination in poliovirus. *J Virol* **73**:8958-65.
46. **Gould, E. A., X. de Lamballerie, P. M. Zanutto, and E. C. Holmes.** 2003. Origins, evolution, and vector/host coadaptations within the genus Flavivirus. *Adv Virus Res* **59**:277-314.
47. **Granwehr, B. P., K. M. Lillibridge, S. Higgs, P. W. Mason, J. F. Aronson, G. A. Campbell, and A. D. Barrett.** 2004. West Nile virus: where are we now? *Lancet Infect Dis* **4**:547-56.
48. **Guirakhoo, F., F. X. Heinz, and C. Kunz.** 1989. Epitope model of tick-borne encephalitis virus envelope glycoprotein E: analysis of structural properties, role of carbohydrate side chain, and conformational changes occurring at acidic pH. *Virology* **169**:90-9.
49. **Guirakhoo, F., K. Pugachev, Z. Zhang, G. Myers, I. Levenbook, K. Draper, J. Lang, S. Ocran, F. Mitchell, M. Parsons, N. Brown, S. Brandler, C. Fournier, B. Barrere, F. Rizvi, A. Travassos, R. Nichols, D. Trent, and T. Monath.** 2004. Safety and efficacy of chimeric yellow Fever-dengue virus tetravalent vaccine formulations in nonhuman primates. *J Virol* **78**:4761-75.
50. **Hahn, C. S., S. Lustig, E. G. Strauss, and J. H. Strauss.** 1988. Western equine encephalitis virus is a recombinant virus. *Proc Natl Acad Sci U S A* **85**:5997-6001.
51. **Hajjou, M., K. R. Hill, S. V. Subramaniam, J. Y. Hu, and R. Raju.** 1996. Nonhomologous RNA-RNA recombination events at the 3' nontranslated region of the Sindbis virus genome: hot spots and utilization of nonviral sequences. *J Virol* **70**:5153-64.

52. **Harvey, T. J., W. J. Liu, X. J. Wang, R. Linedale, M. Jacobs, A. Davidson, T. T. Le, I. Anraku, A. Suhrbier, P. Y. Shi, and A. A. Khromykh.** 2004. Tetracycline-inducible packaging cell line for production of flavivirus replicon particles. *J Virol* **78**:531-8.
53. **Heinz, F. X., W. Tuma, F. Guirakhoo, and C. Kunz.** 1986. A model study of the use of monoclonal antibodies in capture enzyme immunoassays for antigen quantification exploiting the epitope map of tick-borne encephalitis virus. *J Biol Stand* **14**:133-41.
54. **Higgs, S., D. L. Vanlandingham, K. A. Klingler, K. L. McElroy, C. E. McGee, L. Harrington, J. Lang, T. P. Monath, and F. Guirakhoo.** 2006. Growth characteristics of ChimeriVax-Den vaccine viruses in *Aedes aegypti* and *Aedes albopictus* from Thailand. *Am J Trop Med Hyg* **75**:986-93.
55. **Holland, J., K. Spindler, F. Horodyski, E. Grabau, S. Nichol, and S. VandePol.** 1982. Rapid evolution of RNA genomes. *Science* **215**:1577-85.
56. **Holmes, E. C., and S. S. Twiddy.** 2003. The origin, emergence and evolutionary genetics of dengue virus. *Infect Genet Evol* **3**:19-28.
57. **Holmes, E. C., M. Worobey, and A. Rambaut.** 1999. Phylogenetic evidence for recombination in dengue virus. *Mol Biol Evol* **16**:405-9.
58. **Hu, W. S., and H. M. Temin.** 1990. Retroviral recombination and reverse transcription. *Science* **250**:1227-33.
59. **Hu, Y. W., E. Balaskas, M. Furione, P. H. Yen, G. Kessler, V. Scalia, L. Chui, and G. Sher.** 2000. Comparison and application of a novel genotyping method, semiautomated primer-specific and mispair extension analysis, and four other genotyping assays for detection of hepatitis C virus mixed-genotype infections. *J Clin Microbiol* **38**:2807-13.
60. **Huang, C. Y., S. Butrapet, K. R. Tsuchiya, N. Bhamarapavati, D. J. Gubler, and R. M. Kinney.** 2003. Dengue 2 PDK-53 virus as a chimeric carrier for tetravalent dengue vaccine development. *J Virol* **77**:11436-47.
61. **Jarvis, T. C., and K. Kirkegaard.** 1992. Poliovirus RNA recombination: mechanistic studies in the absence of selection. *Embo J* **11**:3135-45.
62. **Jenkins, G. M., A. Rambaut, O. G. Pybus, and E. C. Holmes.** 2002. Rates of molecular evolution in RNA viruses: a quantitative phylogenetic analysis. *J Mol Evol* **54**:156-65.
63. **Kalinina, O., H. Norder, S. Mukomolov, and L. O. Magnius.** 2002. A natural intergenotypic recombinant of hepatitis C virus identified in St. Petersburg. *J Virol* **76**:4034-43.
64. **Kao, J. H., P. J. Chen, M. Y. Lai, P. M. Yang, J. C. Sheu, T. H. Wang, and D. S. Chen.** 1994. Mixed infections of hepatitis C virus as a factor in acute exacerbations of chronic type C hepatitis. *J Infect Dis* **170**:1128-33.
65. **Keck, J. G., G. K. Matsushima, S. Makino, J. O. Fleming, D. M. Vannier, S. A. Stohlman, and M. M. Lai.** 1988. In vivo RNA-RNA recombination of coronavirus in mouse brain. *J Virol* **62**:1810-3.
66. **Keck, J. G., S. A. Stohlman, L. H. Soe, S. Makino, and M. M. Lai.** 1987. Multiple recombination sites at the 5'-end of murine coronavirus RNA. *Virology* **156**:331-41.
67. **Khatchikian, D., M. Orlich, and R. Rott.** 1989. Increased viral pathogenicity after insertion of a 28S ribosomal RNA sequence into the haemagglutinin gene of an influenza virus. *Nature* **340**:156-7.
68. **Khromykh, A. A., M. T. Kenney, and E. G. Westaway.** 1998. trans-Complementation of flavivirus RNA polymerase gene NS5 by using Kunjin virus replicon-expressing BHK cells. *J Virol* **72**:7270-9.

69. **Khromykh, A. A., P. L. Sedlak, and E. G. Westaway.** 2000. cis- and trans-acting elements in flavivirus RNA replication. *J Virol* **74**:3253-63.
70. **Khromykh, A. A., A. N. Varnavski, P. L. Sedlak, and E. G. Westaway.** 2001. Coupling between replication and packaging of flavivirus RNA: evidence derived from the use of DNA-based full-length cDNA clones of Kunjin virus. *J Virol* **75**:4633-40.
71. **Khromykh, A. A., A. N. Varnavski, and E. G. Westaway.** 1998. Encapsidation of the flavivirus kunjin replicon RNA by using a complementation system providing Kunjin virus structural proteins in trans. *J Virol* **72**:5967-77.
72. **Khromykh, A. A., and E. G. Westaway.** 1996. RNA binding properties of core protein of the flavivirus Kunjin. *Arch Virol* **141**:685-99.
73. **Kim, M. J., and C. Kao.** 2001. Factors regulating template switch in vitro by viral RNA-dependent RNA polymerases: implications for RNA-RNA recombination. *Proc Natl Acad Sci U S A* **98**:4972-7.
74. **Kirkegaard, K., and D. Baltimore.** 1986. The mechanism of RNA recombination in poliovirus. *Cell* **47**:433-43.
75. **Klempa, B., H. A. Schmidt, R. Ulrich, S. Kaluz, M. Labuda, H. Meisel, B. Hjelle, and D. H. Kruger.** 2003. Genetic interaction between distinct Dobrava hantavirus subtypes in *Apodemus agrarius* and *A. flavicollis* in nature. *J Virol* **77**:804-9.
76. **Kofler, R. M., J. H. Aberle, S. W. Aberle, S. L. Allison, F. X. Heinz, and C. W. Mandl.** 2004. Mimicking live flavivirus immunization with a noninfectious RNA vaccine. *Proc Natl Acad Sci U S A* **101**:1951-6.
77. **Kofler, R. M., F. X. Heinz, and C. W. Mandl.** 2002. Capsid protein C of tick-borne encephalitis virus tolerates large internal deletions and is a favorable target for attenuation of virulence. *J Virol* **76**:3534-43.
78. **Kofler, R. M., F. X. Heinz, and C. W. Mandl.** 2004. A novel principle of attenuation for the development of new generation live flavivirus vaccines. *Arch Virol Suppl*:191-200.
79. **Kofler, R. M., V. M. Hoenninger, C. Thurner, and C. W. Mandl.** 2006. Functional analysis of the tick-borne encephalitis virus cyclization elements indicates major differences between mosquito-borne and tick-borne flaviviruses. *J Virol* **80**:4099-113.
80. **Kofler, R. M., A. Leitner, G. O'Riordain, F. X. Heinz, and C. W. Mandl.** 2003. Spontaneous mutations restore the viability of tick-borne encephalitis virus mutants with large deletions in protein C. *J Virol* **77**:443-51.
81. **Kopek, B. G., G. Perkins, D. J. Miller, M. H. Ellisman, and P. Ahlquist.** 2007. Three-dimensional analysis of a viral RNA replication complex reveals a virus-induced mini-organelle. *PLoS Biol* **5**:e220.
82. **Kuge, S., N. Kawamura, and A. Nomoto.** 1989. Genetic variation occurring on the genome of an in vitro insertion mutant of poliovirus type 1. *J Virol* **63**:1069-75.
83. **Kummerer, B. M., and C. M. Rice.** 2002. Mutations in the yellow fever virus nonstructural protein NS2A selectively block production of infectious particles. *J Virol* **76**:4773-84.
84. **Lai, M. M.** 1992. RNA recombination in animal and plant viruses. *Microbiol Rev* **56**:61-79.
85. **Lai, M. M., R. S. Baric, S. Makino, J. G. Keck, J. Egbert, J. L. Leibowitz, and S. A. Stohman.** 1985. Recombination between nonsegmented RNA genomes of murine coronaviruses. *J Virol* **56**:449-56.
86. **Lancaster, M. U., S. I. Hodgetts, J. S. Mackenzie, and N. Urosevic.** 1998. Characterization of defective viral RNA produced during persistent infection of Vero cells with Murray Valley encephalitis virus. *J Virol* **72**:2474-82.

87. **Lazzarini, R. A., J. D. Keene, and M. Schubert.** 1981. The origins of defective interfering particles of the negative-strand RNA viruses. *Cell* **26**:145-54.
88. **Liao, C. L., and M. M. Lai.** 1992. RNA recombination in a coronavirus: recombination between viral genomic RNA and transfected RNA fragments. *J Virol* **66**:6117-24.
89. **Lindenbach, B. D., and C. M. Rice.** 2003. Molecular biology of flaviviruses. *Adv Virus Res* **59**:23-61.
90. **Lindenbach, B. D., Thiel, H.-J., Rice, C.M. (ed.).** 2007. *Flaviviridae: the viruses and their replication*, 5th ed. Lippincott Williams & Wilkins Co., Philadelphia.
91. **Liu, Z. L., S. Hennessy, B. L. Strom, T. F. Tsai, C. M. Wan, S. C. Tang, C. F. Xiang, W. B. Bilker, X. P. Pan, Y. J. Yao, Z. W. Xu, and S. B. Halstead.** 1997. Short-term safety of live attenuated Japanese encephalitis vaccine (SA14-14-2): results of a randomized trial with 26,239 subjects. *J Infect Dis* **176**:1366-9.
92. **Ma, L., C. T. Jones, T. D. Groesch, R. J. Kuhn, and C. B. Post.** 2004. Solution structure of dengue virus capsid protein reveals another fold. *Proc Natl Acad Sci U S A* **101**:3414-9.
93. **Mackenzie, J. S., D. J. Gubler, and L. R. Petersen.** 2004. Emerging flaviviruses: the spread and resurgence of Japanese encephalitis, West Nile and dengue viruses. *Nat Med* **10**:S98-109.
94. **Makino, S., J. G. Keck, S. A. Stohlman, and M. M. Lai.** 1986. High-frequency RNA recombination of murine coronaviruses. *J Virol* **57**:729-37.
95. **Mandl, C. W., S. L. Allison, H. Holzmann, T. Meixner, and F. X. Heinz.** 2000. Attenuation of tick-borne encephalitis virus by structure-based site-specific mutagenesis of a putative flavivirus receptor binding site. *J Virol* **74**:9601-9.
96. **Mandl, C. W., M. Ecker, H. Holzmann, C. Kunz, and F. X. Heinz.** 1997. Infectious cDNA clones of tick-borne encephalitis virus European subtype prototypic strain Neudoerfl and high virulence strain Hypr. *J Gen Virol* **78 (Pt 5)**:1049-57.
97. **Markoff, L.** 2003. 5'- and 3'-noncoding regions in flavivirus RNA. *Adv Virus Res* **59**:177-228.
98. **Markoff, L., B. Falgout, and A. Chang.** 1997. A conserved internal hydrophobic domain mediates the stable membrane integration of the dengue virus capsid protein. *Virology* **233**:105-17.
99. **Meyers, G., N. Tautz, E. J. Dubovi, and H. J. Thiel.** 1991. Viral cytopathogenicity correlated with integration of ubiquitin-coding sequences. *Virology* **180**:602-16.
100. **Meyers, G., and H. J. Thiel.** 1996. Molecular characterization of pestiviruses. *Adv Virus Res* **47**:53-118.
101. **Minor, P. D., A. John, M. Ferguson, and J. P. Icenogle.** 1986. Antigenic and molecular evolution of the vaccine strain of type 3 poliovirus during the period of excretion by a primary vaccinee. *J Gen Virol* **67 (Pt 4)**:693-706.
102. **Monath, T. P., F. Guirakhoo, R. Nichols, S. Yoksan, R. Schrader, C. Murphy, P. Blum, S. Woodward, K. McCarthy, D. Mathis, C. Johnson, and P. Bedford.** 2003. Chimeric live, attenuated vaccine against Japanese encephalitis (ChimeriVax-JE): phase 2 clinical trials for safety and immunogenicity, effect of vaccine dose and schedule, and memory response to challenge with inactivated Japanese encephalitis antigen. *J Infect Dis* **188**:1213-30.
103. **Monath, T. P., N. Kanesa-Thanan, F. Guirakhoo, K. Pugachev, J. Almond, J. Lang, M. J. Quentin-Millet, A. D. Barrett, M. A. Brinton, M. S. Cetron, R. S. Barwick, T. J. Chambers, S. B. Halstead, J. T. Roehrig, R. M. Kinney, R. Rico-Hesse, and J. H. Strauss.** 2005. Recombination and flavivirus vaccines: a commentary. *Vaccine* **23**:2956-8.

104. **Monath, T. P., I. Levenbook, K. Soike, Z. X. Zhang, M. Ratterree, K. Draper, A. D. Barrett, R. Nichols, R. Weltzin, J. Arroyo, and F. Guirakhoo.** 2000. Chimeric yellow fever virus 17D-Japanese encephalitis virus vaccine: dose-response effectiveness and extended safety testing in rhesus monkeys. *J Virol* **74**:1742-51.
105. **Monroe, S. S., and S. Schlesinger.** 1983. RNAs from two independently isolated defective interfering particles of Sindbis virus contain a cellular tRNA sequence at their 5' ends. *Proc Natl Acad Sci U S A* **80**:3279-83.
106. **Mukhopadhyay, S., R. J. Kuhn, and M. G. Rossmann.** 2005. A structural perspective of the flavivirus life cycle. *Nat Rev Microbiol* **3**:13-22.
107. **Nagy, P. D., and J. J. Bujarski.** 1995. Efficient system of homologous RNA recombination in brome mosaic virus: sequence and structure requirements and accuracy of crossovers. *J Virol* **69**:131-40.
108. **Nagy, P. D., and J. J. Bujarski.** 1997. Engineering of homologous recombination hotspots with AU-rich sequences in brome mosaic virus. *J Virol* **71**:3799-810.
109. **Nagy, P. D., and J. J. Bujarski.** 1993. Targeting the site of RNA-RNA recombination in brome mosaic virus with antisense sequences. *Proc Natl Acad Sci U S A* **90**:6390-4.
110. **Nagy, P. D., and A. E. Simon.** 1997. New insights into the mechanisms of RNA recombination. *Virology* **235**:1-9.
111. **Nagy, P. D., C. Zhang, and A. E. Simon.** 1998. Dissecting RNA recombination in vitro: role of RNA sequences and the viral replicase. *Embo J* **17**:2392-403.
112. **Negrone, M., M. Ricchetti, P. Nouvel, and H. Buc.** 1995. Homologous recombination promoted by reverse transcriptase during copying of two distinct RNA templates. *Proc Natl Acad Sci U S A* **92**:6971-5.
113. **Onodera, S., X. Qiao, P. Gottlieb, J. Strassman, M. Frilander, and L. Mindich.** 1993. RNA structure and heterologous recombination in the double-stranded RNA bacteriophage phi 6. *J Virol* **67**:4914-22.
114. **Orlinger, K. K., V. M. Hoenninger, R. M. Kofler, and C. W. Mandl.** 2006. Construction and mutagenesis of an artificial bicistronic tick-borne encephalitis virus genome reveals an essential function of the second transmembrane region of protein e in flavivirus assembly. *J Virol* **80**:12197-208.
115. **Patkar, C. G., C. T. Jones, Y. H. Chang, R. Warriar, and R. J. Kuhn.** 2007. Functional Requirements of the Yellow Fever Virus Capsid Protein. *J Virol*.
116. **Perrault, J.** 1981. Origin and replication of defective interfering particles. *Curr Top Microbiol Immunol* **93**:151-207.
117. **Petersen, L. R., and J. T. Roehrig.** 2001. West Nile virus: a reemerging global pathogen. *Emerg Infect Dis* **7**:611-4.
118. **Petersen, L. R., J. T. Roehrig, and J. M. Hughes.** 2002. West Nile virus encephalitis. *N Engl J Med* **347**:1225-6.
119. **Qin, Z., L. Sun, B. Ma, Z. Cui, Y. Zhu, Y. Kitamura, and W. Liu.** 2008. F gene recombination between genotype II and VII Newcastle disease virus. *Virus Res* **131**:299-303.
120. **Raju, R., S. V. Subramaniam, and M. Hajjou.** 1995. Genesis of Sindbis virus by in vivo recombination of nonreplicative RNA precursors. *J Virol* **69**:7391-401.
121. **Reichmann, M. E., and W. M. Schnitzlein.** 1979. Defective interfering particles of rhabdoviruses. *Curr Top Microbiol Immunol* **86**:123-68.
122. **Riegr, M., Nubling, M, Kaiser, R.** 1998. FSME Infektionen durch Rohmilch- welche Rolle spielt dieser in südwestdeutschen FSME-Endemiegebieten. *Virusepidemiologische Information* **60**:348-356.
123. **Romanova, L. I., V. M. Blinov, E. A. Tolskaya, E. G. Viktorova, M. S. Kolesnikova, E. A. Guseva, and V. I. Agol.** 1986. The primary structure of crossover

- regions of intertypic poliovirus recombinants: a model of recombination between RNA genomes. *Virology* **155**:202-13.
124. **Roukens, A. H., and L. G. Visser.** 2008. Yellow fever vaccine: past, present and future. *Expert Opin Biol Ther* **8**:1787-95.
 125. **Sabchareon, A., J. Lang, P. Chanthavanich, S. Yoksan, R. Forrat, P. Attanath, C. Sirivichayakul, K. Pengsaa, C. Pojjaroen-Anant, L. Chambonneau, J. F. Saluzzo, and N. Bhamarapravati.** 2004. Safety and immunogenicity of a three dose regimen of two tetravalent live-attenuated dengue vaccines in five- to twelve-year-old Thai children. *Pediatr Infect Dis J* **23**:99-109.
 126. **Schierup, M. H., C. H. Mordhorst, C. P. Muller, and L. S. Christensen.** 2005. Evidence of recombination among early-vaccination era measles virus strains. *BMC Evol Biol* **5**:52.
 127. **Schlick, P., C. Taucher, B. Schittl, J. L. Tran, R. M. Kofler, W. Schueler, A. von Gabain, A. Meinke, and C. W. Mandl.** 2009. Helices α_2 and α_3 of WNV Capsid Protein are Dispensable for the Assembly of Infectious Virions. *J Virol*.
 128. **Scholle, F., Y. A. Girard, Q. Zhao, S. Higgs, and P. W. Mason.** 2004. trans-Packaged West Nile virus-like particles: infectious properties in vitro and in infected mosquito vectors. *J Virol* **78**:11605-14.
 129. **Schrauf, S., P. Schlick, T. Skern, and C. W. Mandl.** 2008. Functional analysis of potential carboxy-terminal cleavage sites of tick-borne encephalitis virus capsid protein. *J Virol* **82**:2218-29.
 130. **Seligman, S. J., and E. A. Gould.** 2004. Live flavivirus vaccines: reasons for caution. *Lancet* **363**:2073-5.
 131. **Seregin, A., R. Nistler, V. Borisevich, G. Yamshchikov, E. Chaporgina, C. W. Kwok, and V. Yamshchikov.** 2006. Immunogenicity of West Nile virus infectious DNA and its noninfectious derivatives. *Virology* **356**:115-25.
 132. **Serviene, E., N. Shapka, C. P. Cheng, T. Panavas, B. Phuangrat, J. Baker, and P. D. Nagy.** 2005. Genome-wide screen identifies host genes affecting viral RNA recombination. *Proc Natl Acad Sci U S A* **102**:10545-50.
 133. **Shapka, N., and P. D. Nagy.** 2004. The AU-rich RNA recombination hot spot sequence of Brome mosaic virus is functional in tombusviruses: implications for the mechanism of RNA recombination. *J Virol* **78**:2288-300.
 134. **Shriner, D., A. G. Rodrigo, D. C. Nickle, and J. I. Mullins.** 2004. Pervasive genomic recombination of HIV-1 in vivo. *Genetics* **167**:1573-83.
 135. **Shustov, A. V., P. W. Mason, and I. Frolov.** 2007. Production of pseudoinfectious yellow fever virus with a two-component genome. *J Virol* **81**:11737-48.
 136. **Sibold, C., H. Meisel, D. H. Kruger, M. Labuda, J. Lysy, O. Kozuch, M. Pejcoch, A. Vaheri, and A. Plyusnin.** 1999. Recombination in Tula hantavirus evolution: analysis of genetic lineages from Slovakia. *J Virol* **73**:667-75.
 137. **Solomon, T., and D. W. Vaughn.** 2002. Pathogenesis and clinical features of Japanese encephalitis and West Nile virus infections. *Curr Top Microbiol Immunol* **267**:171-94.
 138. **Spann, K. M., P. L. Collins, and M. N. Teng.** 2003. Genetic recombination during coinfection of two mutants of human respiratory syncytial virus. *J Virol* **77**:11201-11.
 139. **Stadler, K., S. L. Allison, J. Schlich, and F. X. Heinz.** 1997. Proteolytic activation of tick-borne encephalitis virus by furin. *J Virol* **71**:8475-81.
 140. **Stiasny, K., and F. X. Heinz.** 2006. Flavivirus membrane fusion. *J Gen Virol* **87**:2755-66.
 141. **Stuhlmann, H., and P. Berg.** 1992. Homologous recombination of copackaged retrovirus RNAs during reverse transcription. *J Virol* **66**:2378-88.

142. **Suzuki, Y., T. Gojobori, and O. Nakagomi.** 1998. Intragenic recombinations in rotaviruses. *FEBS Lett* **427**:183-7.
143. **Tolou, H. J., P. Couissinier-Paris, J. P. Durand, V. Mercier, J. J. de Pina, P. de Micco, F. Billoir, R. N. Charrel, and X. de Lamballerie.** 2001. Evidence for recombination in natural populations of dengue virus type 1 based on the analysis of complete genome sequences. *J Gen Virol* **82**:1283-90.
144. **Tolskaya, E. A., L. I. Romanova, V. M. Blinov, E. G. Viktorova, A. N. Sinyakov, M. S. Kolesnikova, and V. I. Agol.** 1987. Studies on the recombination between RNA genomes of poliovirus: the primary structure and nonrandom distribution of crossover regions in the genomes of intertypic poliovirus recombinants. *Virology* **161**:54-61.
145. **Tsai, K. N., S. F. Tsang, C. H. Huang, and R. Y. Chang.** 2007. Defective interfering RNAs of Japanese encephalitis virus found in mosquito cells and correlation with persistent infection. *Virus Res* **124**:139-50.
146. **Tsiang, M., S. S. Monroe, and S. Schlesinger.** 1985. Studies of defective interfering RNAs of Sindbis virus with and without tRNA^{Asp} sequences at their 5' termini. *J Virol* **54**:38-44.
147. **Twiddy, S. S., and E. C. Holmes.** 2003. The extent of homologous recombination in members of the genus *Flavivirus*. *J Gen Virol* **84**:429-40.
148. **Uzcategui, N. Y., D. Camacho, G. Comach, R. Cuello de Uzcategui, E. C. Holmes, and E. A. Gould.** 2001. Molecular epidemiology of dengue type 2 virus in Venezuela: evidence for in situ virus evolution and recombination. *J Gen Virol* **82**:2945-53.
149. **Wang, S. H., W. J. Syu, and S. T. Hu.** 2004. Identification of the homotypic interaction domain of the core protein of dengue virus type 2. *J Gen Virol* **85**:2307-14.
150. **Weiss, B. G., and S. Schlesinger.** 1991. Recombination between Sindbis virus RNAs. *J Virol* **65**:4017-25.
151. **Welsch, S., S. Miller, I. Romero-Brey, A. Merz, C. K. Bleck, P. Walther, S. D. Fuller, C. Antony, J. Krijnse-Locker, and R. Bartenschlager.** 2009. Composition and three-dimensional architecture of the dengue virus replication and assembly sites. *Cell Host Microbe* **5**:365-75.
152. **Widman, D. G., T. Ishikawa, R. Fayzulin, N. Bourne, and P. W. Mason.** 2008. Construction and characterization of a second-generation pseudoinfectious West Nile virus vaccine propagated using a new cultivation system. *Vaccine* **26**:2762-71.
153. **Worobey, M., and E. C. Holmes.** 1999. Evolutionary aspects of recombination in RNA viruses. *J Gen Virol* **80** (Pt 10):2535-43.
154. **Worobey, M., A. Rambaut, and E. C. Holmes.** 1999. Widespread intra-serotype recombination in natural populations of dengue virus. *Proc Natl Acad Sci U S A* **96**:7352-7.
155. **Yoon, S. W., S. Y. Lee, S. Y. Won, S. H. Park, S. Y. Park, and Y. S. Jeong.** 2006. Characterization of homologous defective interfering RNA during persistent infection of Vero cells with Japanese encephalitis virus. *Mol Cells* **21**:112-20.
156. **Zhang, J., and H. M. Temin.** 1993. Rate and mechanism of nonhomologous recombination during a single cycle of retroviral replication. *Science* **259**:234-8.

Curriculum Vitae

Christian Taucher

Personal data

Date and place of birth: May 9, 1981, Graz
Citizenship: Austrian
Marital status: Married to Cornelia Taucher, since 2007
Child Vinzent Taucher
Name before marriage: Riepl
Home address: Deublergasse 35/1, A-1210 Vienna, Austria

Business address: Institute of Clinical Virology,
Medical University of Vienna
Kinderspitalgasse 15, A-1095 Vienna
Phone: +43-1-40490-79504
Mobil: +43-699-10970028
e-mail: christian.taucher@meduniwien.ac.at

Education

1987-1991 Elementary school in Eferding, Upper Austria
1991-1999 High school in Wilhering, Upper Austria
1999-2000 Student of sociology at Johannes Kepler University
Linz, Upper Austria
2001-2005 Student of genetics and microbiology at
University of Vienna
Sept. 2004-Aug. 2005 Diploma thesis at the biotech company Intercell
Nov. 2005 Awarded M.S. degree in genetics and microbiology by
the University of Vienna
Nov. 2005-2009 Ph.D. thesis at the Institute of Clinical Virology, Vienna